Available online at www.sciencedirect.com
SCIENCE DIRECT®
Physics Reports 412 (2005) 191–275
PHYSICS REPORTS
www.elsevier.com/locate/physrep

# Quantum Zeno effect by general measurements

Kazuki Koshino[a, b, *], Akira Shimizu[c, d]

[a] *Faculty of Systems Engineering, Wakayama University, 930 Sakaedani, Wakayama 640-8510, Japan*
[b] *CREST, Japan Science and Technology Corporation, 4-1-8 Honcho, Kawaguchi 332-0012, Japan*
[c] *Department of Basic Science, University of Tokyo, 3-8-1 Komaba, Tokyo 153-8902, Japan*
[d] *PRESTO, Japan Science and Technology Corporation, 4-1-8 Honcho, Kawaguchi 332-0012, Japan*

Accepted 14 March 2005
Available online 26 April 2005
editor: J. Eichler

**Abstract**

It was predicted that frequently repeated measurements on an unstable quantum state may alter the decay rate of the state. This is called the quantum Zeno effect (QZE) or the anti-Zeno effect (AZE), depending on whether the decay is suppressed or enhanced. In conventional theories of the QZE and AZE, effects of measurements are simply described by the projection postulate, assuming that each measurement is an instantaneous and ideal one. However, real measurements are not instantaneous and ideal. For the QZE and AZE by such general measurements, interesting and surprising features have recently been revealed, which we review in this article. The results are based on the quantum measurement theory, which is also reviewed briefly. As a typical model, we consider a continuous measurement of the decay of an excited atom by a photodetector that detects a photon emitted from the atom upon decay. This measurement is an indirect negative-result one, for which the curiosity of the QZE and AZE is emphasized. It is shown that the form factor is renormalized as a backaction of the measurement, through which the decay dynamics is modified. In a special case of the flat response, where the detector responds to every photon mode with an identical response time, results of the conventional theories are reproduced qualitatively. However, drastic differences emerge in general cases where the detector responds only to limited photon modes. For example, against predictions of the conventional theories, the QZE or AZE may take place even for states that exactly follow the exponential decay law. We also discuss relation to the cavity quantum electrodynamics.


*PACS:* 03.65.Xp; 03.65.Yz; 06.20.Dk

*Keywords:* Quantum Zeno effect

* Corresponding author. Tel./fax: +81 73 457 8302.
*E-mail addresses:* ikuzak@sys.wakayama-u.ac.jp (K. Koshino), shmz@ASone.c.u-tokyo.ac.jp (A. Shimizu).

0370-1573/$ - see front matter © 2005 Elsevier B.V. All rights reserved.
doi:10.1016/j.physrep.2005.03.001

**Contents**

1. Introduction . . . 193
2. Fundamental properties of unstable quantum systems . . . 196
2.1. A typical model of unstable quantum systems . . . 196
2.2. Initial behavior of survival probability . . . 197
2.3. Form factor . . . 198
2.3.1. Interaction mode and the form factor . . . 198
2.3.2. Free space . . . 199
2.3.3. Perfect cavity . . . 200
2.3.4. Leaky cavity . . . 201
2.4. Perturbation theory . . . 202
2.5. Green function method . . . 203
2.6. Decay dynamics under the Lorentzian form factor . . . 204
2.6.1. Exact formulas . . . 204
2.6.2. Symmetric case . . . 206
2.6.3. Asymmetric case . . . 207
3. Conventional theories of quantum Zeno and anti-Zeno effects . . . 208
3.1. Ideal measurement on the target system . . . 208
3.2. Decay rate under repeated measurements . . . 209
3.3. Quantum Zeno effect . . . 211
3.4. Quantum anti-Zeno effect . . . 211
3.5. QZE–AZE phase diagram . . . 212
4. Quantum measurement theory . . . 214
4.1. Ideal measurement . . . 215
4.2. Time evolution of the system and apparatus . . . 216
4.3. von Neumann chain . . . 219
4.3.1. When measurement is completed? . . . 220
4.3.2. Where is the Heisenberg cut? . . . 221
4.3.3. Average over all possible values of the readout . . . 221
4.4. Prescription for analyzing general measurements . . . 222
4.5. Properties of general measurements . . . 223
4.5.1. Response time . . . 223
4.5.2. Measurement error . . . 223
4.5.3. Range of measurement . . . 225
4.5.4. Information obtained by measurement . . . 226
4.5.5. Backaction of measurement . . . 227
4.5.6. Instantaneous measurement and ideal measurement as limiting cases . . . 228
4.6. Various types of measurements . . . 228
4.6.1. Direct versus indirect measurements . . . 229
4.6.2. Positive- versus negative-result measurements . . . 229
4.6.3. Repeated instantaneous measurements versus continuous measurement . . . 229
4.6.4. Unitary approximation . . . 231
4.7. A simple explanation of the Zeno effect using the quantum measurement theory . . . 232
4.8. Additional comments . . . 233
4.8.1. Non-triviality of the uncertainty relations . . . 233
4.8.2. Measurement of time correlations . . . 234
4.8.3. POVM measurement . . . 236
4.8.4. Completeness of the standard laws of quantum theory . . . 237
5. Analysis of Zeno effect by quantum measurement theory . . . 237
5.1. Model for the system and apparatus . . . 237

5.1.1. Hamiltonian for atom–photon–detector system . . . 237
5.1.2. Quantities of interest . . . 239
5.1.3. Relation to direct measurements . . . 240
5.2. Renormalization of form factor by measurement . . . 241
5.3. Continuous measurement with flat response . . . 243
5.3.1. Decay rate under flat response . . . 244
5.3.2. Numerical results . . . 245
5.3.3. Renormalized FGR decay rate . . . 247
5.3.4. QZE–AZE phase diagram . . . 248
5.4. Geometrically imperfect measurement . . . 249
5.5. Quantum Zeno effect by energetically imperfect measurement . . . 251
5.5.1. A model for an exact exponential decay . . . 252
5.5.2. Numerical results . . . 252
5.5.3. Conditions for QZE . . . 253
5.6. Quantum anti-Zeno effect by false measurement . . . 255
5.6.1. Natural linewidth . . . 255
5.6.2. Numerical results . . . 256
5.6.3. Conditions for AZE . . . 257
5.7. Discussions . . . 258
5.7.1. Relation to conventional theories . . . 258
5.7.2. Physical interpretation . . . 258
5.7.3. Discussions and remarks on the model . . . 259
6. Relation to cavity quantum electrodynamics . . . 260
6.1. Relation between the Zeno effect and other phenomena . . . 260
6.2. Modification of form factor in cavity QED . . . 260
6.2.1. Reconstruction of eigenmodes . . . 261
6.2.2. Broadening of eigenenergies . . . 262
6.3. Atom in a homogeneous absorptive medium . . . 262
6.4. Atom in an inhomogeneous absorptive medium . . . 263
6.4.1. Cavity QED . . . 263
6.4.2. Zeno effect by detectors spatially separated from the target atom . . . 265
7. Experimental studies on the Zeno effect . . . 266
7.1. Atomic tunneling phenomenon . . . 267
7.2. Parametric down conversion process . . . 268
7.3. Evasion of the Zeno effect in general experiments . . . 270
8. Summary . . . 270
References . . . 272

## 1. Introduction

The standard quantum theory assumes two principles for time evolution [1,2]; the continuous *unitary evolution* in the absence of measurement, and the projection postulate connecting the pre- and post-measurement states. Using these principles, an interesting prediction was obtained by analyzing the gedanken experiment in which the initial state of a quantum system is unstable and one repeatedly

checks whether the unstable state has decayed or not [3–5]. Until the system is measured, the state vector undergoes the unitary evolution according to the Schrödinger equation. It is then shown that at the very beginning of the decay the survival probability $s(t)$ of the unstable state decreases very slowly as a function of the elapsed time $t$ as $1 - s(t) \propto t^2$, whereas in the later time stage $s(t)$ decreases much faster, typically exponentially. The time scale $t_j$ at which the crossover between these different behaviors takes place is called the *jump time* [6]. On the other hand, the projection postulate tells us that at every moment an observer confirms the survival of the system through the measurement, the quantum state of the system is reset to the initial undecayed one. Combining these two observations, one is led to an interesting conclusion that the decay rate is reduced if the intervals $\tau_i$ of the repeated measurements is shorter than $t_j$. In the limit of $\tau_i/t_j \to +0$, in particular, the decay is completely suppressed, i.e., the system is frozen to the initial undecayed state. This phenomenon is called the *quantum Zeno effect* (QZE) [7–10]. It was also predicted later that for slightly longer $\tau_i$ ($\sim t_j$) the opposite effect, i.e., acceleration of decay, can occur in some quantum systems. This is called the *quantum anti-Zeno effect* (AZE) or inverse Zeno effect [11–14]. The QZE and AZE are sometimes called simply the *Zeno effect*.

Most importantly, the reasoning leading to these predictions is independent of details of quantum systems, and thus the Zeno effect is expected to occur widely in quantum systems. In particular, the complete suppression of the decay in the limit of $\tau_i/t_j \to +0$ is universal, common to all quantum systems. However, the reasoning leading to such interesting and universal conclusions needs to be reexamined, because it assumes that each measurement is an *instantaneous ideal measurement*. Here, the term 'instantaneous' means that the response time $\tau_r$ of the measuring apparatus is much shorter than other relevant time scales such as $\tau_i$. The term 'ideal' means that the post-measurement state is given by the projection postulate, which implies many conditions such as the measurement error is zero. Unfortunately, these conditions are not strictly satisfied in real measurements. Therefore, the Zeno effect by such *general measurements* is interesting and to be explored.

To study the time evolution of quantum systems under general measurements, one must apply the quantum measurement theory, which has been developed for several decades [1,15–23]. The point of the quantum measurement theory is that one must apply the laws of quantum theory to the joint quantum system composed of the target system S of interest and (a part of) the measuring apparatus A. In other words, the 'Heisenberg cut' separating the quantum system and the rest of the world should be located not between S and A but between S+A and the rest A′. Although the boundary between A and A′ can be taken quite arbitrarily, one can obtain the same results if S+A is taken to be large enough, i.e., if the Heisenberg cut is properly located [1]. One can then calculate all relevant quantities, including the response time, measurement error, range of the measurement, and the post-measurement state, and so on. One can thus calculate the decay rate under general measurements as a function of these relevant quantities. Furthermore, although the necessity of the projection postulate in the analysis of the Zeno effect has been a controversial point for a long time [10], the quantum measurement theory gives a clear answer: As far as the Zeno effect is concerned one can analyze it without using the projection postulate at all if S+A is taken to be large enough.

The purpose of the present article is to review results for the Zeno effect by general measurements. We show that the conclusions of the conventional theories, which assume instantaneous ideal measurements, are modified drastically depending on the natures of real measurements. In particular, some of common wisdoms deduced by the conventional theories break in general measurement processes. For example, the

Zeno effect can take place even for systems with $t_j \to +0$ [24,25], for which the conventional theories predicted that the Zeno effect never occurs.

Note that in the original papers of the QZE a truly decaying state was analyzed, for which $s(t)$ in the absence of measurements decreases monotonically. However, the Zeno effect has also been discussed on other classes of states such as states for which $s(t)$ oscillates with $t$ (Rabi oscillation) [26,27]. Furthermore, although the QZE was discussed as a result of measurements in the original papers, some works use the term QZE or AZE for changes of the decay rate induced by any external perturbations such as external noises [28–30]. The former may be called the Zeno effect in the narrow sense, whereas the latter may be called the Zeno effect in the broad sense. Moreover, it is sometimes argued that the Zeno effect is curious or surprising only when the measurements are indirect and negative-result ones [10]. Although these different views concern merely the definition of the terms QZE and AZE, they have been the origins of certain confusion or controversy. We will therefore notice the above points where it is needed.

The present article is organized as follows. In Section 2, we review the *free* quantum dynamics of unstable states, i.e., the dynamics while the system is not being measured, by solving the Schrödinger equation. After presenting a typical model of unstable systems, we describe a simple technique to solve the model, and explain characteristics of the survival probability of the unstable state. By combining the results of Section 2 and the projection postulate, we review in Section 3 the conclusions of the conventional theories of the Zeno effect, which assumed instantaneous ideal measurements. The decay rate under repeated measurements is presented as a function of the measurement intervals $\tau_i$, and the conditions for inducing the QZE or AZE by instantaneous ideal measurements are clarified. The quantum measurement theory is briefly reviewed in Section 4, in such a way that it provides for basic knowledge that are required to understand not only the Zeno effect but also many other topics of quantum measurements. After presenting the prescription for analyzing general measurements, we summarize relevant quantities such as the measurement error and the range of the measurement, as well as useful concepts, such as indirect measurements and negative-result measurements. We also explain why one can analyze the Zeno effect without using the projection postulate. We then give a simple explanation of the Zeno effect using the quantum measurement theory. In Section 5, we analyze the Zeno effect by the quantum measurement theory. We employ a model which describes a continuous indirect negative-result measurement of an unstable state. It is shown that the form factor is renormalized as an inevitable backaction of measurement, and this renormalization plays a crucial role in the Zeno effect. We study the case of a continuous measurement with flat response in Section 5.3, and show that the results almost coincide with those obtained by the conventional theories, which assumed repeated instantaneous ideal measurements. In contrast, we show in Sections 5.4–5.6 that dramatic differences emerge if the response is not flat. In Section 6, relation between the Zeno effect and other phenomena, such as the motional narrowing, is discussed. In particular, we discuss the close relationship between the cavity quantum electrodynamics (QED) and the Zeno effect by a continuous indirect measurement. Using the results of the cavity QED, we touch on the Zeno effect in case where the detectors are spatially separated from the target atom in Section 6.4. InSection 7, we introduce experimental studies on the Zeno effect on monotonically decaying unstable states. We also discuss how to *avoid* the Zeno effect in general experiments, which are designed not to detect the Zeno effect but to measure the free decay rate accurately. Finally, the main points of this article are summarized in Section 8. Since Sections 4 and 5 are rather long, guidelines are given at the beginnings of these sections, which will help the readers who wish to read them faster.

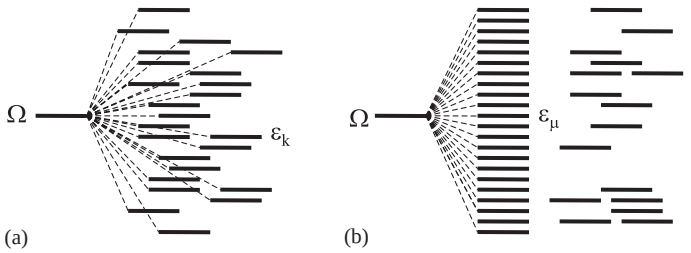


Fig. 1. Schematic energy diagram of the Hamiltonian in (a) the raw form [Eq. (1)], and (b) after the interaction modes are extracted [Eq. (15)].

## 2. Fundamental properties of unstable quantum systems

### *2.1. A typical model of unstable quantum systems*

In this section, we review the intrinsic dynamics of unstable states in quantum systems, which occurs while the system is not being measured. There are many examples of unstable quantum systems: excited atoms [31,32], unstable nuclei [9], and so on. The dynamics of these systems are characterized by irreversibility; the initial unstable state decays with a finite lifetime, and the system never returns to the initial state spontaneously. Such an irreversible dynamics takes place when the initial state is coupled to continua of states, whose energies extend over a wide energy range. In the following, we employ an excited two-level atom with a finite radiative lifetime as a typical example of unstable quantum systems, but the main features of the dynamics are common to most unstable systems.

The system is composed of a two-level atom and a photon field. The eigenmodes of the photon field are labeled by the wavevector $\boldsymbol{k}$ and the polarization $\lambda$. For notational simplicity, we hereafter omit the label $\lambda$ and employ a single label $\boldsymbol{k}$ to discriminate photon eigenmodes. We denote the atomic raising (lowering) operator by $\sigma_+$ ($\sigma_-$), the creation (annihilation) operator of a photon by $b_{\boldsymbol{k}}^\dagger$ ($b_{\boldsymbol{k}}$), and the vacuum state (no atomic excitation and no photons) by $|0\rangle$. At the initial moment ($t = 0$), the atom is in the excited state and there are no photons. Taking $\hbar = c = 1$, the Hamiltonian of this system is given by

$$\hat{H}_S = \Omega\sigma_+\sigma_- + \int \mathrm{d}\boldsymbol{k}\, [(g_{\boldsymbol{k}}\sigma_+ b_{\boldsymbol{k}} + \mathrm{H.c.}) + \epsilon_{\boldsymbol{k}} b_{\boldsymbol{k}}^\dagger b_{\boldsymbol{k}}]\ , \tag{1}$$

where $\Omega$ is the atomic transition energy, $\epsilon_{\boldsymbol{k}}$ is the energy of the mode $\boldsymbol{k}$, and $g_{\boldsymbol{k}}$ is the atom–photon coupling. The schematic energy diagram is shown in Fig. 1(a). Here, the dimension of $\boldsymbol{k}$ is arbitrary, and no specific forms of $\epsilon_{\boldsymbol{k}}$ and $g_{\boldsymbol{k}}$ are assumed.

Regarding the atom–photon interaction, the rotating-wave approximation is employed [31,32], i.e., the counter-rotating terms such as $\sigma_- b_{\boldsymbol{k}}$ and $\sigma_+ b_{\boldsymbol{k}}^\dagger$ are neglected. The effect of counter-rotating terms may be partly incorporated by renormalizing the atom–photon coupling $g_{\boldsymbol{k}}$ for off-resonant photons. Under the rotating-wave approximation, the number of quanta, which is defined by

$$\hat{N} = \sigma_+\sigma_- + \int \mathrm{d}\boldsymbol{k} b_{\boldsymbol{k}}^\dagger b_{\boldsymbol{k}}\ , \tag{2}$$

is conserved in this system, i.e., $[\hat{H}_S, \hat{N}] = 0$. Because we have one quantum (atomic excitation) in the initial state, the state vector evolves restrictedly in the one-quantum space, which is spanned by the

following states:

$$|\mathrm{x}\rangle = \sigma_+|0\rangle \ , \tag{3}$$

$$|\mathrm{g}, \boldsymbol{k}\rangle = b_{\boldsymbol{k}}^\dagger|0\rangle \ , \tag{4}$$

where $|\mathrm{x}\rangle$ and $|\mathrm{g}\rangle$ in the left-hand-side represent the excited and ground states of the atom, respectively. The initial state vector, $|\mathrm{i}\rangle$, is given by $|\mathrm{i}\rangle = |\mathrm{x}\rangle$.

Throughout this article, we employ the Schrödinger picture for describing temporal evolution. The state vector evolves as

$$|\psi(t)\rangle = \exp(-\mathrm{i}\hat{H}_S t)|\mathrm{i}\rangle \ , \tag{5}$$

which may be written as follows:

$$|\psi(t)\rangle = f(t)|\mathrm{x}\rangle + \int \mathrm{d}\boldsymbol{k} f_{\boldsymbol{k}}(t)|\mathrm{g}, \boldsymbol{k}\rangle \ , \tag{6}$$

where

$$f(t) = \langle \mathrm{x}| \exp(-\mathrm{i}\hat{H}_S t)|\mathrm{i}\rangle \ , \tag{7}$$

$$f_{\boldsymbol{k}}(t) = \langle \mathrm{g}, \boldsymbol{k}| \exp(-\mathrm{i}\hat{H}_S t)|\mathrm{i}\rangle \ . \tag{8}$$

$f(t)$ is called the survival amplitude of the initial state, and its square gives the survival probability $s(t)$;

$$s(t) = |f(t)|^2 \ . \tag{9}$$

### 2.2. Initial behavior of survival probability

In this subsection, we briefly discuss short-time behaviors of the survival probability. Expanding $\exp(-\mathrm{i}\hat{H}_S t)$ in Eq. (7) in powers of $t$, $f(t)$ is given by

$$f(t) = \sum_{j=0}^{\infty} \frac{(-\mathrm{i}t)^j}{j!} \langle (\hat{H}_S)^j \rangle \ , \tag{10}$$

where $\langle (\hat{H}_S)^j \rangle = \langle \mathrm{i}|(\hat{H}_S)^j|\mathrm{i}\rangle$.[1] $s(t)$ is thus given by

$$s(t) = 1 - \langle (\Delta \hat{H}_S)^2 \rangle t^2 + \mathcal{O}(t^4) \ , \tag{11}$$

where $\langle (\Delta \hat{H}_S)^2 \rangle \equiv \langle \hat{H}_S^2 \rangle - \langle \hat{H}_S \rangle^2$ is a positive quantity. It is easily confirmed that

$$s(t) = |\langle \exp(-\mathrm{i}\hat{H}_S t) \rangle|^2 = |\langle \exp(\mathrm{i}\hat{H}_S t) \rangle|^2 = s(-t) \ , \tag{12}$$

which implies that $s(t)$ is an even function of $t$ and therefore contains only even powers of $t$. Eq. (11) states that $s(t)$ decreases quadratically in time at the beginning of decay, whereas in a later period $s(t)$

[1] This expansion is valid when $\langle (\hat{H}_S)^j \rangle$ is finite for any $j$. Although this assumption seems to be satisfied in real physical systems, $\langle (\hat{H}_S)^j \rangle$ can diverge if one takes a certain limit, such as the $\Delta \to \infty$ limit taken in Section 5.5.1. Physically, such a limit should be understood as an abbreviated description of the case where $\Delta$ is larger than any other relevant energy scales.

behaves differently depending on details of the system (see Section 2.6 and Refs. [3–5,8,33–35]). The quadratic decrease becomes important when we consider the effects of frequently repeated measurements on the system (see Section 3.3).

### 2.3. Form factor

Before investigating the temporal evolution in the whole time region, we transform the above Hamiltonian $\hat{H}_S$ into a simpler form, where the atom is coupled to a single continuum which is labeled one-dimensionally by the energy.

#### 2.3.1. Interaction mode and the form factor

In order to explain the basic idea, we preliminarily consider a simplified case where the atom interacts only with two photon modes $b_1$ and $b_2$ of the same energy $\mu$. The Hamiltonian for this simplified system is given by

$$\hat{H}_{\rm sim} = \Omega\sigma_+\sigma_- + \mu b_1^\dagger b_1 + \mu b_2^\dagger b_2 + (\gamma_1\sigma_+ b_1 + \gamma_2\sigma_+ b_2 + \text{H.c.}) \ .$$

By the following linear transformation:

$$\begin{pmatrix} B_1 \\ B_2 \end{pmatrix} = \frac{1}{\sqrt{\gamma_1^2+\gamma_2^2}} \begin{pmatrix} \gamma_1 & \gamma_2 \\ -\gamma_2 & \gamma_1 \end{pmatrix} \begin{pmatrix} b_1 \\ b_2 \end{pmatrix} \ ,$$

the Hamiltonian can be recast into the following form:

$$\hat{H}_{\rm sim} = \Omega\sigma_+\sigma_- + \mu B_1^\dagger B_1 + \left[\sqrt{\gamma_1^2+\gamma_2^2}\ \sigma_+ B_1 + \text{H.c.}\right] + \mu B_2^\dagger B_2 \ .$$

Here, only $B_1$ interacts with the atom with the renormalized coupling constant $\sqrt{\gamma_1^2+\gamma_2^2}$, while $B_2$ is decoupled from the atom. We call $B_1$ the *interaction mode* [36,37].

Now we return to the original Hamiltonian $\hat{H}_S$, Eq. (1). We define the interaction mode at energy $\mu$ by

$$B_\mu = g_\mu^{-1} \int \mathrm{d}\boldsymbol{k}\ \delta(\epsilon_{\boldsymbol{k}} - \mu)\ g_{\boldsymbol{k}}\ b_{\boldsymbol{k}} \ , \tag{13}$$

where $g_\mu$ is the *form factor* of the interaction, which is defined by[2]

$$|g_\mu|^2 = \int \mathrm{d}\boldsymbol{k} |g_{\boldsymbol{k}}|^2 \delta(\epsilon_{\boldsymbol{k}} - \mu) \ . \tag{14}$$

Here, $g_\mu$ has been determined so as to normalize $B_\mu$ as $[B_\mu, B_{\mu'}^\dagger] = \delta(\mu - \mu')$. Using these quantities, the Hamiltonian Eq. (1) is transformed into the following form:

$$\hat{H}_S = \Omega\sigma_+\sigma_- + \int \mathrm{d}\mu\ [(g_\mu\sigma_+ B_\mu + \text{H.c.}) + \mu B_\mu^\dagger B_\mu] + \hat{H}_{\rm rest} \ , \tag{15}$$

[2] The phase of $g_\mu$ can be taken arbitrary. For example, one can take it as $g_\mu \geqslant 0$.

where $\hat{H}_{\rm rest}$ consists of modes that do not interact with the atom. The schematic energy diagram after this transformation is shown in Fig. 1(b). Due to our initial condition, the existence of $\hat{H}_{\rm rest}$ does not affect the decay dynamics at all.

In Eq. (15), the atom is coupled to a single continuum $B_\mu$. This type of Hamiltonian is called the Friedrichs model [38]. In this model, the dynamics is determined solely by the functional form of $|g_\mu|^2$. For example, if we apply the Fermi golden rule [39], the radiative decay rate of the atom is given by

$$\Gamma_{\rm FGR} = 2\pi|g_\Omega|^2 = 2\pi \int \mathrm{d}\boldsymbol{k}|g_{\boldsymbol{k}}|^2\delta(\epsilon_{\boldsymbol{k}} - \Omega) \ . \tag{16}$$

In the following parts of this subsection, concrete forms of the form factor are presented for three realistic cases.

*2.3.2. Free space*

Firstly, we consider a case where an atom is placed in a free space [32]. The form factor is dependent on the dimension of the space. Here, we discuss the three-dimensional case as an example. Imposing the periodic boundary condition with the quantization length $L$, and reviving here the index $\lambda$ representing the photonic polarization, the eigenmodes and eigenenergies are given by

$$\boldsymbol{f}_{\boldsymbol{k}\lambda}(\boldsymbol{r}) = L^{-3/2}\,\mathrm{e}^{\mathrm{i}\boldsymbol{k}\cdot\boldsymbol{r}}\boldsymbol{e}_{\boldsymbol{k}\lambda} \ , \tag{17}$$

$$\epsilon_{\boldsymbol{k}\lambda} = |\boldsymbol{k}| \ , \tag{18}$$

where $\boldsymbol{e}_{\boldsymbol{k}\lambda}$ is a unit vector in the direction of polarization, which is normal to the wavevector $\boldsymbol{k}$. $\boldsymbol{k}$ is discretized as $\boldsymbol{k} = 2\pi/L \times (n_x, n_y, n_z)$, where $n_{x,y,z} = 0, \pm1, \pm2, \ldots$ . The atom–photon coupling $g_{\boldsymbol{k}\lambda}$ is given by

$$g_{\boldsymbol{k}\lambda} = -\frac{e}{m}\sqrt{\frac{2\pi}{\epsilon_{\boldsymbol{k}\lambda}}}\langle \mathrm{x}|\boldsymbol{p}\cdot\boldsymbol{f}_{\boldsymbol{k}\lambda}(\boldsymbol{r})|\mathrm{g}\rangle \ , \tag{19}$$

where $m$, $e$, $\boldsymbol{r}$, and $\boldsymbol{p}$ are the mass, charge, position, momentum of the electron in the atom. If the $\boldsymbol{r}$-dependence of $\boldsymbol{f}_{\boldsymbol{k}\lambda}(\boldsymbol{r})$ within the atom is negligible (dipole approximation), we obtain

$$g_{\boldsymbol{k}\lambda} = -\mathrm{i}\Omega\sqrt{\frac{2\pi}{\epsilon_{\boldsymbol{k}\lambda}}}\boldsymbol{\mu}_{\rm atom}\cdot\boldsymbol{f}_{\boldsymbol{k}\lambda}(\boldsymbol{r}) \ , \tag{20}$$

where $\boldsymbol{\mu}_{\rm atom} = e\langle \mathrm{x}|\boldsymbol{r}|\mathrm{g}\rangle$ is the transition dipole moment of the atom.

It should be noted that the atom is coupled only to photons within a finite energy range. The lower-bound originates in the positiveness of the photonic energy. The higher-cutoff $\omega_c$ is introduced by the fact that $\langle \mathrm{x}|\boldsymbol{p}\cdot\boldsymbol{f}_{\boldsymbol{k}\lambda}(\boldsymbol{r})|\mathrm{g}\rangle$ almost vanishes when $|\boldsymbol{k}|$ is large, due to rapid oscillation of $\boldsymbol{f}_{\boldsymbol{k}\lambda}(\boldsymbol{r})$.

Now we determine the form factor, using Eq. (20). The form factor is given, using the formula Eq. (14), by

$$|g_\mu|^2 = \sum_{\boldsymbol{k},\lambda} |g_{\boldsymbol{k}\lambda}|^2\delta(\epsilon_{\boldsymbol{k}} - \mu) \ . \tag{21}$$

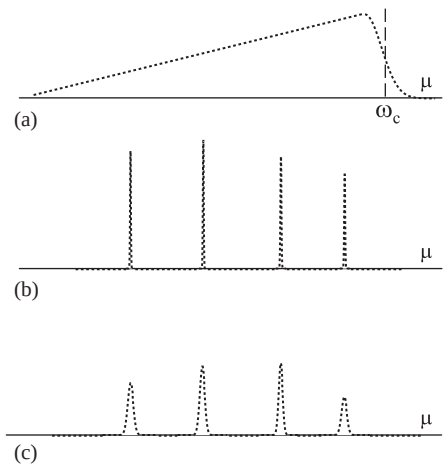


Fig. 2. Schematic view of the form factors in (a) a three-dimensional free space, (b) a perfect cavity, and (c) a leaky cavity.

Taking the $L \to \infty$ limit and replacing the summation over $\boldsymbol{k}$ with the integral, we obtain the following form factor:

$$|g_\mu|^2 = \begin{cases} \dfrac{2\Omega^2 |\boldsymbol{\mu}_{\rm atom}|^2 \mu}{3\pi} & (\mu \lesssim \omega_c) \\ 0 & (\mu \gtrsim \omega_c) \end{cases} . \tag{22}$$

Thus, the form factor has a continuous spectrum in a free space, as shown in Fig. 2(a).

*2.3.3. Perfect cavity*

Next, we discuss a case where the atom is placed in a perfect cavity, whose eigenmodes do not suffer attenuation at all. As a model of such a perfect cavity, we consider a photon field bounded by perfect mirrors placed at $x = 0$ and $l_x$, $y = 0$ and $l_y$, $z = 0$ and $l_z$. The eigenmodes and eigenenergies are given by

$$\boldsymbol{f}_{\boldsymbol{k}\lambda}(\boldsymbol{r}) = \sqrt{\frac{8}{l_x l_y l_z}} \sin(k_x x) \sin(k_y y) \sin(k_z z) \boldsymbol{e}_{\boldsymbol{k}\lambda} , \tag{23}$$

$$\epsilon_{\boldsymbol{k}\lambda} = |\boldsymbol{k}| , \tag{24}$$

where $\boldsymbol{k} = (n_x \pi / l_x, n_y \pi / l_y, n_z \pi / l_z)$ with $n_{x,y,z} = 1, 2, \ldots$ . The atom–photon coupling constant and the form factor are determined by Eqs. (19) and (21), respectively.

A distinct difference from the free-space case is that the photonic modes are discretized. In the present case, the summation over $\boldsymbol{k}$ cannot be replaced with the integral, and the form factor is composed of delta functions located at eigenenergies, as shown in Fig. 2(b). The energy separation becomes larger as the cavity lengths $(l_x, l_y, l_z)$ are decreased. By using a small cavity, one may realize a situation where the atom effectively interacts only with a single eigenmode of the cavity. Then, denoting the annihilation operator of that eigenmode by $a$, the Hamiltonian of the whole system reads

$$\hat{H}_{\rm pc} = \Omega \sigma_+ \sigma_- + (g \sigma_+ a + \text{H.c.}) + \omega_0 a^\dagger a , \tag{25}$$

where $\omega_0$ is the energy of the eigenmode, and $g$ is the coupling constant between the atom and the eigenmode.

*2.3.4. Leaky cavity*

In usual optical cavities, in order that one can input photons into the cavity from external photon modes, one (or more) mirror composing the cavity should be weakly transmissive. In this case, photons inside the cavity gradually escape into external modes through the transmissive mirror, i.e., the cavity is leaky. Considering for simplicity a case where the atom effectively interacts with a single cavity mode, the Hamiltonian for the whole system is given, extending Eq. (25), by

$$\hat{H}_{\rm lc} = \Omega\sigma_+\sigma_- + (g\sigma_+ a + \text{H.c.}) + \omega_0 a^\dagger a + \int \mathrm{d}\omega \left[\sqrt{\frac{\kappa}{2\pi}}(a^\dagger b_\omega + b_\omega^\dagger a) + \omega b_\omega^\dagger b_\omega\right] , \tag{26}$$

where $b_\omega$ denotes the annihilation operator for the external photon mode with energy $\omega$ [40]. The lifetime of the cavity mode is given by $\kappa^{-1}$, and the $Q$-value of the cavity is given by $\omega_0/\kappa$.

It is straightforward to derive the form factor from the above Hamiltonian, by diagonalizing the interaction part of the Hamiltonian between the cavity mode $a$ and the external modes $b_\omega$. To this end, hereafter denoting an infinitesimal positive constant by $\delta$, we define the following operator [41],

$$B_\mu = \alpha(\mu)a + \int \mathrm{d}\omega\beta(\mu,\omega)b_\omega , \tag{27}$$

where

$$\alpha(\mu) = \frac{(\kappa/2\pi)^{1/2}}{\mu - \omega_0 + \mathrm{i}\kappa/2} , \tag{28}$$

$$\beta(\mu,\omega) = \frac{\kappa/2\pi}{(\mu-\omega_0+\mathrm{i}\kappa/2)(\mu-\omega+\mathrm{i}\delta)} + \delta(\mu-\omega) . \tag{29}$$

Note that $B_\mu$ is orthonormalized as $[B_\mu, B_{\mu'}^\dagger] = \delta(\mu-\mu')$. The original operators, $a$ and $b_\omega$, are given in terms of $B_\mu$ by

$$a = \int \mathrm{d}\mu\alpha^*(\mu)B_\mu , \tag{30}$$

$$b_\omega = \int \mathrm{d}\mu\beta^*(\omega,\mu)B_\mu . \tag{31}$$

Using $B_\mu$, Eq. (26) is rewritten as

$$\hat{H}_{\rm lc} = \Omega\sigma_+\sigma_- + \int \mathrm{d}\mu[(g\alpha^*(\mu)\sigma_+ B_\mu + H.c.) + \mu B_\mu^\dagger B_\mu] , \tag{32}$$

in which the atom is coupled to a single continuum of $B_\mu$ and the energy diagram of Fig. 1(b) is realized. Therefore, the form factor takes the following Lorentzian form:

$$|g_\mu|^2 = |g\alpha^*(\mu)|^2 = g^2\frac{\kappa/2\pi}{(\mu-\omega_0)^2 + (\kappa/2)^2} , \tag{33}$$

which satisfies the following sum rule:

$$\int \mathrm{d}\mu |g_\mu|^2 = g^2 \ , \tag{34}$$

which holds for any $\kappa$.

To summarize, when the cavity is perfect and has no leak, the form factor is composed of delta functions, as shown in Fig. 2(b). Contrarily, when the cavity is leaky, each delta function is broadened to be a Lorentzian, keeping the sum rule of Eq. (34), as shown in Fig. 2(c).

### *2.4. Perturbation theory*

In the following part of Section 2, we investigate how the initial unstable state evolves in time by the Schrödinger equation, Eq. (5). Here, we calculate the survival probability *etc* by an elementary perturbation theory. For this purpose, we divide the Hamiltonian Eq. (1) into the diagonal and interaction parts as

$$\hat{H}_S = \hat{H}_0 + \hat{H}_1 \ , \tag{35}$$

$$\hat{H}_0 = \Omega \sigma_+ \sigma_- + \int \mathrm{d}\boldsymbol{k} \epsilon_{\boldsymbol{k}} b^\dagger_{\boldsymbol{k}} b_{\boldsymbol{k}} \ , \tag{36}$$

$$\hat{H}_1 = \int \mathrm{d}\boldsymbol{k} \ (g_{\boldsymbol{k}} \sigma_+ b_{\boldsymbol{k}} + \mathrm{H.c.}) \ . \tag{37}$$

It is easy to derive the following perturbative expansion for the evolution operator $\exp(-\mathrm{i}\hat{H}_S t)$:

$$\begin{aligned} \exp(-\mathrm{i}\hat{H}_S t) = \ & \exp(-\mathrm{i}\hat{H}_0 t) \\ & \times \left[ \hat{1} + (-\mathrm{i}) \int_0^t \mathrm{d}t' \hat{H}_1(t') + (-\mathrm{i})^2 \int_0^t \mathrm{d}t' \int_0^{t'} \mathrm{d}t'' \hat{H}_1(t') \hat{H}_1(t'') + \cdots \right] , \end{aligned} \tag{38}$$

where $\hat{H}_1(t)$ is the interaction representation of $\hat{H}_1$, which is given by

$$\hat{H}_1(t) = \mathrm{e}^{\mathrm{i}\hat{H}_0 t} \hat{H}_1 \mathrm{e}^{-\mathrm{i}\hat{H}_0 t} = \int \mathrm{d}\boldsymbol{k} \ (g_{\boldsymbol{k}} \sigma_+ b_{\boldsymbol{k}} \mathrm{e}^{-\mathrm{i}(\epsilon_{\boldsymbol{k}} - \Omega)t} + \mathrm{H.c.}) \ . \tag{39}$$

Now we calculate the decay amplitude $f_{\boldsymbol{k}}(t)$ defined in Eq. (8) within the lowest-order perturbation, where the second-order and higher powers of $\hat{H}_1$ are neglected in Eq. (38). Then, $f_{\boldsymbol{k}}(t)$ is reduced to the following form:

$$f_{\boldsymbol{k}}(t) \simeq -\mathrm{i}\langle 0 | b_{\boldsymbol{k}} \mathrm{e}^{\mathrm{i}\hat{H}_0 t} \int_0^t \mathrm{d}t' \hat{H}_1(t') \sigma_+ | 0 \rangle = -\mathrm{i} \mathrm{e}^{-\mathrm{i}(\Omega + \epsilon_{\boldsymbol{k}})t/2} \ g^*_{\boldsymbol{k}} \ t \ \mathrm{sinc}[(\epsilon_{\boldsymbol{k}} - \Omega)t/2] \ . \tag{40}$$

The decay probability to the photon $\boldsymbol{k}$ is given by $|f_{\boldsymbol{k}}(t)|^2$. The survival probability is therefore given by

$$s(t) = 1 - \int \mathrm{d}\boldsymbol{k} |f_{\boldsymbol{k}}(t)|^2 = 1 - t^2 \int \mathrm{d}\boldsymbol{k} |g_{\boldsymbol{k}}|^2 \mathrm{sinc}^2[(\epsilon_{\boldsymbol{k}} - \Omega)t/2] \tag{41}$$

$$= 1 - t^2 \int \mathrm{d}\mu |g_\mu|^2 \mathrm{sinc}^2[(\mu - \Omega)t/2] \ . \tag{42}$$

In deriving the last equality, Eq. (14) has been used. Because Eq. (42) is based on the perturbation theory, it is valid only for small $t$; deviation from an exact result becomes significant for large $t$, as we will see in Fig. 6. However, Eq. (42) serves as a convenient tool as long as the short-time behavior is concerned, such as discussion of the QZE and AZE.

Relation to the initial quadratic decay law, Eq. (11), is easily observed. At the very beginning of decay (more strictly, when $t^{-1}$ is much larger than the spectral width of $|g_\mu|^2$), one can regard that $\mathrm{sinc}[(\epsilon_{\boldsymbol{k}} - \Omega)t/2] \simeq 1$, so the right-hand-side of Eq. (42) is approximated as $s(t) \simeq 1 - t^2 \int \mathrm{d}\mu |g_\mu|^2 = 1 - \langle(\Delta \hat{H}_S)^2\rangle t^2$.

### 2.5. Green function method

In the previous subsection, the temporal evolution of unstable system is investigated by the perturbation theory, which is valid only for small $t$ in principle. Here, we summarize the Green function method [42,43], which is standardly used in calculating the temporal evolution of general quantum systems and gives reliable results even for long $t$.

First, we define the *bare* atomic and photon Green functions in the frequency representation. They are given, in terms of the diagonal Hamiltonian $\hat{H}_0$, by

$$A(\omega) = \langle 0|\sigma_- \frac{1}{\omega - \hat{H}_0 + \mathrm{i}\delta} \sigma_+|0\rangle = \frac{1}{\omega - \Omega + \mathrm{i}\delta} , \tag{43}$$

$$P(\omega, \boldsymbol{k}, \boldsymbol{k}') = \langle 0|b_{\boldsymbol{k}'} \frac{1}{\omega - \hat{H}_0 + \mathrm{i}\delta} b^\dagger_{\boldsymbol{k}}|0\rangle = \frac{\delta(\boldsymbol{k} - \boldsymbol{k}')}{\omega - \epsilon_{\boldsymbol{k}} + \mathrm{i}\delta} . \tag{44}$$

These bare Green functions are related, through the Fourier transformation, to the non-interacting dynamics of the atom and the photons. For example,

$$\frac{\mathrm{i}}{2\pi} \int \mathrm{d}\omega \mathrm{e}^{-\mathrm{i}\omega t} A(\omega) = \langle 0|\sigma_- \mathrm{e}^{-\mathrm{i}\hat{H}_0 t}\sigma_+|0\rangle = \mathrm{e}^{-\mathrm{i}\Omega t} . \tag{45}$$

Similarly, we define the *dressed* atomic Green function by

$$\bar{A}(\omega) = \langle 0|\sigma_- \frac{1}{\omega - \hat{H}_S + \mathrm{i}\delta} \sigma_+|0\rangle . \tag{46}$$

The dressed atomic Green function is related to the survival amplitude of the atom $f(t)$ by

$$\frac{\mathrm{i}}{2\pi} \int \mathrm{d}\omega \mathrm{e}^{-\mathrm{i}\omega t} \bar{A}(\omega) = \langle 0|\sigma_- \mathrm{e}^{-\mathrm{i}\hat{H}_S t}\sigma_+|0\rangle \equiv f(t) . \tag{47}$$

It is known that the dressed atomic Green function can be expanded in terms of the bare Green functions as follows,

$$\begin{aligned} \bar{A}(\omega) &= A(\omega) + A(\omega)\Sigma(\omega)A(\omega) + A(\omega)\Sigma(\omega)A(\omega)\Sigma(\omega)A(\omega) + \cdots \\ &= \frac{A(\omega)}{1 - A(\omega)\Sigma(\omega)} , \end{aligned} \tag{48}$$

where the self-energy $\Sigma(\omega)$ is given by

$$\Sigma(\omega) = \int\int \mathrm{d}\boldsymbol{k}_1 \mathrm{d}\boldsymbol{k}_2 g^*_{\boldsymbol{k}_1} g_{\boldsymbol{k}_2} P(\omega, \boldsymbol{k}_1, \boldsymbol{k}_2) = \int \mathrm{d}\boldsymbol{k} \frac{|g_{\boldsymbol{k}}|^2}{\omega - \epsilon_{\boldsymbol{k}} + \mathrm{i}\delta} = \int \mathrm{d}\mu \frac{|g_\mu|^2}{\omega - \mu + \mathrm{i}\delta} . \tag{49}$$

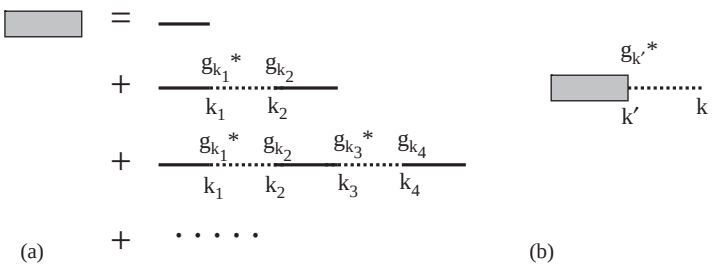


Fig. 3. (a) Feynman diagrams for the dressed atomic Green function. The solid and dotted lines on the right hand side represent the bare atom and photon Green functions $A(\omega)$ and $P(\omega, \boldsymbol{k})$, respectively, while the bold line on the left hand side represents the dressed Green function. (b) Feynman diagram representing the decay to photon $\boldsymbol{k}$.

The Feynman diagrams corresponding to Eq. (48) are drawn in Fig. 3(a). Eq. (14) is used in deriving the third equality of Eq. (49). We can reconfirm by Eqs. (47)–(49) that the decay dynamics of the atom is determined completely by the form factor $g_\mu$.

We also note that, besides the survival amplitude, the decay amplitude to a photon of a specific mode $\boldsymbol{k}$ can be obtained using the dressed atomic Green function as

$$\langle 0|b_{\boldsymbol{k}}\ \frac{1}{\omega-\hat{H}_S+\mathrm{i}\delta}\ \sigma_+|0\rangle=\int \mathrm{d}\boldsymbol{k}'\, g_{\boldsymbol{k}'}^*\bar{A}(\omega)P(\omega,\boldsymbol{k}',\boldsymbol{k})=\frac{g_{\boldsymbol{k}}^*\bar{A}(\omega)}{\omega-\epsilon_{\boldsymbol{k}}+\mathrm{i}\delta}\ . \tag{50}$$

The Feynman diagram corresponding to this amplitude is drawn in Fig. 3(b).

### *2.6. Decay dynamics under the Lorentzian form factor*

The Green function method is applicable to any forms of $\epsilon_{\boldsymbol{k}}$ and $g_{\boldsymbol{k}}$. In this section, we practically use the Green function method to calculate the survival probability of an unstable state. Here, we discuss the case where the form factor is given by a single Lorentzian as follows;

$$|g_\mu|^2=\frac{\gamma}{2\pi}\frac{\Delta^2}{(\mu-\mu_0)^2+\Delta^2}\ . \tag{51}$$

Here, $\mu_0$ and $\Delta$ denote the central energy and the spectral width of the form factor, respectively, and $\gamma/2\pi=|g_{\mu_0}|^2$ characterizes the magnitude of the form factor (see Fig. 4).

Such a Lorentzian form factor is realized, for example, by an atom placed in a leaky optical cavity, as has been shown in Section 2.3.4. Although the form factors of general unstable systems are not necessarily approximated by Lorentzian, it is expected that qualitative features of quantum dynamics are inferable by considering the case of a Lorentzian form factor, as long as the form factor is single-peaked. For example, the decay dynamics in a free space, whose form factor is schematically shown in Fig. 2(a), would be qualitatively reproducible by the Lorentzian form factor if we take $\Omega \ll \mu_0$.

#### *2.6.1. Exact formulas*

In the case of the Lorentzian form factor, we can exactly calculate the self-energy $\Sigma(\omega)$, the dressed Green function $\bar{A}(\omega)$, and the survival amplitude $f(t)=\langle \mathrm{i}|\exp(-\mathrm{i}\mathscr{H}t)|\mathrm{i}\rangle$ as follows:

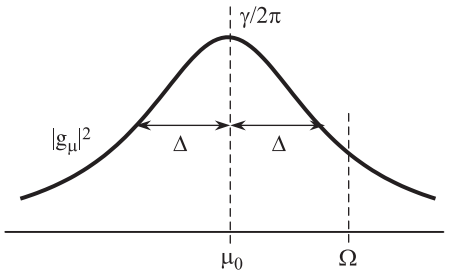


Fig. 4. View of the Lorentzian form factor. The atomic transition energy $\Omega$ is arbitrary.

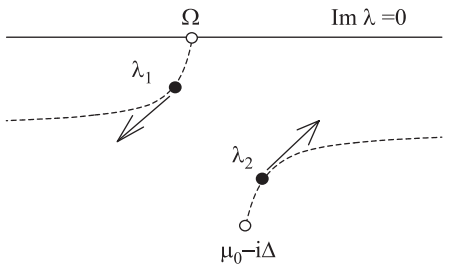


Fig. 5. Solutions $\lambda_1$ and $\lambda_2$ of Eq. (55) are plotted in the complex $\lambda$-plane. Dotted curves show the trajectories when $\gamma$ is changed, and arrows indicate the directions into which $\lambda$'s move as $\gamma$ is increased.

$$\Sigma(\omega) = \frac{\gamma\Delta}{2(\omega - \mu_0 + \mathrm{i}\Delta)} \ , \tag{52}$$

$$\bar{A}(\omega) = \frac{\omega - \mu_0 + \mathrm{i}\Delta}{(\omega - \Omega)(\omega - \mu_0 + \mathrm{i}\Delta) - \gamma\Delta/2} \ , \tag{53}$$

$$f(t) = \frac{\lambda_1 - \mu_0 + \mathrm{i}\Delta}{\lambda_1 - \lambda_2} \exp(-\mathrm{i}\lambda_1 t) + \frac{\lambda_2 - \mu_0 + \mathrm{i}\Delta}{\lambda_2 - \lambda_1} \exp(-\mathrm{i}\lambda_2 t) \ . \tag{54}$$

Here, $\lambda_1$ and $\lambda_2$ are the poles of the dressed Green function $\bar{A}(\omega)$, and satisfy

$$(\omega - \Omega)(\omega - \mu_0 + \mathrm{i}\Delta) - \gamma\Delta/2 = (\omega - \lambda_1)(\omega - \lambda_2) \ . \tag{55}$$

Both of them lie in the lower half plane as shown in Fig. 5, and we choose them to satisfy $|\mathrm{Im}(\lambda_1)| \leqslant |\mathrm{Im}(\lambda_2)|$. The survival probability $s(t)$ is exactly given by

$$s(t) = |f(t)|^2 = \left| \frac{\lambda_1 - \mu_0 + \mathrm{i}\Delta}{\lambda_1 - \lambda_2} \exp(-\mathrm{i}\lambda_1 t) + \frac{\lambda_2 - \mu_0 + \mathrm{i}\Delta}{\lambda_2 - \lambda_1} \exp(-\mathrm{i}\lambda_2 t) \right|^2 \ . \tag{56}$$

On the other hand, the Fermi golden rule, Eq. (16), yields the approximate decay rate as

$$\Gamma_{\mathrm{FGR}} = \gamma \frac{\Delta^2}{\Delta^2 + (\Omega - \mu_0)^2} \ . \tag{57}$$

We will compare $\Gamma_{\mathrm{FGR}}$ with the rigorous result Eq. (56) in the latter part of Section 2.6 (Fig. 7).

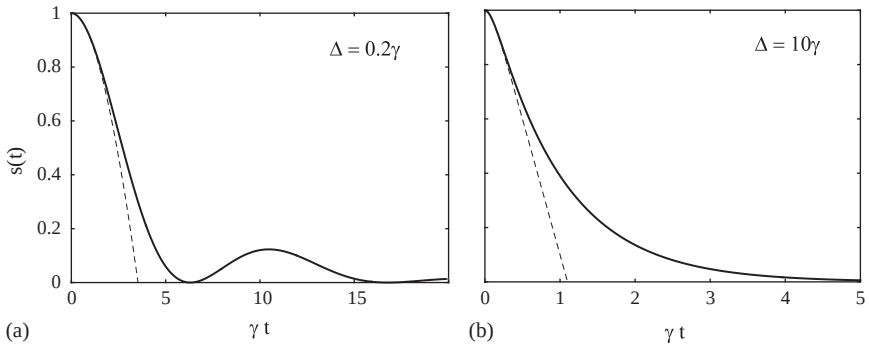


Fig. 6. Temporal evolution of the survival probability $s(t)$, for $\mu_0 - \Omega = 0$. $\Delta = 0.2\gamma$ in (a), and $\Delta = 10\gamma$ in (b). The solid lines are drawn by the exact formula, Eq. (56). The thin dotted lines are the results of perturbation: combining Eqs. (42) and (51), the survival probability is approximately given by $s(t) \simeq 1 - \gamma\Delta^2|\mu_0 - \Omega + \mathrm{i}\Delta|^{-2}t - \gamma\Delta\mathrm{Re}[(1 - \mathrm{e}^{\mathrm{i}(\mu_0-\Omega+\mathrm{i}\Delta)t})(\mu_0 - \Omega + \mathrm{i}\Delta)^{-2}]$.

### 2.6.2. Symmetric case

When the form factor is symmetric about the atomic transition energy, i.e., $\mu_0 = \Omega$, the above equations are particularly simplified;

$$\lambda_{1,2} = \Omega - \mathrm{i}\Delta\frac{1 \pm \sqrt{1 - 2\gamma/\Delta}}{2} , \tag{58}$$

$$f(t) = \frac{1 + \sqrt{1 - 2\gamma/\Delta}}{2\sqrt{1 - 2\gamma/\Delta}} \exp(-\mathrm{i}\lambda_1 t) - \frac{1 - \sqrt{1 - 2\gamma/\Delta}}{2\sqrt{1 - 2\gamma/\Delta}} \exp(-\mathrm{i}\lambda_2 t) . \tag{59}$$

The temporal evolution of the survival probability $s(t)$ is plotted in Fig. 6, for small and large $\Delta$.

First, we discuss a case of small $\Delta$ (satisfying $\Delta < 2\gamma$), in which $\mathrm{Im}(\lambda_1) = \mathrm{Im}(\lambda_2)$ and $\mathrm{Re}(\lambda_1) \neq \mathrm{Re}(\lambda_2)$. In this case, $s(t)$ shows a damped Rabi oscillation, as shown in Fig. 6(a), which implies that the emitted photon may be reabsorbed by the decayed atom. This phenomenon, called the collapse and revival, has actually been observed in an atom in a high-$Q$ cavity [44–46]. In the limit of $\Delta \to 0$ (and simultaneously $\gamma \to \infty$, keeping $\int \mathrm{d}\mu|g_\mu|^2 = \gamma\Delta/2$ at a finite value), the Rabi oscillation continues forever without damping. Obviously, we cannot define the decay rate in the presence of the Rabi oscillation.

Next, we discuss a case of large $\Delta$. In this case, $s(t)$ decreases monotonously as shown in Fig. 6(b). The radiative decay of an atom in free space belongs to this case. In order to clarify the meanings of the parameters $\Delta$ and $\gamma$, we focus on a case of $\Delta \gg \gamma$ in the following. Then, $\lambda_1$ and $\lambda_2$ are approximated by

$$\lambda_1 \simeq \Omega - \mathrm{i}\gamma/2 , \tag{60}$$

$$\lambda_2 \simeq \Omega - \mathrm{i}\Delta . \tag{61}$$

At the beginning of the decay, one can easily confirm, by expanding Eq. (59) in powers of $t$, that $s(t)$ decreases quadratically as

$$s(t) = 1 - \gamma\Delta t^2/2 + \mathcal{O}(t^4) . \tag{62}$$

Noticing that $\langle(\Delta\hat{H}_S)^2\rangle = \gamma\Delta/2$ in our example, Eq. (62) is in accordance with Eq. (11). On the other hand, in the later stage of the decay ($t \gtrsim \Delta^{-1}$), the second term of Eq. (59) becomes negligible and $s(t)$

follows the exponential decay law as

$$s(t) \simeq \mathscr{Z} \exp(-\Gamma(\infty)t) \ , \tag{63}$$

where

$$\mathscr{Z} = \left| \frac{\lambda_1 - \mu_0 + \mathrm{i}\Delta}{\lambda_1 - \lambda_2} \right|^2 \ , \tag{64}$$

$$\Gamma(\infty) = -2\,\mathrm{Im}(\lambda_1) \ . \tag{65}$$

The decay rate in the later stage of decay ($t \gtrsim \Delta^{-1}$) is rigorously given by Eq. (65). We confirm that the rigorous rate $\Gamma(\infty)$ agrees to the lowest order of $\gamma/\Delta$ with the golden-rule decay rate $\Gamma_{\mathrm{FGR}}$, which is given by Eq. (57). Thus, $\Gamma_{\mathrm{FGR}}$ serves as a good approximation of $\Gamma(\infty)$, as long as $\Delta \gg \gamma$.

In concluding this subsection, we summarize the results for the case of $\Delta \gg \gamma$, which is satisfied in most unstable states of interest. At the beginning of decay $s(t)$ decreases quadratically obeying Eq. (62), and later follows the exponential decay law, Eq. (63). The transition between these two behaviors occurs at

$$t \sim \Delta^{-1} \equiv t_{\mathrm{j}} \ , \tag{66}$$

which is called the *jump time* [3] [6]. The decay rate $\Gamma(\infty)$ in the later stage is approximated well by the golden-rule decay rate $\Gamma_{\mathrm{FGR}}$.

*2.6.3. Asymmetric case*

Now we discuss the asymmetric case, where $\mu_0$ is not necessarily equal to $\Omega$. The crossover between the damped Rabi oscillation and the monotonous decrease, which was observed in Fig. 6, is also observed in this case. Here we focus on the latter situation assuming $\Delta \gg \gamma$, which is usually satisfied in most of monotonically decaying systems.

Throughout this article, much attentions are paid to the decay rate of an unstable quantum state. The decay rate at time $t$ is conventionally defined by

$$\Gamma_{\mathrm{con}}(t) = -\left(\frac{\mathrm{d}s}{\mathrm{d}t}\right) \Big/ s = -\frac{\mathrm{d}}{\mathrm{d}t} \ln s(t) \ . \tag{67}$$

In Fig. 7(a), $\Gamma_{\mathrm{con}}(t)$ is plotted for three different values of $|\mu_0 - \Omega|$. However, in the discussion of the Zeno effect, the following quantity is more significant:

$$\Gamma(t) = -\frac{\ln s(t)}{t} \ . \tag{68}$$

In Section 3.3, it will be revealed that $\Gamma(\tau_{\mathrm{i}})$ gives the decay rate under repeated instantaneous ideal measurements with intervals $\tau_{\mathrm{i}}$. $\Gamma(t)$ is plotted in Fig. 7(b). Comparing Figs. 7(a) and (b), we find that the discrepancy between $\Gamma_{\mathrm{con}}(t)$ and $\Gamma(t)$ is significant in the early time stage, $t \lesssim t_{\mathrm{j}}$; in particular, at the beginning of decay, $\Gamma_{\mathrm{con}}(t) = 2\Gamma(t)$. However, the discrepancy becomes less significant as time evolves.

Focusing on $\Gamma(t)$, the following features are observed in common in three lines in Fig. 7(b): Initially ($t \ll t_{\mathrm{j}}$), $s(t)$ is given by Eq. (62) regardless of $|\mu_0 - \Omega|$. Therefore, $\Gamma(t)$ is approximately given by a linear

[3] Note that definition of the jump time is slightly different from the original one: In Ref. [6], the jump time is defined as $t_{\mathrm{j}} \equiv \Gamma(\infty)/\langle(\Delta\hat{H}_S)^2\rangle$, which is reduced here to $t_{\mathrm{j}} \simeq 2\Delta/[\Delta^2 + (\Omega - \mu_0)^2]$.

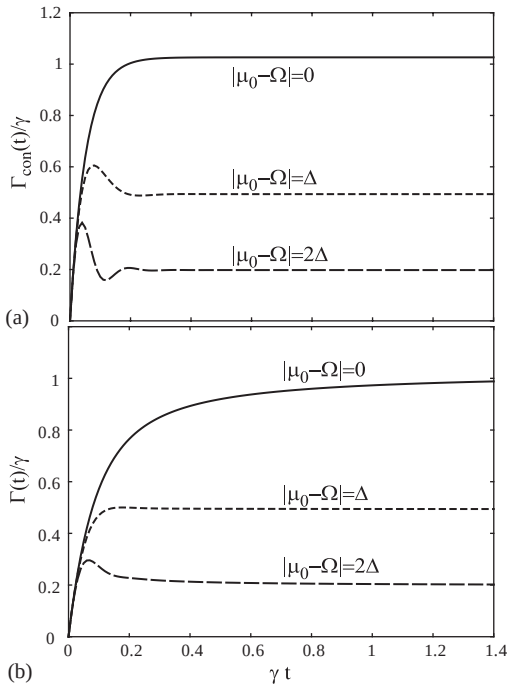


Fig. 7. Temporal evolution of (a) $\Gamma_{\rm con}(t)$ and (b) $\Gamma(t)$. We take $\Delta=20\gamma$ ($t_{\rm j}=0.05\gamma^{-1}$), and $|\mu_0-\Omega|=0$, $\Delta$, $2\Delta$. The corresponding golden-rule decay rates, $\Gamma_{\rm FGR}=2\pi|g_\Omega|^2$, are $\gamma$, $0.5\gamma$, and $0.2\gamma$, respectively.

function of $t$, $\Gamma(t)=\gamma\Delta t$. Sufficiently after the jump time ($t\gg t_{\rm j}$), $\Gamma(t)$ approaches a constant value, $\Gamma(\infty)$, which is given by Eq. (65). As is observed in Fig. 7, $\Gamma(\infty)$ is in good agreement with the golden-rule decay rate, $\Gamma_{\rm FGR}$.

On the other hand, there is a remarkable qualitative difference in the intermediate time region, $t\sim t_{\rm j}$. For the case of $|\mu_0-\Omega|=0$, $\Gamma(t)$ is a monotonously increasing function of $t$ and $\Gamma(t)<\Gamma(\infty)$ for any $t$. Contrarily, for the case of $|\mu_0-\Omega|=2\Delta$, $\Gamma(t)$ is not a monotonic function and there exists a time region in which $\Gamma(t)>\Gamma(\infty)$. This difference is crucial in determining whether repeated measurements result in suppression of decay (QZE) or enhancement of decay (AZE), as will be discussed in Section 3.4.

## 3. Conventional theories of quantum Zeno and anti-Zeno effects

In this section, we summarize the main results of conventional theories of the quantum Zeno and anti-Zeno effects, where it is assumed that instantaneous and ideal measurements to check the decay of the unstable state are repeated frequently.

### *3.1. Ideal measurement on the target system*

In the previous section, we have reviewed the *free* unitary time evolution of an unstable quantum state, where the system is not being measured. When one performs a measurement, on the other hand,

the measurement accompanies considerable backaction on the measured system, according to quantum theory. If the measurement is an ideal one, its influence on the quantum state of the measured system is described as follows. Let us consider a situation in which one measures a physical quantity $Q$ of the system, whose operator $\hat{Q}$ is assumed to have discrete eigenvalues. The projection operator onto the subspace belonging to the eigenvalue $q$ of $\hat{Q}$ is denoted by $\hat{\mathscr{P}}(q)$, and the state vector before the measurement is denoted by $|\psi\rangle$. Then, the probability of obtaining $q$ as a measured value is given by

$$P(q) = \|\hat{\mathscr{P}}(q)|\psi\rangle\|^2 = \langle\psi|\hat{\mathscr{P}}(q)|\psi\rangle \ , \tag{69}$$

and the state vector just after the measurement is given by

$$|\psi_q\rangle = \frac{1}{\sqrt{P(q)}}\hat{\mathscr{P}}(q)|\psi\rangle \ , \tag{70}$$

which is called the *projection postulate* of measurement [1].

Now we apply this prescription to a situation in which an observer makes a measurement on the atom to check whether the atom has decayed or not. In this case, the physical quantity to be measured is the number of excitations in the atom, $\sigma_+\sigma_-$. The eigenvalues of the operator $\sigma_+\sigma_-$ are 1 and 0, and the corresponding projection operators are given by

$$\hat{\mathscr{P}}(1) = |\mathrm{x}\rangle\langle\mathrm{x}| = \sigma_+|0\rangle\langle 0|\sigma_- \ , \tag{71}$$

$$\hat{\mathscr{P}}(0) = \int \mathrm{d}\boldsymbol{k}|\mathrm{g},\boldsymbol{k}\rangle\langle\mathrm{g},\boldsymbol{k}| = \int \mathrm{d}\boldsymbol{k} b_{\boldsymbol{k}}^\dagger|0\rangle\langle 0|b_{\boldsymbol{k}} \ . \tag{72}$$

If the state vector at $t = 0$ is given by $|\mathrm{i}\rangle = |\mathrm{x}\rangle = \sigma_+|0\rangle$, the state vector at time $t$ is given by Eq. (6). The probability of observing the survival of the atom is given, using Eqs. (69) and (71), by

$$P(1) = |f(t)|^2 = s(t) \ , \tag{73}$$

and the state vector just after this observation is given, using Eqs. (70), (71), and (73), by

$$|\psi_1\rangle = \sigma_+|0\rangle = |\mathrm{i}\rangle \ , \tag{74}$$

neglecting an irrelevant phase factor $f(t)/|f(t)|$. Thus, when the survival of the atom is confirmed, the state vector is reset to the initial one (the product of the atomic excited state and the photon vacuum) as a backaction of the measurement.

### *3.2. Decay rate under repeated measurements*

In the preceding subsection, we have summarized the influence of a single ideal measurement on the atomic state. We now investigate, using the projection postulate, how the decay dynamics is affected by repeated measurements to check the decay of the atom, assuming that each measurement is instantaneous and ideal.

Suppose that instantaneous ideal measurements are performed periodically at $t = j\tau_\mathrm{i}$ ($j = 1, 2, \ldots$), where $\tau_\mathrm{i}$ is the intervals between measurements. We hereafter denote the survival probability just after the $n$th measurement by $S(t = n\tau_\mathrm{i})$. This probability is identical to the probability of confirming survival of the atom in all measurements ($j = 1, 2, \ldots, n$), because, once the atom has decayed and emitted a photon, the revival probability is negligibly small in monotonically decaying systems. Noticing that

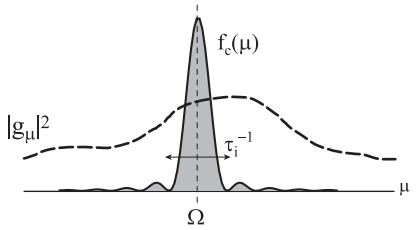


Fig. 8. Calculation of the decay rate $\Gamma(\tau_\mathrm{i})$ under repeated measurement. $\Gamma(\tau_\mathrm{i})$ is given by integrating the form factor $|g_\mu|^2$ with a weight function $f_\mathrm{c}(\mu)$.

(i) if the atom is in the excited state at $t = 0$, the survival probability at $t = \tau_\mathrm{i}$ is given by $s(\tau_\mathrm{i})$, and that (ii) the state is reset to the atomic excited state after every confirmation of survival, we obtain $S(t = n\tau_\mathrm{i})$ simply as

$$S(t = n\tau_\mathrm{i}) = [s(\tau_\mathrm{i})]^n = [s(\tau_\mathrm{i})]^{t/\tau_\mathrm{i}} \ . \tag{75}$$

Therefore, the decay rate $\Gamma$ under such repeated measurements is given, as a function of the measurement intervals $\tau_\mathrm{i}$, by

$$\Gamma(\tau_\mathrm{i}) = -\tau_\mathrm{i}^{-1} \ln s(\tau_\mathrm{i}) \ . \tag{76}$$

This equation clearly demonstrates that the decay rate depends not only on the original unitary dynamics of the system [which determines $s(t)$] but also on the measurement intervals $\tau_\mathrm{i}$.

Throughout this article, our main concern is focused on the case of short $\tau_\mathrm{i}$. As we have observed in Section 2.4, the initial behavior of the survival probability $s(t)$ can be well evaluated by Eq. (42). Using Eq. (42), Eq. (76) is recast into the following form [51]:

$$\Gamma(\tau_\mathrm{i}) = \int \mathrm{d}\mu |g_\mu|^2 \times f_\mathrm{c}(\mu) \ , \tag{77}$$

$$f_\mathrm{c}(\mu) = \tau_\mathrm{i} \ \mathrm{sinc}^2 \left[ \frac{\tau_\mathrm{i}(\mu - \Omega)}{2} \right] \ . \tag{78}$$

Namely, the decay rate under repeated instantaneous ideal measurements is given by integrating the form factor $|g_\mu|^2$ with a weight function $f_\mathrm{c}(\mu)$, as illustrated in Fig. 8. The weight function $f_\mathrm{c}(\mu)$ has the following properties: (i) $f_\mathrm{c}(\mu)$ is a positive function centered at the atomic transition energy $\Omega$ with a spectral width $\sim \tau_\mathrm{i}^{-1}$, and (ii) $f_\mathrm{c}(\mu)$ is normalized as $\int \mathrm{d}\mu f_\mathrm{c}(\mu) = 2\pi$.

As a reference, we first consider a situation where the unstable state is not measured, namely, $\tau_\mathrm{i} \to \infty$. In this limit, the weight function is reduced to a delta function as $f_\mathrm{c}(\mu) \to 2\pi\delta(\mu - \Omega)$, so $\Gamma \to 2\pi|g_\Omega|^2$. This is nothing but the Fermi golden rule for an unobserved system, Eq. (16).

Generally, $\Gamma(\tau_\mathrm{i})$ depends on the measurement intervals $\tau_\mathrm{i}$ through the width of the weight function $f_\mathrm{c}(\mu)$. However, there exists a notable exception: a system whose form factor is a constant function as $|g_\mu|^2 = \gamma/2\pi$. It is known that such a system follows an exact exponential decay law, $s(t) = \mathrm{e}^{-\gamma t}$, as can be seen by taking the $\Delta \to \infty$ limit of the results of Section 2.6. For such a system, the measurement-modified decay rate, Eq. (77), is always reduced to the *free* decay rate $\gamma$, irrespective of $\tau_\mathrm{i}$. Thus, we are led to a well-known conclusion that the decay rate of exactly exponentially decaying systems are not

affected by repeated measurements at all. Note, however, that we have assumed that each measurement is instantaneous and ideal. For general measurements, the above conclusion is *not* necessarily true, as will be shown in Section 5.

### 3.3. Quantum Zeno effect

In the preceding subsection, it is observed that the decay rate $\Gamma$ is generally modified by repeated measurements, and $\Gamma$ is dependent on the measurement intervals $\tau_{\rm i}$. A particularly interesting phenomenon is expected when $\tau_{\rm i}$ is extremely short: for very small $t$, the behavior of $s(t)$ is described by the quadratic decay law, Eq. (11). Combining Eqs. (11) and (76), the decay rate under very frequent measurements is given by

$$\Gamma(\tau_{\rm i}) = \langle(\Delta\hat{H}_S)^2\rangle\tau_{\rm i} \ , \tag{79}$$

which states that the decay rate is proportional to the measurement intervals $\tau_{\rm i}$.[4] Thus, as one measures the system more frequently (i.e., as $\tau_{\rm i}$ is made shorter), the decay of the system is more suppressed. In the limit of infinitely frequent measurements ($\tau_{\rm i} \to 0$), the decay of the system is perfectly inhibited. This phenomenon is called the *quantum Zeno effect* [5] (or several other names [47–49]), which is hereafter abbreviated as the QZE.

Note that the above argument does not invoke any system-dependent features. Thus, the QZE is a universal phenomenon, which is expected in general quantum systems if instantaneous ideal measurements are possible for the unstable states of interest.

### 3.4. Quantum anti-Zeno effect

In the preceding subsection, the QZE is derived by combining the initial quadratic decrease, Eq. (11), and the measurement-modified decay rate, Eq. (76). However, Eq. (11) holds only for extremely small $t$, and hence Eq. (79) is not applicable for longer measurement intervals $\tau_{\rm i}$. In this subsection, we study the case of longer $\tau_{\rm i}$. For simplicity, we focus on an unstable state with the Lorentzian form factor, for which the rigorous form of $s(t)$ is known for any $t$, as discussed in Section 2.6.

Combining Eqs. (56) and (76), we can obtain the decay rate for general values of $\tau_{\rm i}$. Since the decay rate under repeated instantaneous ideal measurements is given by Eq. (76), $\Gamma(\tau_{\rm i})$ has already been plotted in Fig. 7(b), if one regards the horizontal axis as the measurement intervals $\tau_{\rm i}$ (in units of $\gamma^{-1}$). In order to emphasize the effect of measurements, we plot the normalized decay rate $\Gamma(\tau_{\rm i})/\Gamma(\infty)$ in Fig. 9, where $\Gamma(\infty)$ is the free decay rate. The three curves correspond to three different values (0, $\Delta$, and $2\Delta$) of the energy discrepancy between the atomic transition energy $\Omega$ and the central energy of the form factor $\mu_0$. It should be recalled that the jump time is related to the width of the form factor and is roughly evaluated as $t_{\rm j} \sim \Delta^{-1}$. [Since a multiplicative factor of order unity is unimportant, we have defined $t_{\rm j}$ as $t_{\rm j} \equiv \Delta^{-1}$ in Eq. (66).]

The following points are observed in common: (i) When the measurement intervals $\tau_{\rm i}$ is long ($\tau_{\rm i} \gg t_{\rm j}$), the decay rate is almost unaffected by measurement, i.e., $\Gamma(\tau_{\rm i}) \simeq \Gamma(\infty)$. (ii) A large deviation from the

[4] Eq. (79) can also be obtained by Eqs. (77) and (78); When $\tau_{\rm i}$ is very short [$\tau_{\rm i}^{-1} \gg$ (spectral width of $|g_\mu|^2$)], $f_{\rm C}(\mu) \simeq \tau_{\rm i}$ and $\Gamma(\tau_{\rm i}) \simeq \tau_{\rm i} \times \int {\rm d}\mu |g_\mu|^2 = \tau_{\rm i}\langle(\Delta\hat{H}_S)^2\rangle$.

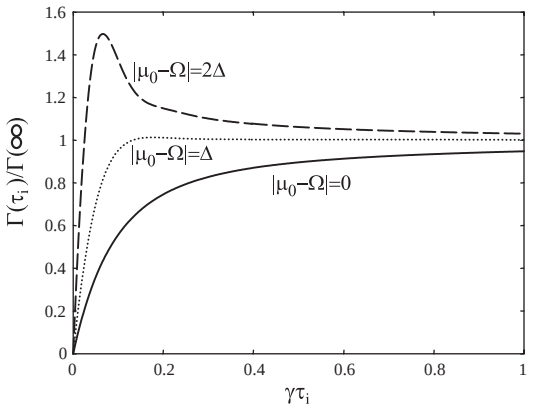


Fig. 9. The decay rate $\Gamma(\tau_i)$, normalized by the free decay rate $\Gamma(\infty)$, under repeated instantaneous ideal measurements with intervals $\tau_i$, for the case of the Lorentzian form factor, Eq. (51). The parameters are chosen as follows: $\Delta = 20\gamma$ (which gives $t_j \sim 0.05\gamma^{-1}$) and $|\Omega - \mu_0| = 0, \Delta, 2\Delta$. In the case of $|\Omega - \mu_0| = 2\Delta$ and $\tau_i \sim t_j$, it is observed that the decay is accelerated from the unobserved case (the anti-Zeno effect). The decay rate is maximized when $\tau_i \simeq 0.066\gamma^{-1}$.

unobserved decay rate is observed when $\tau_i$ is short enough to satisfy

$$\tau_i \lesssim t_j \ . \tag{80}$$

This condition is in accordance with our expectation, because $s(t)$ significantly deviates from the exponential law only for $t \lesssim t_j$. (iii) When $\tau_i$ is extremely short ($\tau_i \ll t_j$), $\Gamma(\tau_i)$ is proportional to $\tau_i$, in accordance with Eq. (79).

Qualitative difference is observed in the intermediate region, $\tau_i \sim t_j$. In the case of $\Omega - \mu_0 = 0$, $\Gamma(\tau_i)$ is always smaller than the free decay rate $\Gamma(\infty)$. The decay is more suppressed as the measurements become more frequent. Thus, in this case, the argument of Section 3.3 can be smoothly extended to a larger $\tau_i$ region without qualitative change. Contrarily, in the case of $\Omega - \mu_0 = 2\Delta$, $\Gamma(\tau_i)$ is not a monotonous function of $\tau_i$, and $\Gamma(\tau_i)$ may become larger than the free decay rate for $\tau_i \sim t_j$. Thus, the decay is *accelerated* by successive measurements. This opposite effect is called the *quantum anti-Zeno effect* [12,13,50–52], which is hereafter abbreviated as the AZE, or the *inverse-Zeno effect* [14,53,54]. The QZE and AZE are sometimes called simply the *Zeno effect*.

### 3.5. QZE–AZE phase diagram

It should be remarked that, whereas the QZE may be observed for any unstable quantum system if $\tau_i$ is sufficiently small, the AZE does not necessarily takes place; a counterexample is the case of $|\Omega - \mu_0| = 0$, where decay is always suppressed for any $\tau_i$ (see Fig. 9). From this respect, quantum unstable states can be classified into the following two types: (a) The QZE is always observed for any value of $\tau_i$, and (b) the QZE is observed for $\tau_i < \tau^*$, whereas the AZE is observed for $\tau_i > \tau^*$, i.e., the QZE–AZE transition takes place at $\tau_i = \tau^*$.

By analyzing Eqs. (56) and (76), a phase diagram discriminating the QZE and AZE is generated in Fig. 10 for the case of the Lorentzian form factor, Eq. (51), as a function of $|\Omega - \mu_0|$ and $\tau_i$. The phase

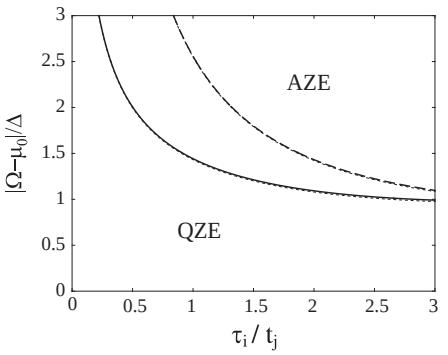


Fig. 10. The phase diagram of the QZE and AZE under repeated instantaneous ideal measurements, for the case of the Lorentzian form factor [Eq. (51)]. The solid line divides the QZE region and the AZE region. The broken line shows the optimum measurement intervals $\tau_i$, at which the decay rate is maximized, for each value of $|\Omega - \mu_0|$. Although $\Delta = 40\gamma$ in this figure, the results are insensitive to the value of $\Delta$. In fact, the thin dotted lines, for which $\Delta = 20\gamma$, almost overlap the corresponding lines for $\Delta = 40\gamma$.

boundary (solid line) is drawn by solving the following equation:

$$\Gamma(\tau^*) = \Gamma(\infty) \ . \tag{81}$$

If Eq. (81) has a solution in $0 < \tau^* < \infty$, the unstable system belongs to type (b). In case of the Lorentzian form factor, Fig. 10 indicates that the system belongs to type (a) if $|\Omega - \mu_0| < \Delta$, and to type (b) if $|\Omega - \mu_0| > \Delta$.

In order to judge whether Eq. (81) has a solution or not, it is useful to remember the fact that, $s(t)$ generally follows the exponential decay law in the later stage of decay as $s(t) \simeq \mathscr{Z} \exp(-\Gamma(\infty)t)$, where $\mathscr{Z}$ is a positive constant. For example, in the case of Lorentzian form factor, $s(t)$ behaves as Eq. (63) in the later stage of decay. Therefore, the asymptotic form of $\Gamma(t)$ is given by $\Gamma(t) = \Gamma(\infty) - \ln \mathscr{Z}/t$. We thus find that, as $t \to \infty$, $\Gamma(t)$ approaches to $\Gamma(\infty)$ from below when $\mathscr{Z} > 1$, and from above when $\mathscr{Z} < 1$. Combining this fact and the fact that $\Gamma(t) \to 0$ as $t \to 0$, one is intuitively led to the following criterion: a system belongs to type (a) when $\mathscr{Z} > 1$, and to type (b) when $\mathscr{Z} < 1$ [14,53].

Now we check the validity of this criterion for the case of Lorentzian form factor, as an example. In this case, $\mathscr{Z}$ is given by Eq. (64), where $\lambda_1$ and $\lambda_2$ are given by Eq. (55). When $\gamma$ is small, $\lambda_1$ and $\lambda_2$ are approximated as

$$\lambda_1 = \Omega + \frac{\gamma\Delta}{2}\frac{1}{\Omega - \mu_0 + \mathrm{i}\Delta} \ , \tag{82}$$

$$\lambda_2 = \mu_0 - \mathrm{i}\Delta - \frac{\gamma\Delta}{2}\frac{1}{\Omega - \mu_0 + \mathrm{i}\Delta} \ . \tag{83}$$

$\mathscr{Z}$ is therefore approximately given by

$$\mathscr{Z} \simeq \left|1 - \frac{\gamma\Delta}{2(\Omega - \mu_0 + \mathrm{i}\Delta)^2}\right|^2 \simeq 1 - \gamma\Delta\frac{(\Omega - \mu_0)^2 - \Delta^2}{|\Omega - \mu_0 + \mathrm{i}\Delta|^4} \ . \tag{84}$$

Thus, the condition of type (a), i.e., $\mathscr{Z} > 1$, is reduced to $|\Omega - \mu_0| < \Delta$. This is in agreement with numerical results (see Fig. 10), which indicates the validity of the criterion.

To summarize this subsection, there are two types of unstable systems. In type (a), only the QZE is induced by repeated measurements. The decay is more suppressed as the measurements become more frequent. In type (b), whereas the QZE is induced when the measurements are very frequent, the opposite effect—the AZE—takes place when the measurements are less frequent. The decay rate depends on $\tau_{\mathrm{i}}$ in a non-monotonous way. The former (latter) type of systems satisfy $\mathscr{Z} > 1$ ($\mathscr{Z} < 1$), where $\mathscr{Z}$ is the prefactor of the exponential decay law in the later stage of decay.

These conclusions have been drawn under the assumptions that each measurement is instantaneous and ideal. However, as we will discuss in Section 4.5.6, such measurements are unrealistic and in some sense unphysical. Therefore, we must explore the Zeno effect in realistic measurement processes. For this purpose, we should apply the quantum measurement theory, which is briefly summarized in the next section.

## 4. Quantum measurement theory

Since quantum systems exhibit probabilistic natures, one has to perform many runs of measurements in an experiment. In ordinary experiments, one resets the system before each run in order to prepare the same quantum state $|\psi\rangle$ for all runs. Or, alternatively, one prepares many equivalent systems in the same state $|\psi\rangle$, and performs the same measurement independently for each system. In either case, one does not need to know the *post-measurement state* $|\psi'\rangle$ (i.e., the state after the measurement) in order to predict or analyze the results of the experiment.

However, one can perform another measurement (of either the same observable or a different observable) on $|\psi'\rangle$ before he resets the system. That is, one can perform two subsequent measurements in each run, one for the pre-measurement state $|\psi\rangle$ and the other for the post-measurement state $|\psi'\rangle$. Or, alternatively, if one prepares many equivalent systems in the same state $|\psi\rangle$, he can perform the two subsequent measurements for each system. In order to predict or analyze the results of such subsequent measurements, one needs to know $|\psi'\rangle$, i.e., the state after the first measurement. To calculate $|\psi'\rangle$, one must use something like the so-called projection postulate (Section 4.1). By many studies in the last several decades, it has been revealed *both theoretically and experimentally* that a naive application of the projection postulate gives wrong results that do *not* agree with experiments on subsequent measurements. To resolve this discrepancy, the quantum measurement theory has been developed [1,15–23], which will be briefly explained in this section. Although Landau and Lifshitz [55] were pessimistic about the possibility of the calculations of the post-measurement states, it has been revealed that the calculations *are* possible in many cases. Furthermore, most importantly, the results of the calculations have been *confirmed by many experiments* (mostly on quantum optics; see, e.g., Refs. [21,32]). This demonstrates the power of the quantum measurement theory.

To explain all the points which may be questioned in studying the Zeno effect, we describe all the basic things of the quantum measurement theory in this section. As a result, this section provides for basic knowledge that are required to understand not only the Zeno effect but also many other topics of quantum measurements. Actually, the full powers of the quantum measurement theory are manifest in studying the other topics, such as those in Refs. [16–20,22,23,56–61], whereas in studying the Zeno effect one can make great simplifications for the reasons explained in Section 4.7 if the underlying logic and

approximations are taken for granted. Hence, if the reader is interested only in the Zeno effect and wish to read this section faster, we suggest the reader to read only Sections 4.1, 4.2, 4.3.2, 4.3.3, 4.6, and 4.7.[5] When a question arises on the underlying logic upon reading later sections, the reader can go back to the rest of this section.

### 4.1. Ideal measurement

Consider measurement of an observable $Q$ of a quantum system S. The observable $Q$ can be either the position, momentum, spin, or any other observable. However, for simplicity, we assume throughout this section that the operator $\hat{Q}$ representing $Q$ has discrete eigenvalues. The case of continuous eigenvalues can be described in a similar manner, which, however, requires some technical cares concerning the mathematical treatment of continuous eigenvalues.

In an early stage of the development of quantum theory, measurement of $Q$ is formulated simply as follows. The probability $P_R^{\text{ideal}}(r)$ of getting a value $r$ of the readout observable $R$ of a measuring apparatus is given by

$$P_R^{\text{ideal}}(r) = \begin{cases} P(q) & \text{for } r = q, \text{ an eigenvalue of} \hat{Q} \ , \\ 0 & \text{otherwise} \ , \end{cases} \tag{85}$$

where

$$P(q) \equiv \left\| \hat{\mathscr{P}}(q)|\psi\rangle \right\|^2 \tag{86}$$

is the probability given by the Born rule. Here, $\hat{\mathscr{P}}(q)$ denotes the projection operator onto the subspace belonging to the eigenvalue $q$ of $\hat{Q}$, and $|\psi\rangle$ is the *pre-measurement state*, i.e., the state vector of S just before the measurement. When an eigenvalue $q$ is obtained as readout $r$ of this measurement, the *post-measurement state* $|\psi_q^{\text{ideal}}\rangle$, i.e., the state vector of S just after the measurement, is given by

$$|\psi_q^{\text{ideal}}\rangle = \frac{1}{\sqrt{P(q)}} \hat{\mathscr{P}}(q)|\psi\rangle \ , \tag{87}$$

where the prefactor $1/\sqrt{P(q)}$ is simply a normalization factor. In other words, the density operator of S just after the measurement is given by

$$\hat{\rho}_q^{\text{ideal}} = |\psi_q^{\text{ideal}}\rangle\langle\psi_q^{\text{ideal}}| = \frac{1}{P(q)} \hat{\mathscr{P}}(q)|\psi\rangle\langle\psi|\hat{\mathscr{P}}(q) \ . \tag{88}$$

This postulate is often called the *projection postulate* after the work of von Neumann [1], although he considered not $\hat{\rho}_q^{\text{ideal}}$ but the following mixture;

$$\hat{\rho}_{\text{vN}}^{\text{ideal}} \equiv \sum_q P(q)\hat{\rho}_q^{\text{ideal}} = \sum_q \hat{\mathscr{P}}(q)|\psi\rangle\langle\psi|\hat{\mathscr{P}}(q) \ , \tag{89}$$

which we call the *von Neumann mixture*. Its physical meaning will be described in Section 4.3.3.

[5] The readers who are quite familiar with the quantum measurement theory can skip directly to Section 4.7, and then to Section 5.

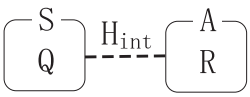


Fig. 11. A schematic diagram of a general measurement of an observable $Q$ of a quantum system S using a measuring apparatus A, whose readout observable is $R$.

A measurement process satisfying Eqs. (85) and (87) is called an *ideal measurement* or a *projective measurement*.[6] The conventional theories of the Zeno effect in Section 3 assumed that measurements are ideal (and instantaneous). However, real measurement processes do not satisfy Eqs. (85) and (87) strictly, and thus are called *general measurements* or *imperfect measurements* or *non-ideal measurements*. For example, a real measuring apparatus has a non-vanishing error, and thus Eqs. (85) and (87) are satisfied only approximately. In order to analyze such general measurements, one has to use the quantum measurement theory.

### *4.2. Time evolution of the system and apparatus*

The starting point of the quantum measurement theory is the key observation that not only the system S to be observed but also the measuring apparatus A should obey the laws of quantum theory. Therefore, one must analyze the time evolution of the joint quantum system S+A using the laws of quantum theory, as schematically shown in Figs. 11 and 12 [1,16–21,56,57,62]. In this case, A is sometimes called a *probe quantum system*.

If S and A can be described by the Hilbert spaces $\mathbf{H}_{\mathrm{S}}$ and $\mathbf{H}_{\mathrm{A}}$, respectively, then the joint system S+A can be described by the product space $\mathbf{H}_{\mathrm{S+A}} \equiv \mathbf{H}_{\mathrm{S}} \otimes \mathbf{H}_{\mathrm{A}}$. If the Hamiltonians of S and A are $\hat{H}_{\mathrm{S}}$ (which operates on $\mathbf{H}_{\mathrm{S}}$) and $\hat{H}_{\mathrm{A}}$ (on $\mathbf{H}_{\mathrm{A}}$), respectively, the Hamiltonian of S+A is given by

$$\hat{H}_{\mathrm{S+A}} = \hat{H}_{\mathrm{S}} \otimes \hat{1} + \hat{1} \otimes \hat{H}_{\mathrm{A}} + \hat{H}_{\mathrm{int}} \ , \tag{90}$$

which is simply written as $\hat{H}_{\mathrm{S+A}} = \hat{H}_{\mathrm{S}} + \hat{H}_{\mathrm{A}} + \hat{H}_{\mathrm{int}}$.

Assuming that any correlations are erased during the preparation processes of the measurement, we can take the pre-measurement state (i.e., the state just before the measurement at $t = 0$) of S+A as a simple product state,

$$|\Psi(0)\rangle = |\psi\rangle|\psi_{\mathrm{A}}\rangle \quad (\in \mathbf{H}_{\mathrm{S+A}}), \tag{91}$$

where $|\psi\rangle$ ($\in \mathbf{H}_{\mathrm{S}}$) and $|\psi_{\mathrm{A}}\rangle$ ($\in \mathbf{H}_{\mathrm{A}}$) denote the pre-measurement states of S and A, respectively. Here, we assume for simplicity that the pre-measurement states are pure states. The generalization to a mixed state is straightforward, and one will then find that the main conclusions and ideas that will be explained in the following are not changed at all.

[6] It is sometimes called a *first-kind measurement*. However, this term is also used for a general measurement in which the post-measurement state is in the subspace that is spanned by the eigenvectors belonging to eigenvalues which are close to the readout $r$. If $[\hat{Q}, \hat{H}_{\mathrm{S}}] = 0$, in particular, a first-kind measurement in this sense is called a *quantum non-demolition measurement* [19,58,59]. A measurement which is not of the first kind is said to be of the second kind. In this article, however, we do not use these terms in order to avoid possible confusions.

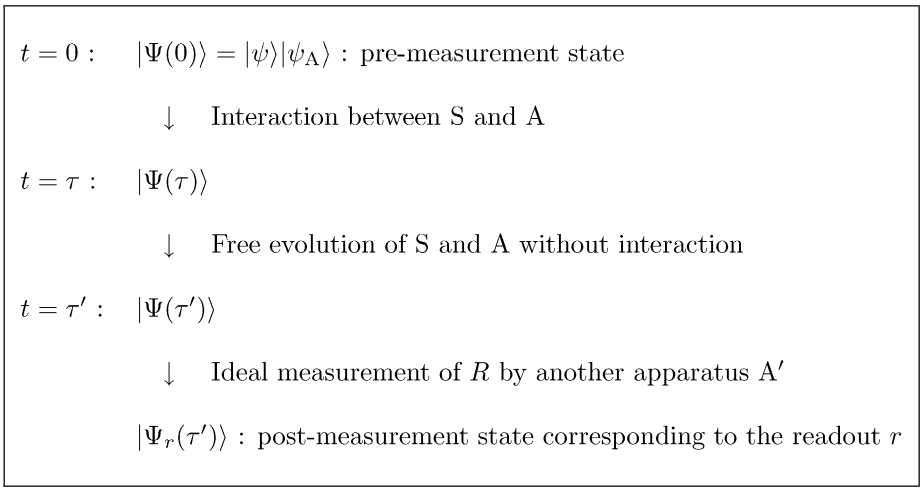


Fig. 12. The time evolution of the joint quantum system which is shown in Fig. 11. The unitary evolution during $0 \leqslant t \leqslant \tau$, by which correlations between the observable $Q$ and the readout observable $R$ is established, is called the *unitary part* of the measurement. See the text for details.

Let $|q, l\rangle$'s ($\in \mathbf{H}_{\rm S}$) be orthonormalized eigenvectors of $\hat{Q}$, the operator representing the observable $Q$ to be measured. Here, $q$ is an eigenvalue of $\hat{Q}$ and $l$ denotes a set of quantum numbers labeling degenerate eigenvectors. Since $|q, l\rangle$'s form a complete set of $\mathbf{H}_{\rm S}$, we can expand the pre-measurement state of S as

$$|\psi\rangle = \sum_{q,l} \psi(q, l)|q, l\rangle \ . \tag{92}$$

The readout is an observable of $A$, because it will be observed by another apparatus or an observer (see Section 4.3 for details). It is denoted by $R$, and the operator (on $\mathbf{H}_{\rm A}$) representing it by $\hat{R}$. Let $|r, m\rangle$'s ($\in \mathbf{H}_{\rm A}$) be orthonormalized eigenvectors of $\hat{R}$, where $r$ is an eigenvalue of $\hat{R}$ and $m$ denotes a set of quantum numbers labeling degenerate eigenvectors. We can expand the pre-measurement state of A as

$$|\psi_{\rm A}\rangle = \sum_{m} \psi_{\rm A}(m)|r_0, m\rangle \ , \tag{93}$$

where $r_0$ is the pre-measurement value of the readout. Note that every operator of S commutes with every operator of A. For example, $[\hat{Q}, \hat{R}] = [\hat{Q}, \hat{H}_{\rm A}] = [\hat{H}_{\rm S}, \hat{R}] = [\hat{H}_{\rm S}, \hat{H}_{\rm A}] = 0$, which will be used in the following calculations.

If S+A can be regarded as an isolated system in the time interval $0 \leqslant t \leqslant \tau$ during which the interaction between S and A takes place, its state vector evolves into

$$|\Psi(\tau)\rangle = {\rm e}^{-{\rm i}\hat{H}_{\rm S+A}\tau}|\psi\rangle|\psi_{\rm A}\rangle \tag{94}$$

$$= \sum_{q,l}\sum\nolimits_{m} \psi(q, l)\psi_{\rm A}(m){\rm e}^{-{\rm i}\hat{H}_{\rm S+A}\tau}|q, l\rangle|r_0, m\rangle \ . \tag{95}$$

Let us express the factor in the last line as the superposition of $|q', l'\rangle|r', m'\rangle$'s as

$$\mathrm{e}^{-\mathrm{i}\hat{H}_{\mathrm{S+A}}\tau}|q, l\rangle|r_0, m\rangle = \sum_{q',l'}\sum_{r',m'} u_{q,l,m}^{q',l',r',m'}|q', l'\rangle|r', m'\rangle \ , \tag{96}$$

where the coefficient $u_{q,l,m}^{q',l',r',m'}$ is a function of $\hat{H}_{\mathrm{S+A}}$, $\tau$ and $r_0$, all of which can be tuned by tuning the experimental setup.[7] Then, Eq. (95) can be expressed as

$$|\Psi(\tau)\rangle = \sum_{q,l}\left[\psi(q, l)\sum_{q',l'}\left(|q', l'\rangle\sum_{m,r',m'}\psi_{\mathrm{A}}(m)u_{q,l,m}^{q',l',r',m'}|r', m'\rangle\right)\right] \ . \tag{97}$$

As we will show shortly, the results for a general measurement reduce to those for an ideal one if $u_{q,l,m}^{q',l',r',m'}$ takes the following form;[8]

$$u_{q,l,m}^{q',l',r',m'} = u_{q,m}^{m'}\delta_{q',q}\delta_{l',l}\delta_{r',q} \ . \tag{99}$$

In this case, Eq. (97) reduces to

$$|\Psi(\tau)\rangle = \sum_{q,l}\left[\psi(q, l)|q, l\rangle\left(\sum_{m,m'}\psi_{\mathrm{A}}(m)u_{q,m}^{m'}|q, m'\rangle\right)\right] \ , \tag{100}$$

which clearly shows that S and A get entangled,[9] by the interaction $\hat{H}_{\mathrm{int}}$ in $\hat{H}_{\mathrm{S+A}}$, in such a way that $Q$ and $R$ are strongly correlated. This is the main part of the measurement process, which we call the *unitary part*, because it is described as a unitary evolution due to the Schrödinger equation. Since $Q$ and $R$ are correlated, one can get information about $Q$ by measuring $R$, as shown below. For general measurements, the correlation between $Q$ and $R$ may be weaker than that in Eq. (100). However, non-vanishing correlation *should* be established in order to get non-vanishing information. Since non-vanishing information should be obtained by any measurement (see Section 4.5.4), $\hat{H}_{\mathrm{int}}$ should be such an interaction that creates non-vanishing correlation between $Q$ and $R$.

For $t > \tau$, for which the interaction is over (or ineffective),[10] the state vector further evolves as

$$|\Psi(t)\rangle = \mathrm{e}^{-\mathrm{i}(\hat{H}_{\mathrm{S}}+\hat{H}_{\mathrm{A}})(t-\tau)}|\Psi(\tau)\rangle \tag{101}$$

until the readout $R$ is measured by another apparatus or an observer A′ at $t = \tau'$ ($\geqslant\tau$). If this measurement of $R$ at $t = \tau'$ can be regarded as an instantaneous ideal measurement of $R$ (*not* of $Q$), then the probability

[7] Note that one can tune not only $\hat{H}_{\mathrm{S+A}}$ and $\tau$ but also $r_0$. The significance of this fact is discussed in Refs. [19,20].

[8] A more general form of Eq. (99) is

$$u_{q,l,m}^{q',l',r',m'} = u_{q,m}^{m'}\delta_{q',q}\delta_{l',l}\delta_{r',f(q)} \ . \tag{98}$$

where $f$ is an invertible function of $q$. By relabeling $r$ appropriately, we can reduce this to Eq. (99).

[9] That is, this state is not generally a simple product of two vectors, one is in $\mathbf{H}_{\mathrm{S}}$ and the other is in $\mathbf{H}_{\mathrm{A}}$.

[10] For example, when the wavefunction of S takes a wavepacket form the interaction becomes ineffective after the wavepacket passes through the apparatus.

$P_R(r)$ of getting a readout $r$ (which is an eigenvalue of $\hat{R}$) is given by

$$P_R(r) = \|\hat{\mathscr{P}}_R(r)|\Psi(\tau')\rangle\|^2 \tag{102}$$

$$= \|\hat{\mathscr{P}}_R(r)\mathrm{e}^{-\mathrm{i}(\hat{H}_\mathrm{S}+\hat{H}_\mathrm{A})(\tau'-\tau)}|\Psi(\tau)\rangle\|^2 \ . \tag{103}$$

Here, $\hat{\mathscr{P}}_R(r)$ denotes the projection operator onto the subspace belonging to the eigenvalue $r$ of $\hat{1}\otimes\hat{R}$;

$$\hat{\mathscr{P}}_R(r) \equiv \hat{1}\otimes\sum_m |r,m\rangle\langle r,m| \ . \tag{104}$$

When an eigenvalue $r$ is thus obtained as the readout, the post-measurement state $|\Psi_r(\tau')\rangle$ of S+A is given by

$$|\Psi_r(\tau')\rangle = \frac{1}{\sqrt{P_R(r)}}\hat{\mathscr{P}}_R(r)|\Psi(\tau')\rangle \tag{105}$$

$$= \frac{1}{\sqrt{P_R(r)}}\hat{\mathscr{P}}_R(r)\mathrm{e}^{-\mathrm{i}(\hat{H}_\mathrm{S}+\hat{H}_\mathrm{A})(\tau'-\tau)}|\Psi(\tau)\rangle \ . \tag{106}$$

If we denote the trace operation over $\mathbf{H}_\mathrm{A}$ by $\mathrm{Tr}_\mathrm{A}$, the post-measurement state of S is represented by the reduced density operator,

$$\hat{\rho}_r(\tau') = \mathrm{Tr}_\mathrm{A}(|\Psi_r(\tau')\rangle\langle\Psi_r(\tau')|) \ , \tag{107}$$

because the expectation value $\langle X\rangle_r$ of any observable $X$ of S is given by

$$\langle X\rangle_r = \langle\Psi_r(\tau')|\hat{X}|\Psi_r(\tau')\rangle = \mathrm{Tr}[\hat{\rho}_r(\tau')\hat{X}] \ . \tag{108}$$

Since the entanglement of S and A is not generally dissolved in $|\Psi_r(\tau')\rangle$, $\rho_r(\tau')$ generally becomes a mixed state.

Eqs. (102) and (107) for a general measurement of $Q$ should be compared with Eqs. (85) and (88) for an ideal measurement. The general equations reduce to the ideal ones if Eq. (99) is satisfied. In fact, we have in this case

$$\hat{\mathscr{P}}_R(r)|\Psi(\tau)\rangle = \begin{cases} \left(\sum_l \psi(q,l)|q,l\rangle\right)\left(\sum_{m,m'}\psi_\mathrm{A}(m)u^{m'}_{q,m}|q,m'\rangle\right) & \text{for } r=q, \text{ an eigenvalue of } \hat{Q}, \\ 0 & \text{otherwise.} \end{cases} \tag{109}$$

Since we can take $\tau'=\tau$ as will be discussed in Section 4.3.1, and noting that $\sum_l \psi(q,l)|q,l\rangle = \mathscr{P}(q)|\psi\rangle$, we find that Eqs. (102) and (107) reduce in this case to Eqs. (85) and (88), respectively. Therefore, in order to realize an ideal measurement, one must construct an experimental setup by which Eq. (99) is satisfied. Implications of this condition will be discussed in Section 4.5.6.

### *4.3. von Neumann chain*

In the above argument, the observable $Q$ of the quantum system S is measured by the apparatus A, and the readout observable $R$ of A is measured by another apparatus or an observer A′ [1]. Such a sequence, as shown in Fig. 13, is sometimes called the *von Neumann chain*. We here describe its basic notions.

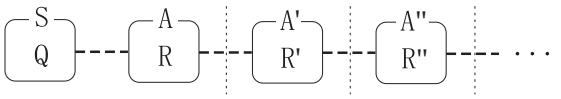


Fig. 13. The *von Neumann chain*. To measure an observable $Q$ of a quantum system S, an apparatus A is coupled to S and the information on $Q$ is transferred to an observable $R$ of A. To measure $R$, another apparatus A$'$ is coupled to A and the information on $R$ is transferred to an observable $R'$ of A$'$, and so on. The vertical dotted lines indicate possible locations of the *Heisenberg cut* (see Section 4.3.2), inside which the laws of quantum theory are applied whereas the outside is just taken as a device for measuring $R$ (or $R'$, or $R''$, ..., depending on the location of the Heisenberg cut).

*4.3.1. When measurement is completed?*

The measurement process described above is completed at $t = \tau'$. We now show, however, that one can also say that the measurement is completed at $t = \tau$.

To show this, let us calculate the state after $\tau'$. For $t > \tau'$, S and A evolve freely, hence the state vector of S+A at $t$ ($> \tau'$) is given by

$$|\Psi_r(t)\rangle = \mathrm{e}^{-\mathrm{i}(\hat{H}_\mathrm{S}+\hat{H}_\mathrm{A})(t-\tau')}|\Psi_r(\tau')\rangle \tag{110}$$

$$= \frac{1}{\sqrt{P_R(r)}}\,\mathrm{e}^{-\mathrm{i}(\hat{H}_\mathrm{S}+\hat{H}_\mathrm{A})(t-\tau')}\hat{\mathscr{P}}_R(r)\mathrm{e}^{-\mathrm{i}(\hat{H}_\mathrm{S}+\hat{H}_\mathrm{A})(\tau'-\tau)}|\Psi(\tau)\rangle\ . \tag{111}$$

For the apparatus A to work well, the readout $R$ should be stable for $t \geqslant \tau$. That is,

$$P_R(r) = \text{independent of } \tau'\ , \tag{112}$$

to a good approximation. This is satisfied if

$$[\hat{R}, \hat{H}_\mathrm{A}] = 0\ , \tag{113}$$

because this implies $[\hat{\mathscr{P}}_R(r), \hat{H}_\mathrm{A}] = 0$, and Eq. (103) then reduces to

$$P_R(r) = \|\mathrm{e}^{-\mathrm{i}(\hat{H}_\mathrm{S}+\hat{H}_\mathrm{A})(\tau'-\tau)}\hat{\mathscr{P}}_R(r)|\Psi(\tau)\rangle\|^2 = \|\hat{\mathscr{P}}_R(r)|\Psi(\tau)\rangle\|^2 = \text{independent of } \tau'\ . \tag{114}$$

Although Eq. (113) is not a necessary condition but a sufficient condition for Eq. (112),[11] we henceforth assume Eq. (113) for simplicity.[12] Then, Eq. (111) reduces to

$$|\Psi_r(t)\rangle = \frac{1}{\sqrt{P_R(r)}}\mathrm{e}^{-\mathrm{i}(\hat{H}_\mathrm{S}+\hat{H}_\mathrm{A})(t-\tau)}\hat{\mathscr{P}}_R(r)|\Psi(\tau)\rangle\ , \tag{116}$$

which is independent of $\tau'$. Therefore,

$$\hat{\rho}_r(t) = \mathrm{Tr}_\mathrm{A}(|\Psi_r(t)\rangle\langle\Psi_r(t)|) \tag{117}$$

---

[11] Condition (113) implies Eq. (114) for *every* vector $|\Psi(\tau)\rangle$ in $\mathbf{H}_{\mathrm{S+A}}$. However, it is sufficient for Eq. (112) that Eq. (114) is satisfied only for $|\Psi(\tau)\rangle$ given by Eq. (95).

[12] It is worth mentioning that Eq. (113) is a natural assumption if $R$ and $H_\mathrm{A}$ are macroscopic variables, because then they must be additive observables [63,64] and the volume $V_\mathrm{A}$ of A is quite large, and thus Eq. (113) is *always* satisfied to a good approximation in the sense that [64]

$$\left[\frac{\hat{R}}{V_\mathrm{A}}, \frac{\hat{H}_\mathrm{A}}{V_\mathrm{A}}\right] = O\left(\frac{1}{V_\mathrm{A}}\right)\ . \tag{115}$$

is also independent of $\tau'$. We thus find that the state of S+A, as well as the state of S, for $t > \tau'$ (i.e., after the measurement is completed) are independent of $\tau'$, the instance at which $R$ is read by another apparatus or an observer.

Because of this reasonable property, one can take $\tau'$ as an arbitrary time after $\tau$. In particular, we can take $\tau' = \tau$, from which *we can say that the measurement is completed at* $t = \tau$.

*4.3.2. Where is the Heisenberg cut?*

In the above argument, apparatus A has been treated as a quantum system that evolves according to the Schrödinger equation. On the other hand, another apparatus or an observer A′ which measures R of A has been treated as a device that performs the measurement of R. This means that we have assumed in the von Neumann chain a *hypothetical* boundary between A and A′, inside which the laws of quantum theory are applied, whereas the outside is just taken as such a device. Such a boundary is called the *Heisenberg cut*. Since this boundary is hypothetical and artificial, it must be able to be moved to a large extent freely, without causing any observable effects, for quantum theory to be consistent. von Neumann called this property the *psychophysical parallelism* [1]. He showed that quantum theory indeed has this property in the following sense.[13]

Suppose that the Heisenberg cut is moved to the boundary between A′ and A″ of Fig. 13, and that both the measurement of $R$ by A′ (at $t = \tau' > \tau$) and that of $R'$ by A″ (at $t = \tau'' > \tau'$) are ideal (and instantaneous, for simplicity). By calculating the time evolution of the enlarged joint system S+A+A′ in a manner similar to the calculations of Sections 4.2 and 4.3.1, one can calculate the probability distribution $P'_{R'}(r')$ of the readout $r'$ as well as the reduced density operator $\hat{\rho}'_{r'}(t)$ of S for $t > \tau''$. From such calculations, one can show that $P'_{R'}(r')$ and $\hat{\rho}'_{r'}(t)$ coincide with $P_R(r)$ and $\hat{\rho}_r(t)$, which have been obtained above as Eqs. (102) and (107), respectively. That is,

$$P'_{R'}(\cdot) = P_R(\cdot) \ , \tag{118}$$

$$\hat{\rho}'_{r'}(t) = \hat{\rho}_r(t) \ \text{ for every pair of } r' \text{and } r \text{ such that } r' = r \ . \tag{119}$$

This shows that the Heisenberg cut can be located either between A and A′ or between A′ and A″, without causing any observable effects. In contrast, the Heisenberg cut *cannot* be moved to the boundary between S and A for general measurements, because it would then give Eqs. (85) and (88), which do not agree with the correct equations (102) and (107).

Therefore, we conclude that *the Heisenberg cut can be located at any place at which the interaction process can be regarded as the unitary part* (in the terminology of Section 4.2) *of an ideal measurement*.

*4.3.3. Average over all possible values of the readout*

Suppose that the Heisenberg cut is located between A and A′. The post-measurement state corresponding to each readout $r$ is given by

$$\hat{\rho}_r(\tau) = \mathrm{Tr}_{\mathrm{A}}(|\Psi_r(\tau)\rangle\langle\Psi_r(\tau)|) \ , \tag{120}$$

where we have taken $\tau' = \tau$ as discussed in Section 4.3.1. The expectation value $\langle X\rangle_r$ of an observable $X$ of S is calculated, for each readout $r$, as

$$\langle X\rangle_r = \mathrm{Tr}[\hat{\rho}_r(\tau)\hat{X}] \ . \tag{121}$$

[13] Although he showed this for the von Neumann mixture $\hat{\rho}_{\mathrm{vN}}$, we here show it more generally for $\hat{\rho}_r$.

In some cases, the mixture of $\hat{\rho}_r(\tau)$'s over all possible values of $r$,

$$\hat{\rho}_{\rm vN}(\tau) \equiv \sum_r P_R(r)\hat{\rho}_r(\tau) \ , \tag{122}$$

is also used as the post-measurement state. As in the case of an ideal measurement (Section 4.1), we call it the *von Neumann mixture*. This density operator is useful when one discusses *average* properties of the post-measurement states. That is, when one is interested in the average $\langle X\rangle_{\rm vN}$ of $\langle X\rangle_r$ over all possible values of $r$, it can be calculated as

$$\langle X\rangle_{\rm vN} = \sum_r P_R(r)\langle X\rangle_r = \sum_r P_R(r){\rm Tr}[\hat{\rho}_r(\tau)\hat{X}] = {\rm Tr}[\hat{\rho}_{\rm vN}(\tau)\hat{X}] \ . \tag{123}$$

In this case, $\hat{\rho}_{\rm vN}(\tau)$ is equivalent to the set of $\{P_R(r), \hat{\rho}_r(\tau)\}$. Notice, however, that $\hat{\rho}_{\rm vN}(\tau)$ has less information in more general cases, such as the case where one is interested in properties of the post-measurement state corresponding to *each* value of $r$. In fact, the decomposition of $\hat{\rho}_{\rm vN}(\tau)$ into the form of the right-hand side of Eq. (122) is not unique, and hence one *cannot* get the set of $\{P_R(r), \hat{\rho}_r(\tau)\}$ uniquely from $\hat{\rho}_{\rm vN}(\tau)$.

Eq. (123) can be simplified if we note that $[\hat{X}, \hat{\mathscr{P}}_R(r)] = 0$ for all $r$ (because $X$ is an observable of S whereas $R$ is an observables of A). Using this and $\hat{\mathscr{P}}_R(r)\hat{\mathscr{P}}_R(r) = \hat{\mathscr{P}}_R(r)$ and $\sum_r \hat{\mathscr{P}}_R(r) = \hat{1}$, we can rewrite Eq. (123) as

$$\langle X\rangle_{\rm vN} = \sum_r \langle\Psi(\tau)|\hat{\mathscr{P}}_R(r)\hat{X}\hat{\mathscr{P}}_R(r)|\Psi(\tau)\rangle = \sum_r \langle\Psi(\tau)|\hat{\mathscr{P}}_R(r)\hat{X}|\Psi(\tau)\rangle = \langle\Psi(\tau)|\hat{X}|\Psi(\tau)\rangle \ . \tag{124}$$

This shows that one can calculate $\langle X\rangle_{\rm vN}$ from $|\Psi(\tau)\rangle$, which is the final state of the unitary part (in the terminology of Section 4.2). Therefore, *when one is interested only in* $\langle X\rangle_{\rm vN}$, *it is sufficient to calculate the unitary part of the measurement process*, and one can forget about the ideal measurement of $R$ by A′, for which we have used the projection postulate. Note, however, that this is not generally the case for repeated measurements, as will be discussed in Section 4.6.3.

### *4.4. Prescription for analyzing general measurements*

From discussions in Sections 4.2 and 4.3, we can deduce the prescription for analyzing general measurements as follows:

1. Write down the von Neumann chain S, $\rm A_1$, $\rm A_2$, ... .
2. Find a place at which the interaction process can be regarded as the unitary part of an ideal measurement. Locate the Heisenberg cut there. Although two or more such places may be found, you can choose any of them. However, to simplify calculations, it is better to choose the one that is closest to S.
3. If the Heisenberg cut thus located lies between $\rm A_k$ and $\rm A_{k+1}$, apply the laws of quantum theory to the joint system S+$\rm A_1 + \cdots A_k$, taking $\rm A_{k+1}$ as a device that performs an ideal measurement of the readout observable $\rm R_k$ of $\rm A_k$. If the interaction in the joint system is effective during the time interval $0 \leqslant t \leqslant \tau$, one can say that the measurement is performed during this interval.
4. Evaluate the probability distribution of the readout $r_k$ of $\rm R_k$ and the post-measurement state, in the same way as we have done in Section 4.2.

We can regard the subsystem $A_1 + \cdots A_k$ of the joint system $S+A_1 + \cdots A_k$ as system A of Section 4.2, and $A_{k+1}$ as A′. We can therefore apply the formulation of Section 4.2 to general cases. We will thus use the equations and notations of Section 4.2 in the following discussions.

### 4.5. Properties of general measurements

#### 4.5.1. Response time

In an early stage of the development of quantum theory, it was sometimes argued that the measurement should be made instantaneously. Such a measurement is called an *instantaneous measurement*. However, as we will discuss in Section 4.5.6, any physical measurement takes a finite time. This finite time $\tau$ has been defined in Section 4.2 as the time after which the interaction between S and A becomes ineffective. Therefore, if the Hamiltonian $\hat{H}_{S+A}$ and the pre-measurement state $|\Psi(0)\rangle$ are known, one can evaluate $\tau$ by solving the Schrödinger equation. This $\tau$ is usually called the *response time* of the apparatus.[14]

To be more precise, $\tau$ should be called the *lower limit of the response time*, because *practical* response times of real experiments usually become longer for many practical reasons. In the model of Section 5, for example, $\tau$ (which will be denoted by $\tau_r$ there) is the time required for generating an elementary excitation in the detector. Such a microscopic excitation should be magnified to obtain a macroscopic signal. Due to possible delays in the magnification and the signal transmission processes, the practical response time will become longer in real experiments.

However, in discussing fundamental physics, the limiting value is more significant than practical values,[15] which depend strongly on detailed experimental conditions. For this reason, we simply call $\tau$ the *response time* in this article. For the same reason, we shall drop in the following subsections the words 'lower limit of' or 'upper limit of' from the terms such as the *lower limit of the measurement error*, the *upper limit of the range of measurement*, the *upper limit of the amount of information obtained by measurement*, and the *lower limit of the backaction of measurement*.

It is worth stressing that if one makes $\tau$ shorter without increasing the strength of $\hat{H}_{int}$ then the measurement error would be increased. Therefore, there is a tradeoff between (the reduction of) the response time and (that of) the measurement error. This and related tradeoffs, as well as their deep implications, were discussed in Ref. [20].

#### 4.5.2. Measurement error

For general measurements, the probability distribution $P_R(r)$ of the readout of measuring apparatus is different from that for an ideal measurement, $P_R^{ideal}(r)$. This means that a general measurement has a non-vanishing measurement error.

For example, consider a special case where $|\psi\rangle$ is an eigenstate of $\hat{Q}$;

$$|\psi\rangle = \sum_l \varphi_q(l)|q, l\rangle \equiv |\varphi_q\rangle \ , \tag{125}$$

[14] See Section 4.6.3 for the response time of continuous measurements.

[15] For example, suppose that the measurement of the readout $R$ by A′ is performed not at $t = \tau$ but at a later time $t = \tau' > \tau$. Then the total response time of the experiment becomes longer. However, we have shown in Section 4.3.1 that the value of $\tau'$ is irrelevant.

where $\varphi_q(l)$'s are arbitrary coefficients satisfying $\sum_l |\varphi_q(l)|^2 = 1$. In this case, $P_R^{\rm ideal}(r) = \delta_{r,q}$ from Eqs. (85) and (86), whereas $P_R(r)$ (for $\tau' = \tau$) is evaluated from Eqs. (95), (96) and (102) as

$$\begin{aligned} P_R(r) &= \|\hat{\mathscr{P}}_R(r) \mathrm{e}^{-\mathrm{i}\hat{H}_{\mathrm{S+A}}\tau} |\varphi_q\rangle|\psi_{\mathrm{A}}\rangle\|^2 \\ &= \left\| \sum_l \varphi_q(l) \sum_m \psi_{\mathrm{A}}(m) \sum_{q',l',m'} u_{q,l,m}(q',l',r,m') |q',l'\rangle|r,m'\rangle \right\|^2 . \end{aligned} \tag{126}$$

It is then clear that $P_R(r) \neq P_R^{\rm ideal}(r)$ in general, except when condition (99) is satisfied.

Since the predictions of quantum theory are of probabilistic nature, the definition of the measurement error is not so trivial, as will be discussed shortly. In principle, however, the measurement error should be quantified by an appropriate measure of the difference between $P_R(r)$ and $P_R^{\rm ideal}(r)$. For example, it may be quantified by the *Kullback–Leider distance* or *relative entropy* [65];

$$D(P_R^{\rm ideal} \| P_R) \equiv \sum_r P_R^{\rm ideal}(r) \log \frac{P_R^{\rm ideal}(r)}{P_R(r)} . \tag{127}$$

One can also use $D(P_R \| P_R^{\rm ideal})$, which is not equal to $D(P_R^{\rm ideal} \| P_R)$ in general. Or, one can use other measures which are used in probability theory and/or information theory [65].

However, it is customary, and sometimes convenient, to quantify the measurement error in a different way using a few parameters. One of such parameters is the difference between the expectation values of the two probability distributions,

$$\begin{aligned} \delta r_{\rm bias} &\equiv \langle R \rangle - \langle R \rangle^{\rm ideal} \\ &\equiv \sum_r r P_R(r) - \sum_r r P_R^{\rm ideal}(r) \\ &= \langle \Psi(\tau) | \hat{R} | \Psi(\tau) \rangle - \langle \psi | \hat{Q} | \psi \rangle . \end{aligned} \tag{128}$$

When $\delta r_{\rm bias} = 0$, the measurement is said to be *unbiased*. In certain cases, one can easily calibrate (i.e., relabel) $r$ in such a way that the unbiased condition is satisfied.

Another parameter used to quantify the measurement error is related to the standard deviation. When the pre-measurement state is an eigenstate of $\hat{Q}$, $|\varphi_q\rangle$, the readout $r$ of an ideal measurement always agrees with $q$, showing no fluctuation. Hence, its standard deviation

$$\delta r_{\rm sd}^{\rm ideal} \equiv [\langle (\Delta R)^2 \rangle^{\rm ideal}]^{1/2} \equiv \left[ \sum_r (r - \langle R \rangle^{\rm ideal})^2 P_R^{\rm ideal}(r) \right]^{1/2} \tag{129}$$

vanishes. On the other hand, for the same state $|\varphi_q\rangle$, the standard deviation of the readout of a general measurement

$$\delta r_{\rm sd} \equiv [\langle (\Delta R)^2 \rangle]^{1/2} \equiv \left[ \sum_r (r - \langle R \rangle)^2 P_R(r) \right]^{1/2} \tag{130}$$

is finite. Therefore, a set of $\delta r_{\rm bias}$ and $\delta r_{\rm sd}$ may be used to quantify the measurement error when the pre-measurement state is an eigenstate of $\hat{Q}$. However, for a general pre-measurement state $|\psi\rangle$, the

readout fluctuates even for an ideal measurement, i.e., $\delta r_{\rm sd}^{\rm ideal} \geqslant 0$. As a result, there exist various ways of quantifying the measurement error by (something like) the standard deviation. For example, many works on quantum non-demolition measurement [17,58,59] quantified it by a set of $\delta r_{\rm bias}$ and the increase of the variance [19,20,56,57,62],

$$(\delta r_{\rm sd})^2 - (\delta r_{\rm sd}^{\rm ideal})^2 \ . \tag{131}$$

Although this quantification is convenient for many applications, one of its disadvantages is that its vanishment (along with $\delta r_{\rm bias} = 0$) does not guarantee $P_R(r) = P_R^{\rm ideal}(r)$. Another important work [23] quantified the measurement error by

$$\langle \Psi_{\rm H}|(\hat{R}_{\rm H}(\tau) - \hat{Q}_{\rm H}(0))^2|\Psi_{\rm H}\rangle \ , \tag{132}$$

where $\hat{R}_{\rm H}$, $\hat{Q}_{\rm H}$, $|\Psi_{\rm H}\rangle$ are $\hat{R}$, $\hat{Q}$, $|\Psi\rangle$ in the Heisenberg picture, respectively, i.e., $|\Psi_{\rm H}\rangle = |\Psi(0)\rangle$ and so on. Although this quantity has good mathematical properties, its physical meaning is not clear enough. For example, suppose that we are given two pieces of apparatus A and $\mathrm{A}^{\rm ideal}$ which perform general and ideal measurements, respectively. By performing two experiments, one using A and the other using $\mathrm{A}^{\rm ideal}$, we can measure all of $\delta r_{\rm bias}$, $\delta r_{\rm sd}$, $\delta r_{\rm sd}^{\rm ideal}$ and $D(P_R^{\rm ideal} \| P_R)$, for any states. However, it is impossible to measure the quantity of Eq. (132) using A and $\mathrm{A}^{\rm ideal}$ for general states.

In the following, we do not specify the detailed quantification of the measurement error $\delta q_{\rm err}$ except when it is needed.[16] However, we simply say that $\delta q_{\rm err} = 0$ when $P_R(r) = P_R^{\rm ideal}(r)$.

### *4.5.3. Range of measurement*

Let us denote the eigenvalue spectrum of $\hat{Q}$ by $\mathcal{Q}$, and the number of eigenvalues by $|\mathcal{Q}|$. For example, when $\hat{Q}$ is the $z$ component of the spin of a spin-$S$ system, $\mathcal{Q} = \{-S\hbar, \ldots, (S-1)\hbar, S\hbar\}$ and $|\mathcal{Q}| = 2S+1$.

Consider the case where the pre-measurement state is an eigenstate $|\varphi_q\rangle$ of $\hat{Q}$. Then, $\delta q_{\rm err}$ can be taken as a set of $\delta r_{\rm bias}$ and $\delta r_{\rm sd}$. Note that both $\delta r_{\rm bias}$ and $\delta r_{\rm sd}$ are generally functions of $q$, i.e., $\delta q_{\rm err}$ varies in $\mathcal{Q}$. Let $\delta q_{\rm err}^*$ be the upper limit of the measurement error allowable for the purpose of the experiment. For example, if $Q$ is a component of a spin and if one wants to distinguish different spin states, then $\delta q_{\rm err}^*$ should be less than $\hbar/2$, say $\delta q_{\rm err}^* = \hbar/4$. In this case, $\delta q_{\rm err}^*$ is of the same order of magnitude as the minimum spacing $\Delta q_{\rm min}$ between the eigenvalues of $\hat{Q}$. On the other hand, $\delta q_{\rm err}^* \gg \Delta q_{\rm min}$ in many optical experiments on condensed-matter physics using photodetectors, in which $Q$ is the photon number and thus $\Delta q_{\rm min} = 1$.

If $\delta q_{\rm err} \leqslant \delta q_{\rm err}^*$ in a region $\mathcal{Q}_{\rm range}$ in $\mathcal{Q}$, we say that the *range* of the measurement (or of the measuring apparatus) is $\mathcal{Q}_{\rm range}$ [19,20]. For an ideal measurement, $\delta q_{\rm err} = 0$ everywhere in $\mathcal{Q}$, and hence $\mathcal{Q}_{\rm range} = \mathcal{Q}$. In this case, we say that the range of the measurement covers the whole spectrum of $\hat{Q}$. This is not necessarily the case for general measurements. For example, a photon counter cannot count the photon number correctly if the number is too large.

Although the importance of the range of the measurement has not been stressed in many theoretical works, it often plays crucial roles as stressed in Refs. [19,20], and as will be explained in Sections 4.5.4, 5.4 and 5.6.

---

[16] If the reader feels uneasy about this, you can assume for example that $\delta q_{\rm err}$ of an apparatus is defined only for eigenstates of $\hat{Q}$, and that $\delta q_{\rm err}$ is a set of $\delta r_{\rm bias}$ and $\delta r_{\rm sd}$.

*4.5.4. Information obtained by measurement*

We have seen that for general measurements the measurement error $\delta q_{\rm err}$ may be non-zero and the range $\mathcal{Q}_{\rm range}$ of the measurement may be narrower than the spectrum $\mathcal{Q}$ of the observable $\hat{Q}$ to be measured. This implies that the amount $I$ of information that is obtained by the measurement is smaller for a general measurement than for an ideal measurement [19,20,60].

To see this, consider again the case where the pre-measurement state is an eigenstate $|\varphi_q\rangle$ of $\hat{Q}$, for which $\delta q_{\rm err}$ is specified by $\delta r_{\rm bias}$ and $\delta r_{\rm sd}$. We assume that $\delta r_{\rm bias}=0$ for simplicity, so that $\delta q_{\rm err}=\delta r_{\rm sd}$. Let $J$ be the number of different eigenstates that can be distinguished from each other by this measurement. As will be illustrated shortly, $J$ depends on $\delta q_{\rm err}$ and $\mathcal{Q}_{\rm range}$. We may define $I$ by

$$I \equiv \log_2 J. \tag{133}$$

Although more elaborate definition of $I$ would be possible, this simple definition will suffice the present discussion.

For an ideal measurement, $\delta q_{\rm err}=0$ and $J=|\mathcal{Q}|$. Therefore, $I$ takes the maximum value,

$$I^{\rm ideal} = \log_2 |\mathcal{Q}| \ . \tag{134}$$

For a general measurement, however, $I \leqslant I^{\rm ideal}$ in general. For example, when $\delta q_{\rm err}$ is smaller than the minimum spacing $\Delta q_{\rm min}$ between the eigenvalues of $\hat{Q}$, we have $J \simeq |\mathcal{Q}_{\rm range}|$, hence

$$I \simeq \log_2 |\mathcal{Q}_{\rm range}| \leqslant I^{\rm ideal} \ . \tag{135}$$

When $\delta q_{\rm err} \gtrsim \Delta q_{\rm min}$, on the other hand, one cannot distinguish between $|\varphi_q\rangle$ and $|\varphi_{q'}\rangle$ with certainty if $|q-q'|<\delta q_{\rm err}$. Therefore, $J<|\mathcal{Q}_{\rm range}|$ and $I$ becomes even smaller.

It should be stressed that *an interaction process between S and A can be called a measurement process only when I is large enough* (at least $I \gtrsim 1$),[17] because measurement of $Q$ is a process by which an observer gets information about $Q$. For example, as the temperature of A is increased $I$ is generally decreased because of the thermal noise, until $I \simeq 0$ at a high temperature.[18] In such a case, the interaction process between S and A is not a measurement process because an observer cannot get any information about $Q$. Hence, it should be called a *non-informative disturbance* of S by A. Another, rather trivial, example of non-informative disturbances is the case where $\hat{H}_{\rm int}$ is such an interaction that does not generate the correlation between $Q$ and $R$. It is obvious that such an interaction is possible.

The distinction between measurement and a non-informative disturbance is crucial when discussing many problems about measurement, such as the quantum non-demolition measurement [19,20] and the reversible measurement [60]. For example, the state before the interaction with A can be physically recovered only for a non-informative disturbance [60]. In discussions of the Zeno effect, however, the distinction was sometimes disregarded in the literature. That is, there are two ways of defining the Zeno effect: one is as an effect of measurements, which may be called the Zeno effect *in the narrow sense*, while the other, which may be called the Zeno effect *in the broad sense*, is as an effect of any kinds of

[17] This is common to both quantum and classical physics.

[18] This may be seen simply as follows: Since $R$ can change through the interaction with S, the change of $R$ is not forbidden by a boundary condition which could be imposed on A. Then, according to the fluctuation–dissipation theorem [67], $R$ fluctuates at a finite temperature $T$, and the magnitude of the fluctuation is proportional to $T$ (apart from possible $T$ dependence of the response function). Therefore, with increasing $T$, $\delta r_{\rm sd}$ increases, and thus $\delta q_{\rm err}$ increases, and consequently $I$ decreases, approaching zero at the high-temperature limit.

disturbances including non-informative disturbances. In the latter sense, it was concluded for example that the Zeno effect would become stronger as the temperature of A is increased [66]. Furthermore, the well-known shortening of lifetimes of quasi-particles with increasing the temperature of solids could be called the AZE. However, these are *not* the Zeno effect in the narrow sense because one cannot get information from a high-temperature apparatus. It should be noticed that universal conclusions, which are independent of details of models, can be drawn only for the Zeno effect in the narrow sense (see Section 4.7).

*4.5.5. Backaction of measurement*

If the measurement were not made (i.e., if $\hat{H}_{\rm int} = 0$), the state of S at $t = \tau$ would be given by

$$\hat{\rho}^{\rm free} = {\rm e}^{-{\rm i}\hat{H}_{\rm S}\tau}|\psi\rangle\langle\psi|{\rm e}^{{\rm i}\hat{H}_{\rm S}\tau} \ . \tag{136}$$

When defining the backaction, however, $\tau$ in this expression is often taken 0 in order to exclude the effect of the trivial change induced by $\hat{H}_{\rm S}$. We will not specify which is used for $\hat{\rho}^{\rm free}$, except when the specification is needed.

If the measurement has been made, the post-measurement state corresponding to each readout $r$ is given by Eq. (120). When quantifying the backaction, however, it is customary to take the von Neumann mixture $\hat{\rho}_{\rm vN}(\tau)$, Eq. (122), as the post-measurement state. We call the difference between $\hat{\rho}_{\rm vN}(\tau)$ (or $\hat{\rho}_r(\tau)$) and $\hat{\rho}^{\rm free}$ the *backaction* of the measurement. Its magnitude should be quantified by a measure of the difference between the two density operators. For example, it may be quantified by the *quantum relative entropy* [68,69];

$$D(\hat{\rho}^{\rm free}\|\hat{\rho}_{\rm vN}(\tau)) \equiv {\rm Tr}[\hat{\rho}^{\rm free}(\log_2\hat{\rho}^{\rm free} - \log_2\hat{\rho}_{\rm vN}(\tau))] \ . \tag{137}$$

One can also use $D(\hat{\rho}_{\rm vN}(\tau)\|\hat{\rho}^{\rm free})$, which is not equal to $D(\hat{\rho}^{\rm free}\|\hat{\rho}_{\rm vN}(\tau))$ in general. Or, one can use other measures which are used in quantum information theory [68,69].

However, it is customary, and sometimes convenient, to quantify the backaction in the following way. If an ideal measurement of an observable $X$ of S is performed for the post-measurement state $\hat{\rho}_{\rm vN}(\tau)$, its probability distribution will be

$${\rm Tr}[\hat{\rho}_{\rm vN}(\tau)\hat{\mathscr{P}}_X(x)] \equiv P_X^{\rm vN}(x) \ , \tag{138}$$

where $\hat{\mathscr{P}}_X(x)$ denotes the projection operator onto the subspace belonging to an eigenvalue $x$ of $\hat{X}$. For $\hat{\rho}^{\rm free}$, on the other hand, the probability distribution would be

$${\rm Tr}[\hat{\rho}^{\rm free}\hat{\mathscr{P}}_X(x)] \equiv P_X^{\rm free}(x) \ . \tag{139}$$

The backaction is sometimes quantified by the difference between $P_X^{\rm vN}(x)$ and $P_X^{\rm free}(x)$ of properly chosen observables, such as $Q$ and/or its canonical conjugate $P$.[19] In particular, the difference between $P_Q^{\rm vN}(q)$ and $P_Q^{\rm free}(q)$ is called the *backaction on the measured observable*, whereas the difference between $P_P^{\rm vN}(p)$ and $P_P^{\rm free}(p)$ may be called the *backaction on the conjugate observable* [17,58,59].

The difference between $P_X^{\rm vN}(x)$ and $P_X^{\rm free}(x)$ can be quantified, for example, by the relative entropies. However, they are sometimes quantified more simply by the differences between the averages, $\langle X\rangle_{\rm vN}$ and

[19] When $Q$ is a position coordinate, for example, $P$ is the conjugate momentum.

$\langle X\rangle^{\rm free}$, and the variances, $\langle(\Delta X)^2\rangle_{\rm vN}$ and $\langle(\Delta X)^2\rangle^{\rm free}$, of $P_X^{\rm vN}(x)$ and $P_X^{\rm free}(x)$;

$$\delta\langle X\rangle \equiv \langle X\rangle_{\rm vN} - \langle X\rangle^{\rm free} , \tag{140}$$

$$\delta\langle(\Delta X)^2\rangle \equiv \langle(\Delta X)^2\rangle_{\rm vN} - \langle(\Delta X)^2\rangle^{\rm free} . \tag{141}$$

In this quantification, the backaction on the measured observable is represented by the set of $\delta\langle Q\rangle$ and $\delta\langle(\Delta Q)^2\rangle$, whereas the backaction on the conjugate observable by the set of $\delta\langle P\rangle$ and $\delta\langle(\Delta P)^2\rangle$. Heisenberg used $\delta\langle(\Delta P)^2\rangle$ in his famous gedanken experiment on the uncertainty principle. It may thus be tempting to think that the measurement error and the backaction would be related simply by Heisenberg's uncertainty relation. However, *this is false*, as we will explain in Section 4.8.1.

In the following, we do not specify the detailed quantification of the backaction except when it is needed.

### *4.5.6. Instantaneous measurement and ideal measurement as limiting cases*

It is sometimes assumed that the response time $\tau \to +0$. In order to get a non-vanishing information $I$, however, such an *instantaneous measurement* is possible only in the limit of infinite coupling constant $\xi$ of $\hat{H}_{\rm int}$. In fact, if $\xi$ is finite we have

$$\lim_{\tau\to+0} |\Psi(\tau)\rangle = \lim_{\tau\to+0} {\rm e}^{-{\rm i}\hat{H}_{\rm S+A}\tau}|\psi\rangle|\psi_{\rm A}\rangle = |\psi\rangle|\psi_{\rm A}\rangle , \tag{142}$$

which clearly shows that one cannot get any information about S by measuring $R$ of A. Since the coupling constant of any physical interaction is finite, an instantaneous measurement is, in its exact definition, an unphysical limit. It becomes physical only in the sense that $\tau$ is shorter than any other relevant time scales.

On the other hand, an ideal measurement can be regarded as the following limit of a general measurement; $\delta q_{\rm err} \to 0$, and $\mathcal{Q}_{\rm range} \to \mathcal{Q}$, and $I \to \log_2|\mathcal{Q}|$, and the backaction $\to D(\hat{\rho}^{\rm free}\|\hat{\rho}^{\rm ideal}_{\rm vN})$. These conditions are satisfied if Eq. (99) is satisfied for every $q, l, m, q', l', r', m'$. Therefore, to realize an ideal measurement, one must construct an experimental setup whose $\hat{H}_{\rm S+A}$, $\tau$ and $r_0$ satisfy this condition. This is generally very hard and somewhat unrealistic, particularly when the size of A is small [70,61]. Moreover, a fundamental tradeoff among the measurement error, range, and backaction has been suggested for measurements of a certain classes of physical quantities,[20] such as the photon number [20]. Furthermore, it is sometimes assumed that $\tau \to +0$ for ideal measurements, although such a limit is unphysical as mentioned above. To avoid confusion, we call such an ideal measurement as an *instantaneous ideal measurement*.

Since most of real measurements do not satisfy these limiting conditions, it is important to explore properties of general measurements.

## *4.6. Various types of measurements*

In discussing the Zeno effect, more characterizations of measurements are used, which are explained in this subsection.

[20] Although such quantities can be measured, it is not obvious whether they can be called observables if the word "observable" is used only for a quantity of which an ideal measurement is possible, at least in principle, to an arbitrarily good approximation.

*4.6.1. Direct versus indirect measurements*

Suppose that S can be decomposed into two parts, $S_0$ and S′. This does not necessarily mean that $S_0$ and S′ are spatially separated. They can be, for example, different sets of variables such as different quantized fields. Let $Q$ and $Q'$ be observables of $S_0$ and S′, respectively, and assume that they are correlated strongly, where $Q$ is the observable to be measured. For example, $Q$ may be the electron energy in an excited atom, by measurement of which one can detect the decay of the atom, and $Q'$ the energy of photons emitted from the atom: They are strongly correlated with each other because of the energy conservation.

Because of the strong correlation, the information about $Q$ can be obtained through either an interaction between $S_0$ and A or another interaction between S′ and A. In the former case, the measurement is called a *direct measurement* because apparatus A interacts directly with $S_0$ which includes $Q$, whereas in the latter case it is called an *indirect measurement* because A does not interact directly with $S_0$.[21] When discussing decay of an unstable state, for example, $Q'$ may be regarded as a *decay product*, which is produced by the decay. In such a case, an indirect measurement is a measurement of a decay product(s). Note that in indirect measurements properties of the measurement of $Q'$ become important. For example, the range $\mathcal{Q}'_{\text{range}}$ of the measurement of $Q'$ plays crucial roles in Sections 5.5 and 5.6.

It is often criticized that the Zeno effect by direct measurements is not the 'genuine' Zeno effect [10], because the appearance of change of $Q$ is not very surprising if an apparatus acts directly on $S_0$. It seems therefore that theories and experiments on the Zeno effect by indirect measurements are to be explored more intensively.

*4.6.2. Positive- versus negative-result measurements*

Consider an excited atom, which will emit a photon when it decays to the ground state. If one monitors the decay by a photodetector that detects a photon emitted from the atom, the photodetector reports no signal if the decay does not occur. One can confirm that the atom does not decay by the fact that nothing happens. Such a measurement, in which one can get information even when a measuring apparatus reports no signal, is called a *negative-result measurement*. In terms of the formulation of Section 4.2, this means that one can get information even when $r = r_0$. On the other hand, when the spin of an electron is measured by the Stern–Gerlach apparatus, the apparatus reports either $r = +\hbar/2$ or $-\hbar/2$, whereas $r_0$ takes another value, say $r_0 = 0$. Such a measurement, in which $r$ after the measurement is always different from $r_0$, is called a *positive-result measurement*.

The Zeno effect looks more interesting when it is induced by negative-result measurements than by positive-result measurements, because seemingly nothing happens in the former case [10]. In Section 5, we will analyze the Zeno effect induced by indirect negative-result measurements.

*4.6.3. Repeated instantaneous measurements versus continuous measurement*

Assume that the Heisenberg cut is located between A and A′ in Fig. 13. Suppose that a measurement of Q is performed, in which the apparatus A interacts with S during $0 \leqslant t \leqslant \tau$ and $R$ of A is measured by A′ at $t = \tau$.[22] Then, suppose that another measurement is performed, in which A interacts with S again

[21] It might be tempting to regard S′ in a indirect measurement as a part of a measuring apparatus. However, this is not recommended because they are different in the following point: S′ always couples to $S_0$, whereas the apparatus couples to $S_0$ (or S′) only during a measuring process.

[22] Although we assume in the following equations for simplicity that the measurements of $R$ by $A'$ are ideal and instantaneous, it is easy to generalize the equations to the case of general measurements of $R$ using, e.g., the operator $\hat{\mathcal{O}}_m(r)$ of the POVM measurement of Section 4.8.3.

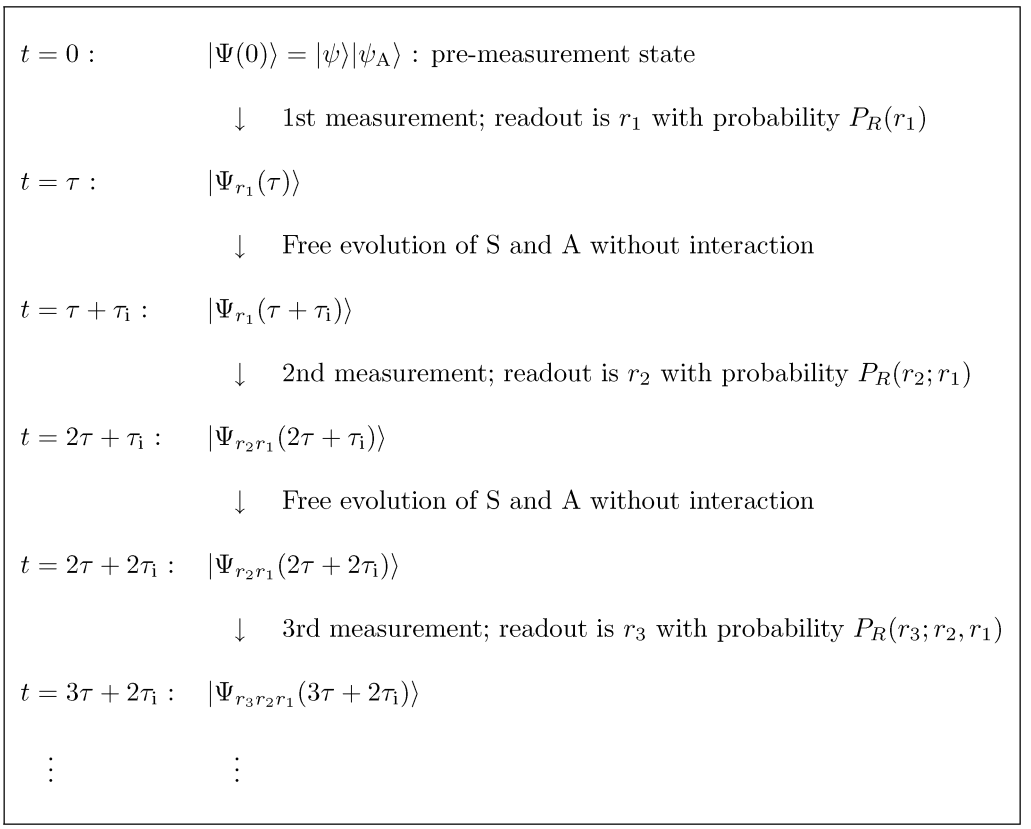


Fig. 14. Repeated measurements with time intervals $\tau_{\rm i}$.

during $\tau + \tau_{\rm i} \leqslant t \leqslant 2\tau + \tau_{\rm i}$ and $R$ is again measured by A$'$ at $t = 2\tau + \tau_{\rm i}$. By repeating such sequences, one can perform *repeated measurements* of $Q$ of S with time intervals $\tau_{\rm i}$, as shown in Fig. 14.

Repeated measurements in the limit of $\tau \to +0$ (while keeping $\tau_{\rm i}$ finite) may be called *repeated instantaneous measurements*.[23] To keep $I$ of each measurement constant in this case, one has to increase the coupling constant $\xi$ of $\hat{H}_{\rm int}$ to infinity, as discussed in Section 4.5.6. Therefore, the repeated instantaneous measurements is a rather unphysical limit.

On the other hand, one can change $\tau_{\rm i}$ freely without changing $I$, because $\tau_{\rm i}$ is basically independent of $I$ of each measurement. Therefore, the limit of $\tau_{\rm i} \to +0$ is a physical and realistic limit, which is widely performed in real experiments. Since the apparatus A interacts continuously with S in such repeated measurements, it may be called a *continuous measurement*.[24]

[23] It is sometimes called *pulsed measurements*. To avoid possible confusion, however, we do not use this term in this article.

[24] This term is widely used when A interacts continuously with S, even when the times and properties (i.e., whether ideal or general and whether instantaneous or not) of measurements of $R$ by $A'$ are not specified. As will be shown in Section 4.6.4, such times and properties become irrelevant if one employs the 'unitary approximation' and is interested only in $\langle X\rangle_{\rm vN}$ and/or $\langle R\rangle_{\rm vN}$, where $X$ is an observable of S.

Despite the above-mentioned difference between the two limits, it is sometimes argued that repeated instantaneous measurements for which $(\tau_{\rm i}, \tau) = (T, 0)$ is equivalent to continuous measurement for which $(\tau_{\rm i}, \tau) = (0, KT)$, where $K$ is a positive constant of order unity. However, this equivalence holds only for certain limited cases. In fact, the results of Section 5 show that they are not equivalent, sometimes much different, in general.

Note that the definition of the response time $\tau$ becomes ambiguous in the case of continuous measurement, because $\hat{H}_{\rm int}$ is effective for all $t \geqslant 0$. In this case, $\tau$ may be defined as the time scale $\tau_{\rm r}$ on which the probability distribution $P_R(r)$ becomes significantly different from the initial distribution $P_R(r) = \delta_{r,r_0}$. Although only the order of magnitude can be determined according to this definition, it suffices for discussions on the Zeno effect induced by continuous measurement. Therefore, we will use this definition in Section 5.

Properties of repeated measurements can be calculated simply as a sequence of general measurements, which we have discussed so far. In fact, by repeatedly applying Eqs. (94), (102) and (105) (with $\tau' = \tau$), we obtain

$$P_R(r_n; r_{n-1}, \ldots, r_1) = \|\hat{\mathscr{P}}_R(r_n) {\rm e}^{-{\rm i}\hat{H}_{\rm S+A}\tau} |\Psi_{r_{n-1}\cdots r_1}((n-1)(\tau+\tau_{\rm i}))\rangle\|^2 \ , \tag{143}$$

$$|\Psi_{r_n\cdots r_1}(n\tau + (n-1)\tau_{\rm i})\rangle = \frac{\hat{\mathscr{P}}_R(r_n){\rm e}^{-{\rm i}\hat{H}_{\rm S+A}\tau}}{\sqrt{P_R(r_n; r_{n-1}, \ldots, r_1)}} |\Psi_{r_{n-1}\cdots r_1}((n-1)(\tau+\tau_{\rm i}))\rangle \ , \tag{144}$$

$$|\Psi_{r_n\cdots r_1}(n(\tau+\tau_{\rm i}))\rangle = {\rm e}^{-{\rm i}\hat{(}H_{\rm S}+H_{\rm A})\tau_{\rm i}} |\Psi_{r_n\cdots r_1}(n\tau + (n-1)\tau_{\rm i})\rangle \ , \tag{145}$$

for $n = 1, 2, \ldots$ . From these formulas, one can calculate everything about repeated measurements, including the Zeno effect. For example, the expectation value $\langle W\rangle_{r_n\cdots r_1}$ of an observable $W$ (of S or A) for the state after $n$ measurements, for which the readouts are $r_1, \ldots, r_n$, is given by

$$\langle W\rangle_{r_n\ldots r_1} = \langle \Psi_{r_n\cdots r_1}(n\tau + (n-1)\tau_{\rm i})|\hat{W}|\Psi_{r_n\cdots r_1}(n\tau + (n-1)\tau_{\rm i})\rangle \ . \tag{146}$$

*4.6.4. Unitary approximation*

In some cases, one is only interested in the average of $\langle W\rangle_{r_n\cdots r_1}$ over all possible values of the readouts. Such an average $\langle W\rangle_{\rm vN}$ is given by

$$\langle W\rangle_{\rm vN} = \sum_{r_1,\ldots,r_n} P_R(r_n; r_{n-1}, \ldots, r_1) P_R(r_{n-1}; r_{n-2}, \ldots, r_1) \cdots P_R(r_1) \langle W\rangle_{r_n\cdots r_1} \ . \tag{147}$$

Using Eq. (143), and taking $\tau_{\rm i} = 0$ for simplicity,[25] we can rewrite this equation as

$$\begin{aligned}
\langle W\rangle_{\rm vN} = & \sum_{r_1,\ldots,r_n} P_R(r_{n-1}; r_{n-2}, \ldots, r_1) \cdots P_R(r_1) \\
& \times \langle \Psi_{r_{n-1}\cdots r_1}((n-1)\tau)|{\rm e}^{{\rm i}\hat{H}_{\rm S+A}\tau} \hat{\mathscr{P}}_R(r_n) \hat{W} \hat{\mathscr{P}}_R(r_n) {\rm e}^{-{\rm i}\hat{H}_{\rm S+A}\tau} |\Psi_{r_{n-1}\cdots r_1}((n-1)\tau)\rangle, \\
= & \sum_{r_1,\ldots,r_n} \langle \Psi(0)|{\rm e}^{{\rm i}\hat{H}_{\rm S+A}\tau} \hat{\mathscr{P}}_R(r_1) \cdots {\rm e}^{{\rm i}\hat{H}_{\rm S+A}\tau} \hat{\mathscr{P}}_R(r_n) \hat{W} \hat{\mathscr{P}}_R(r_n) \\
& \times {\rm e}^{-{\rm i}\hat{H}_{\rm S+A}\tau} \cdots \hat{\mathscr{P}}_R(r_1) {\rm e}^{-{\rm i}\hat{H}_{\rm S+A}\tau} |\Psi(0)\rangle \ .
\end{aligned} \tag{148}$$

[25] The corresponding formula for $\tau_{\rm i} > 0$ can also be obtained easily.

In practical calculations, this is often approximated by[26]

$$\langle W\rangle_{\rm vN} \simeq \langle\Psi(0)|e^{i\hat{H}_{\rm S+A}n\tau}\hat{W}e^{-i\hat{H}_{\rm S+A}n\tau}|\Psi(0)\rangle \ . \tag{149}$$

According to this approximate formula, one can evaluate $\langle W\rangle_{\rm vN}$ by simply calculating the unitary evolution, generated by $e^{-i\hat{H}_{\rm S+A}t}$, of the initial state $|\Psi(0)\rangle$ of the composite system S+A. That is, one does not have to use the projection postulate at all. We thus call this approximation the *unitary approximation*. For *each* model of S+A, the validity of this approximation can be checked by comparing the result obtained from Eq. (149) with that obtained from Eq. (148).

Note, however, that *general* justification of the unitary approximation is not so simple. In Eq. (148), the role of the sum of the projection operators $\sum_{r_j}\hat{\mathscr{P}}_R(r_j)$ $(j=1, 2, \ldots, n)$ is to destroy quantum interference between states corresponding to different values of $r_j$'s. Therefore, if environments surrounding S+A are taken into account, decoherence by the environments would induce the same effects as theirs [72]. It might thus be tempting to consider that one could reduce Eq. (148) to Eq. (149) simple by using this equivalence. However, such decoherence effects generally induce noise terms in the Schrödinger equation, which thus turns into a stochastic one. In general, the time evolution by such a stochastic Schrödinger equation cannot be described by a unitary evolution such as Eq. (149). In particular, Eq. (149) is obviously wrong in the limit of $\tau\to 0$ (while keeping $n\tau$ finite) because then the Zeno effect on $R$ should take place. Therefore, to show the general validity of the unitary approximation one needs to show that Eq. (148) (or the stochastic Schrödinger equation) reduces to Eq. (149) under certain conditions.

When $W = X$ or $R$, where $X$ is an observable of S, a sufficient condition for the validity of the unitary approximation would be that $R$ is a macroscopic variable, for the following reason. If $R$ is a macroscopic variable, the quantum interference destroyed by $\sum_{r_j}\hat{\mathscr{P}}_R(r_j)$ is that between macroscopically distinct states. Such quantum interference can become significant only in limited cases such as (i) a certain observable is measured which can detect such interference, (ii) the state will evolve back closely to the initial state, or (iii) the Zeno effect on $R$ occurs. Neither $X$ nor $R$ can be such an observable of case (i). Furthermore, it seems unlikely that the 'recurrent' process of case (ii) could occur in the time scale of a practical value of $\tau$ if $R$ is a macroscopic variable, because then A is a macroscopic system which generally has many degrees of freedom and complicated dynamics. Moreover, the time scale of case (iii) seems much shorter than the time scale of the Zeno effect on $Q$, which is a microscopic variable.

Actually, the unitary approximation is used widely in studying the Zeno effect without confirming its validity, even when $R$ is taken as a microscopic variable. However, it is generally believed (and confirmed empirically) that results obtained by this approximation are much better than the results of a naive application of the projection postulate on S. In Section 5, we will employ the unitary approximation and discuss its validity for the proposed model.

### *4.7. A simple explanation of the Zeno effect using the quantum measurement theory*

When a quantum system S is not measured, its state $|\psi\rangle$ evolves freely as $|\psi(t)\rangle = \exp[-i\hat{H}_S t]|\psi\rangle$, and the expectation value of an observable $Q$ of S evolves as $\langle\psi(t)|\hat{Q}|\psi(t)\rangle \equiv \langle Q(t)\rangle^{\rm free}$. To measure $Q$, on

[26] Unlike formula (124) for single measurement, Eq. (149) is not a rigorous formula because $\hat{R}$ does not commute with $\hat{H}_{\rm S+A}$ (since if they did then $R$ would not change by the interaction, and thus no information would be transferred to $R$), except for the trivial case where $[\hat{X}, \hat{H}_{\rm S+A}] = 0$ and $\hat{W} = \hat{X}$, for which $\langle W\rangle_{\rm vN} = \langle\Psi(0)|\hat{W}|\Psi(0)\rangle$.

the other hand, one must couple S with an apparatus A via an interaction $\hat{H}_{\rm int}$ between them in such a way that non-vanishing correlation is established between $Q$ and an readout $R$ of A, as discussed in Section 4.2. As a result, S and A evolve as a coupled system as $|\Psi(t)\rangle = \exp[-{\rm i}(\hat{H}_{\rm S} + \hat{H}_{\rm int} + \hat{H}_{\rm A})t]|\psi\rangle|\psi\rangle_{\rm A}$, and the expectation value of $Q$ now evolves as $\langle\Psi(t)|\hat{Q}|\Psi(t)\rangle \equiv \langle Q(t)\rangle^{\rm int}$. Since $Q$ and $R$ undergo a coupled motion by $\hat{H}_{\rm int}$, $\langle Q(t)\rangle^{\rm int}$generally evolves differently from $\langle Q(t)\rangle^{\rm free}$. Even when A reports no signal (i.e., a negative-result measurement), the presence of $\hat{H}_{\rm int}$ does have an effect. Obviously, the effect becomes larger as the coupling constant $\xi$ of $\hat{H}_{\rm int}$ is increased.

Suppose that one performs repeated measurements, each takes $\tau$ seconds, with vanishing intervals ($\tau_{\rm i} = 0$). To make the measurements more frequent (i.e., to reduce $\tau$) without reducing the amount of information $I$ obtained by each measurement, one must increase $\xi$. Therefore, as $\tau$ is decreased without reducing $I$, the effect of $\hat{H}_{\rm int}$ on S becomes larger. If $\tau$ can thus be reduced sufficiently short by increasing $\xi$ enough, the difference between $\langle Q(t)\rangle^{\rm int}$ and $\langle Q(t)\rangle^{\rm free}$ (for a given $t$) becomes larger, and it will become possible to detect the difference by experiments. This is the Zeno effect when $Q$ represents an observable that distinguishes the status (whether the system is decayed or not) of an unstable state.

Note that an *arbitrary* interaction with an external system does *not* necessarily affect the expectation value of $Q$. The essence of the Zeno effect is that *the form of* $\hat{H}_{\rm int}$ *is limited and its strength* $\xi$ *is lower bounded* by the requirement that $\hat{H}_{\rm int}$ should create sufficient correlation between $Q$ and $R$ in order to extract non-vanishing information. For this reason, the lifetime is *always* modified in the limit of $\tau_{\rm i} \to 0$ and $\tau \to 0$, because this implies $\xi \to \infty$. Such a universal conclusion can never be drawn for general interactions with (or perturbations from) external systems.

However, as explained in Section 4.5.6, an instantaneous ideal measurement is an unrealistic limit of real measurements. Therefore, the following questions need to be answered: (i) Is the Zeno effect induced by real measurements? (ii) Under what conditions does it occur? (iii) How does the decay rate of the unstable state behave as a function of the measurement parameters, such as the measurement error, response time, range, and so on? We will answer these questions in Sections 5 and 6.

Note that for analyzing the Zeno effect it is sufficient to calculate the averages, over all possible values of the readout, of expectation values of a few observables. In fact, one is most interested in the lifetime of an unstable state, which is the average time at which the decay occurs. This can be expressed as the average of the expectation value of an appropriate observable. Therefore, as explained in Section 4.6.4, *for analyzing the Zeno effect it is sufficient to calculate the unitary part of the measurement process if one employs the unitary approximation*.[27] That is, unlike the conventional theories of Section 3, one does not have to use the projection postulate. To *understand* this point, however, the full framework, which we have explained so far in this section, of the quantum measurement theory is necessary.

### *4.8. Additional comments*

We have explained all things necessary to apply the quantum measurement theory to the Zeno effect. To be more complete, however, we will describe a few more points which will help the reader.

#### *4.8.1. Non-triviality of the uncertainty relations*

The Zeno effect is a sort of backaction of measurements. It might thus be tempting to think that the Zeno effect could simply be described using the uncertainty relations. However, this is false. We here explain this point, assuming the canonical commutation relation $[\hat{Q}, \hat{P}] = {\rm i}\hbar$ for simplicity.

[27] As explained there, this approximation should be good if $R$ is taken as a macroscopic variable.

The uncertainty relation that is described in most textbooks is the following inequality,

$$\delta q\, \delta p \geqslant \hbar/2\ . \tag{150}$$

Here, $(\delta q)^2 \equiv \langle\psi|(\Delta\hat{Q})^2|\psi\rangle$ and $(\delta p)^2 \equiv \langle\psi|(\Delta\hat{P})^2|\psi\rangle$, where $\Delta\hat{Q} \equiv \hat{Q} - \langle\psi|\hat{Q}|\psi\rangle$ and $\Delta\hat{P} \equiv \hat{P} - \langle\psi|\hat{P}|\psi\rangle$. This inequality is derived directly from $[\hat{Q}, \hat{P}] = i\hbar$. On the other hand, in his famous gedanken experiment on the uncertainty principle, Heisenberg claimed the following inequality,

$$\delta q_{\rm err}\, \delta p_{ba} \geqslant \hbar/2\ , \tag{151}$$

where $\delta q_{\rm err}$ and $\delta p_{ba}$ are the measurement error in a measurement of $Q$ and its backaction on $P$, respectively, which are quantified by the square roots of Eqs. (131) and (141).

As stressed by Lamb [71], inequalities (150) and (151) are totally different from each other. In the former, $\delta q$ and $\delta p$ represent the standard deviation of experimental data that are obtained from *error-less* measurements of $Q$ and $P$, respectively, which are performed independently of each other. Properties of the measuring apparatus are not included at all. In this sense, inequality (150) can be understood as the uncertainty relation *of the pre-measurement state*. On the other hand, $\delta q_{\rm err}$ and $\delta p_{ba}$ in inequality (151) are the measurement error and backaction, respectively, *of the measuring apparatus*. They are obviously different from $\delta q$ and $\delta p$; e.g., $\delta q_{\rm err}$ can be large even when $\delta q = 0$. Furthermore, inequality (150) is never violated by any quantum states whereas relation (151) *can* be violated. For example, suppose that we have an approximately error-less measuring apparatus $\mathrm{A}^{\rm errless}$ of $Q$ of a particle, and a momentum modulator M, which limits the range of momentum in some finite range. We can let the pre-measurement wavefunction enter in $\mathrm{A}^{\rm errless}$, and then pass through M. Since the location of the Heisenberg cut and the time at which the measurement is completed can be taken arbitrary, we can regard this composite system $\mathrm{A}^{\rm errless}$+M as a single apparatus A. For this apparatus, $\delta q_{\rm err} \simeq 0$ (by $\mathrm{A}^{\rm errless}$) whereas $\delta p_{ba}$ is upper limited (by M). Therefore, $\delta q_{\rm err}\, \delta p_{ba} \simeq 0$, and inequality (151) is violated.

As might be understood from this simple example, one can construct many different "uncertainty products" by combining two of $\delta q$, $\delta q_{\rm err}$, $\delta q_{\rm ba}$, $\delta p$, $\delta p_{\rm err}$, and $\delta p_{\rm ba}$. The lower limits, if exist, of different uncertainty products can have different values. Furthermore, inequality (150) assumes that the measurements of $Q$ and $P$ are performed not simultaneously but separately. When $Q$ and $P$ are measured simultaneously, on the other hand, the uncertainty becomes larger as $\delta q\, \delta p \geqslant \hbar$ [22]. To explore these uncertainty products, the quantum measurement theory is necessary. Recently, Ozawa [23] have found certain universal relations among them, using the rather mathematical definition (132).

It is clear from these considerations that the Zeno effect cannot be discussed simply using uncertainty relations.

### *4.8.2. Measurement of time correlations*

Suppose that an observable $X$ is measured at $t = 0$ using an apparatus $A_X$, and subsequently another observable $Y$ is measured at time $t\,(>0)$ using another apparatus $A_Y$. The expectation value of the product of the two readouts $R_X$ and $R_Y$ is called the *time correlation*, which we denote as $\langle Y(t)X(0)\rangle$. As a quantum-theoretical expression of this quantity, the following one is often employed:

$$\langle\psi_{\rm H}|\hat{Y}_{\rm H}(t)\hat{X}_{\rm H}(0)|\psi_{\rm H}\rangle\ , \tag{152}$$

where the subscript H denotes the corresponding quantities in the Heisenberg picture. However, as stressed first by Glauber [16], this expression is wrong except for a special case. The correct expression is obtained, in a manner similar to discussions of Section 4.6.3, as follows.

From Eqs. (94) and (102) (with $\tau' = \tau \equiv \tau_X$, the response time of $\mathrm{A}_X$), the probability distribution of the value $r_X$ of $R_X$ is given by

$$P_{R_X}(r_X) = \|\hat{\mathscr{P}}_{R_X}(r_X)\mathrm{e}^{-\mathrm{i}\hat{H}_{\mathrm{S+A}}\tau_X}|\psi\rangle|\psi_{\mathrm{A}}\rangle\|^2 \ , \tag{153}$$

where A denotes the joint system of $\mathrm{A}_X$ and $\mathrm{A}_Y$, and the post-measurement state is

$$|\Psi_{r_X}(\tau_X)\rangle = \frac{1}{\sqrt{P_{R_X}(r_X)}}\hat{\mathscr{P}}_{R_X}(r_X)\mathrm{e}^{-\mathrm{i}\hat{H}_{\mathrm{S+A}}\tau_X}|\psi\rangle|\psi_{\mathrm{A}}\rangle \ . \tag{154}$$

This state evolves into $\mathrm{e}^{-\mathrm{i}\hat{(}H_{\mathrm{S}}+H_{\mathrm{A}})(t-\tau_X)}|\Psi_{r_X}(\tau_X)\rangle$ at time $t$ ($\geqslant\tau_X$), which becomes the pre-measurement state of the measurement of $Y$. The probability distribution of the value $r_Y$ of $R_Y$ is therefore given by

$$P_{R_Y}(r_Y; r_X) = \|\hat{\mathscr{P}}_{R_Y}(r_Y)\mathrm{e}^{-\mathrm{i}\hat{H}_{\mathrm{S+A}}\tau_Y}\mathrm{e}^{-\mathrm{i}\hat{(}H_{\mathrm{S}}+H_{\mathrm{A}})(t-\tau_X)}|\Psi_{r_X}(\tau_X)\rangle\|^2 \ , \tag{155}$$

where $\tau_Y$ is the response time of $\mathrm{A}_Y$. From these equations, the time correlation is calculated as

$$\begin{aligned}\langle Y(t)X(0)\rangle &= \sum_{r_X,r_Y} r_Y r_X P_{R_Y}(r_Y; r_X) P_{R_X}(r_X) \\ &= \sum_{r_X,r_Y} r_Y r_X \|\hat{\mathscr{P}}_{R_Y}(r_Y)\mathrm{e}^{-\mathrm{i}\hat{H}_{\mathrm{S+A}}\tau_Y}\mathrm{e}^{-\mathrm{i}\hat{(}H_{\mathrm{S}}+H_{\mathrm{A}})(t-\tau_X)} \\ &\quad\times \hat{\mathscr{P}}_{R_X}(r_X)\mathrm{e}^{-\mathrm{i}\hat{H}_{\mathrm{S+A}}\tau_X}|\psi\rangle|\psi_{\mathrm{A}}\rangle\|^2 \ .\end{aligned} \tag{156}$$

If both measurements are ideal and instantaneous,[28] and if $[\hat{X}, \hat{Y}] = [\hat{X}, \hat{H}_{\mathrm{S}}] = 0$, then from Eq. (109) this formula reduces to

$$\langle Y(t)X(0)\rangle = \sum_{x,y} yx\|\hat{\mathscr{P}}_Y(y)\mathrm{e}^{-\mathrm{i}\hat{H}_{\mathrm{S}}t}\hat{\mathscr{P}}_X(x)|\psi\rangle\|^2 = \langle\psi_{\mathrm{H}}|\hat{Y}_{\mathrm{H}}(t)\hat{X}_{\mathrm{H}}(0)|\psi_{\mathrm{H}}\rangle \ . \tag{157}$$

For general measurements, however, one must use the correct formula (156), which states that the value of the time correlation depends on properties of the measuring apparatus. In particular, the value strongly depends on the backaction of A, because it determines the post-measurement state $|\Psi_{r_X}(\tau_X)\rangle$, which evolves into the pre-measurement state of the subsequent measurement of $Y$. Therefore, if one has two sets of pieces of apparatus ($\mathrm{A}_X$, $\mathrm{A}_Y$) and ($\mathrm{A}'_X$, $\mathrm{A}'_Y$), the value of $\langle Y(t)X(0)\rangle$ depends on which set is used as the measuring apparatus, even when their measurement errors are negligibly small. Examples and experimental demonstrations of this fact are presented, e.g., in books on quantum optics [21,32].

An important implication of the discussions of this subsection is that the Zeno effect would also depend on properties of measuring apparatus. This is indeed the case, as will be demonstrated in Section 5.

---

[28] As noted in Section 4.5.6, this means that the coupling constant $\xi$ of $\hat{H}_{\mathrm{int}}$ is infinite, and hence $\hat{H}_{\mathrm{S+A}}\tau_X \nrightarrow 0$ although $\tau_X \to 0$.

*4.8.3. POVM measurement*

From Eqs. (94) and (102) (with $\tau' = \tau$), the probability distribution of the readout can be expressed as

$$\begin{aligned} P_R(r) &= \mathrm{Tr}_{\mathrm{S+A}}[\hat{\mathscr{P}}_R(r)\mathrm{e}^{-\mathrm{i}\hat{H}_{\mathrm{S+A}}\tau}|\psi\rangle|\psi_{\mathrm{A}}\rangle\langle\psi_{\mathrm{A}}|\langle\psi|\mathrm{e}^{\mathrm{i}\hat{H}_{\mathrm{S+A}}\tau}\hat{\mathscr{P}}_R(r)] \\ &= \mathrm{Tr}\left[\sum_m \langle r,m|\mathrm{e}^{-\mathrm{i}\hat{H}_{\mathrm{S+A}}\tau}|\psi\rangle|\psi_{\mathrm{A}}\rangle\langle\psi_{\mathrm{A}}|\langle\psi|\mathrm{e}^{\mathrm{i}\hat{H}_{\mathrm{S+A}}\tau}|r,m\rangle\right] , \end{aligned} \tag{158}$$

where $\mathrm{Tr}_{\mathrm{S+A}}$ and Tr denotes the trace operations over $\mathbf{H}_{\mathrm{S+A}}$ and $\mathbf{H}_{\mathrm{S}}$, respectively. If we define the operator $\hat{\mathscr{O}}_m(r)$ on $\mathbf{H}_{\mathrm{S}}$ by

$$\hat{\mathscr{O}}_m(r)|\psi\rangle \equiv \langle r,m|\mathrm{e}^{-\mathrm{i}\hat{H}_{\mathrm{S+A}}\tau}|\psi\rangle|\psi_{\mathrm{A}}\rangle \quad \text{for } \forall|\psi\rangle \in \mathbf{H}_{\mathrm{S}} , \tag{159}$$

then the above equation can be written as

$$P_R(r) = \mathrm{Tr}\left[\sum_m \hat{\mathscr{O}}_m(r)\hat{\rho}(0)\hat{\mathscr{O}}_m^\dagger(r)\right] , \tag{160}$$

where $\hat{\rho}(0) = |\psi\rangle\langle\psi|$. Furthermore, the post-measurement state can be expressed as

$$\begin{aligned} \hat{\rho}_r(\tau) &= \frac{1}{P_R(r)}\mathrm{Tr}_{\mathrm{A}}[\hat{\mathscr{P}}_R(r)\mathrm{e}^{-\mathrm{i}\hat{H}_{\mathrm{S+A}}\tau}|\psi\rangle|\psi_{\mathrm{A}}\rangle\langle\psi_{\mathrm{A}}|\langle\psi|\mathrm{e}^{\mathrm{i}\hat{H}_{\mathrm{S+A}}\tau}\hat{\mathscr{P}}_R(r)] \\ &= \frac{1}{\mathrm{Tr}\left[\sum_m \hat{\mathscr{O}}_m(r)\hat{\rho}(0)\hat{\mathscr{O}}_m^\dagger(r)\right]} \sum_m \hat{\mathscr{O}}_m(r)\hat{\rho}(0)\hat{\mathscr{O}}_m^\dagger(r) . \end{aligned} \tag{161}$$

Therefore, we can calculate both $P_R(r)$ and $\hat{\rho}_r(\tau)$ from the pre-measurement state $\hat{\rho}(0)$ if the set of operators $\{\hat{\mathscr{O}}_m(r)\}$ is given. General properties of $\{\hat{\mathscr{O}}_m(r)\}$ is easily obtained from its definition (159). For example,

$$\sum_r \sum_m \hat{\mathscr{O}}_m^\dagger(r)\hat{\mathscr{O}}_m(r) = \hat{1} \tag{162}$$

because $\sum_r \sum_m \langle\psi_1|\hat{\mathscr{O}}_m^\dagger(r)\hat{\mathscr{O}}_m(r)|\psi_2\rangle = \langle\psi_1|\psi_2\rangle$ for arbitrary vectors $|\psi_1\rangle$ and $|\psi_2\rangle$.

If $\Delta$ is a set of values of $r$, then the probability of getting the readout in $\Delta$ is given by

$$\sum_{r\in\Delta} P_R(r) = \mathrm{Tr}\left[\sum_{r\in\Delta}\sum_m \hat{\mathscr{O}}_m(r)\hat{\rho}(0)\hat{\mathscr{O}}_m^\dagger(r)\right] . \tag{163}$$

Helstrom [68] derived a similar expression in a different manner, by considering mathematical requirements for general measurements. He called the association between $\Delta$ and the linear map

$$\hat{\rho} \mapsto \sum_{r\in\Delta}\sum_m \hat{\mathscr{O}}_m(r)\hat{\rho}\hat{\mathscr{O}}_m^\dagger(r) \tag{164}$$

a *positive operator-valued measure* (POVM). Therefore, a general measurement is sometimes called a *POVM measurement*.

One can in principle calculate the correct POVM using Eq. (159) for each model of the measurement process. However, for certain purposes, it is sufficient to *assume* some reasonable form of the POVM by hand. This simplifies discussions greatly. Such a phenomenological theory is widely used, e.g., in quantum information theory [68,69]. The Zeno effect can also be analyzed using such a phenomenological theory, although we shall not use it in this article.

#### *4.8.4. Completeness of the standard laws of quantum theory*

In concluding this section, we want to stress that the results of this section show the completeness of the standard laws of quantum theory, which include Born's rule and the projection postulate. One can surely obtain the correct results by applying these laws if the Heisenberg cut is located at an appropriate position, although wrong results might be obtained if one naively assumed the Heisenberg cut between S and A. Furthermore, we have *derived* formula for POVM measurements in Section 4.8.3, although some recent textbooks employed POVM measurements as one of the fundamental laws of quantum theory. Therefore, the standard laws of quantum theory are complete if correctly applied.

## 5. Analysis of Zeno effect by quantum measurement theory

In the previous Section, we have reviewed the quantum measurement theory, according to which (in particular, Section 4.6.4) one should analyze the unitary temporal evolution of both the target system S of measurements and (a part of) measuring apparatus A. Many of theoretical analyses of the Zeno effect employed this formalism [48,49,73–79]. In this section, taking a photon-counting measurement on the decay of an excited atom as an example, we study the Zeno effect with this formalism, and compare the results with those obtained in Section 3.

This section is organized as follows: In Section 5.1, a concrete Hamiltonian for the system-apparatus interaction, as well as the physical quantities of interest, is presented. In Section 5.2, the effect of the system-apparatus interaction is investigated analytically; it is shown that the system-apparatus interaction results in the renormalization of the form factor, through which the decay rate of the atom is modified. In Section 5.3, we consider an idealized situation where the detector satisfies the flat-response condition, Eq. (192); it is observed that the conventional projection-based theory discussed in Section 3 is essentially reproduced under this condition. On the contrary, in Sections 5.4–5.6, we consider the effects of imperfect measurements, where the flat-response condition is not satisfied and various phenomena beyond the conventional theory appear.

### *5.1. Model for the system and apparatus*

#### *5.1.1. Hamiltonian for atom–photon–detector system*

As an example of an unstable system and a measuring apparatus for checking its decay, we discuss the case where the radiative decay of an excited atom is continuously monitored by counting the emitted photon. This is a sort of a continuous measurement (Section 4.6.3), where the observer judges that the atom has decayed if the detector (measuring apparatus) has counted a photon. Note that this measurement is classified as a negative-result and indirect measurement, for which the curiousness of the Zeno effect is most emphasized (see Sections 4.6.1 and 4.6.2).

We present again the Hamiltonian of the measured system S, i.e., an atom and a photon field:

$$\hat{H}_S = \Omega\sigma_+\sigma_- + \int \mathrm{d}\boldsymbol{k}\ [(g_{\boldsymbol{k}}\sigma_+ b_{\boldsymbol{k}} + \mathrm{H.c.}) + \epsilon_{\boldsymbol{k}} b_{\boldsymbol{k}}^\dagger b_{\boldsymbol{k}}]\ . \tag{165}$$

The unobserved decay dynamics of this system has already been discussed in Section 2. We now couple a detector A–S. In usual photodetectors, photons are converted to elementary excitations (typically, electron–hole pairs) in the detector. Here, we model the detector by a spatially homogeneous absorptive medium, whose Hamiltonian is given by

$$\hat{H}_A = \sum_j \int \mathrm{d}\boldsymbol{k}\ \epsilon_{\boldsymbol{k}j} c_{\boldsymbol{k}j}^\dagger c_{\boldsymbol{k}j}\ . \tag{166}$$

Here, $\epsilon_{\boldsymbol{k}j}$ and $c_{\boldsymbol{k}j}$ denote the energy and an annihilation operator, respectively, of the elementary excitation with the momentum $\boldsymbol{k}$ and a set of other quantum numbers $j$.[29] We treat $c_{\boldsymbol{k}j}$ as a bosonic operator, which satisfies $[c_{\boldsymbol{k}j}, c_{\boldsymbol{k}'j'}^\dagger] = \delta(\boldsymbol{k}-\boldsymbol{k}')\delta_{j,j'}$, and thus the detector is here modeled by non-interacting bosons. Such a treatment is allowed as long as the density of excitations is low,[30] which is valid in usual photodetection processes. Usually, elementary excitations form a continuum in energy, and the conversion from a photon to an excitation occurs irreversibly. The interaction between photons and the elementary excitations may be described by adding the following photon–detector interaction term [79,82]:

$$\hat{H}_{\mathrm{int}} = \sum_j \int \mathrm{d}\boldsymbol{k}(\xi_{\boldsymbol{k}j} b_{\boldsymbol{k}}^\dagger c_{\boldsymbol{k}j} + \ H.c.)\ . \tag{167}$$

Here, the photon (of mode) $\boldsymbol{k}$ does not couple to elementary excitations with a different momentum $\boldsymbol{k}'(\neq \boldsymbol{k})$, due to the translational symmetry inherent in spatially homogeneous systems.

Throughout this section, we assume that there is no excitation in the detector initially. Then, following Section 2.3, we can transform Eqs. (166) and (167) into the following form:

$$\hat{H}_A = \int\int \mathrm{d}\boldsymbol{k}\,\mathrm{d}\omega\ \omega c_{\boldsymbol{k}\omega}^\dagger c_{\boldsymbol{k}\omega}\ , \tag{168}$$

$$\hat{H}_{\mathrm{int}} = \int\int \mathrm{d}\boldsymbol{k}\,\mathrm{d}\omega(\xi_{\boldsymbol{k}\omega} b_{\boldsymbol{k}}^\dagger c_{\boldsymbol{k}\omega} + \ H.c.)\ , \tag{169}$$

where $c_{\boldsymbol{k}\omega}$ is normalized as $[c_{\boldsymbol{k}\omega}, c_{\boldsymbol{k}'\omega'}^\dagger] = \delta(\boldsymbol{k}-\boldsymbol{k}')\delta(\omega-\omega')$. $\xi_{\boldsymbol{k}\omega}$ is the form factor for the photon–detector interaction, for a photon with momentum $\boldsymbol{k}$.

The photon–detector coupling $\xi_{\boldsymbol{k}\omega}$ generally introduces two effects on the photonic modes: The coupling makes the lifetimes of photons finite, as well as it introduces slight shifts in the photonic energies. The latter effect appears when $\xi_{\boldsymbol{k}\omega}$ is not a symmetric function of $\omega$ about the photon energy $\varepsilon_{\boldsymbol{k}}$ (see Section 6.3). Here, in order to neglect the energy shifts of photons, which bring about uninteresting

[29] For example, $\boldsymbol{k}$ is the center-of-mass momentum of an electron-hole pair, and $j$ is a set of other quantum numbers for the electron–hole relative motion.

[30] States excited by photons are in the charge-neutral sector of electron–hole states. Such states can always be mapped to states of *interacting* bosons [80,81]. When the density of excitations is low, then the density of bosons in the mapped state is low, and thus the interactions among the bosons are negligible. For details, see, e.g., Refs. [80,81].

complexity from the viewpoint of the Zeno effect, we neglect $\omega$-dependence of $\xi_{\boldsymbol{k}\omega}$ and take the following form:

$$\xi_{\boldsymbol{k}\omega} = \sqrt{\eta_{\boldsymbol{k}}/2\pi}\ , \tag{170}$$

which is called the *flat-band approximation*. By this choice of photon–detector coupling, the photon $\boldsymbol{k}$ will be converted into an excitation in the detector at a rate $\eta_{\boldsymbol{k}}$. The response time of the detector for the photon $\boldsymbol{k}$ is therefore given by

$$\tau_{\boldsymbol{k}} \equiv \eta_{\boldsymbol{k}}^{-1}\ . \tag{171}$$

In realistic experimental situations, the photon–detector coupling $\eta_{\boldsymbol{k}}$ often depends on $\boldsymbol{k}$. For example, if the detector has a finite detection energy band, $\eta_{\boldsymbol{k}}$ is non-zero only for photons whose energy falls in the detection energy band. Therefore, we retain $\boldsymbol{k}$-dependence of $\eta_{\boldsymbol{k}}$ in order to treat such cases.

In real photodetectors, photogenerated excitations are magnified to yield macroscopic signals. Here we neglect the magnification processes, regarding it as the apparatus A′ that performs an ideal measurement of the number of excitation quanta (Section 4.2), although actually it would not be ideal in general. Such an approximation has been successfully applied to many problems in quantum optics [16,21,32].

*5.1.2. Quantities of interest*

In studying the Zeno effect, one is interested only in the averages of a few observables (such as $s(t)$, $\varepsilon(t)$ and $r(t)$, described below) over all possible values of the readouts of the measurements. Furthermore, since this model does not corresponds to either of the limiting cases (i)–(iii) of Section 4.6.4, [31] the unitary approximation of Section 4.6.4 is expected to be good for this model. Therefore, within the unitary approximation, it is sufficient to investigate the unitary time evolution of the joint quantum system S+A, as explained in Section 4.7. Therefore, the projection postulate is no more necessary; the counteraction of measurement onto S is naturally introduced through the interaction $\hat{H}_{\rm int}$ between the measured system and the measuring apparatus.

The Hamiltonian of S+A is given by the sum of Eqs. (165), (168) and (169);

$$\hat{H} = \hat{H}_S + \hat{H}_{\rm int} + \hat{H}_A\ . \tag{172}$$

The pre-measurement state is $\sigma_+|0\rangle|0_A\rangle$, where $|0_A\rangle$ denotes the vacuum state for $c_{\boldsymbol{k}\omega}$. Hereafter, we denote the vacuum state for the enlarged system S+A, $|0\rangle|0_A\rangle$, by $|0\rangle$ for simplicity. Since the number of total quanta, $\hat{N} = \sigma_+\sigma_- + \int \mathrm{d}\boldsymbol{k} b_{\boldsymbol{k}}^\dagger b_{\boldsymbol{k}} + \int\int \mathrm{d}\boldsymbol{k}\,\mathrm{d}\omega c_{\boldsymbol{k}\omega}^\dagger c_{\boldsymbol{k}\omega}$, is conserved ($=1$) in this enlarged system, the state vector at time $t$ can be written in the following form:

$$|\psi(t)\rangle = \exp(-\mathrm{i}\mathscr{H}t)|\mathrm{i}\rangle = f(t)\sigma_+|0\rangle + \int \mathrm{d}\boldsymbol{k} f_{\boldsymbol{k}}(t) b_{\boldsymbol{k}}^\dagger|0\rangle + \int\int \mathrm{d}\boldsymbol{k}\,\mathrm{d}\omega f_{\boldsymbol{k}\omega}(t) c_{\boldsymbol{k}\omega}^\dagger|0\rangle\ . \tag{173}$$

We define the following three probabilities of physical interest:

$$s(t) = |f(t)|^2\ , \tag{174}$$

[31] For example, the time scale of the recurrent process is infinite because A of this model has a continuous spectrum.

$$\varepsilon(t) = \int \mathrm{d}\boldsymbol{k} |f_{\boldsymbol{k}}(t)|^2 \ , \tag{175}$$

$$r(t) = \int\int \mathrm{d}\boldsymbol{k}\, \mathrm{d}\omega |f_{\boldsymbol{k}\omega}(t)|^2 \ . \tag{176}$$

$s(t)$ is the survival probability of the atom under the photoncounting measurement. $\varepsilon(t)$ is the probability that the atom has decayed and emitted a photon but the emitted photon has not been detected. We therefore call $\varepsilon(t)$ the measurement error.[32] $r(t)$ is the probability that the atom has decayed and the emitted photon has been detected. Neglecting the signal magnification process, we can interpret $r(t)$ as the probability of getting the detector response. One of the merits of the present analysis of measurement is that all of these quantities of interest can be calculated.

In the following part of Section 5, we will investigate how the decay probability $1-s(t)$ is perturbed by the interaction with measuring apparatus, $\hat{H}_{\mathrm{int}}$. If $1-s(t)$ is suppressed (enhanced) compared to the case of free decay where $\hat{H}_{\mathrm{int}} = 0$, we regard that the QZE (AZE) is taking place. One might feel strange why this judgment is not done through $r(t)$, which is directly accessible by an observer. This is because $r(t)$ does not necessarily reflect the decay probability $1 - s(t)$ faithfully in general measurement processes: In good measurements, $1 - s(t)$ well coincides with $r(t)$ as observed in Fig. 17(b), but such an optimal response is expected only when the response time of detector is much shorter than the atomic lifetime, and when the detector is active for all relevant photons. If the detector response is slow [see Fig. 17(a)] or if the detector is inactive for some photons [see Figs. 23, 25 and 29], $r(t)$ largely deviates from $1 - s(t)$. Note that the atomic state does have decayed if $1 - s(t) = 1$ even when $r(t) \simeq 0$.

*5.1.3. Relation to direct measurements*

As stated at the beginning of Section 5.1.1, the model presented in Section 5.1.1 describes a case of an indirect measurement. However, it is shown here that a model for a *direct* measurement can also be recast into the same form, and therefore that the results presented in Section 5 are applicable not only to indirect measurements but also to direct measurements.

As the unstable quantum system, we again employ an excited atom undergoing radiative decay, but we slightly change the notation: denoting the excited and ground states by $|a\rangle$ and $|b\rangle$, and taking the energy of $|b\rangle$ as the origin of energy, we rewrite the unobserved system Hamiltonian as

$$\hat{H}_{\mathrm{S}}^{\mathrm{direct}} = \Omega |a\rangle\langle a| + \int \mathrm{d}\boldsymbol{k}\ [(g_{\boldsymbol{k}} b_{\boldsymbol{k}} |a\rangle\langle b| + \mathrm{H.c.}) + \epsilon_{\boldsymbol{k}} b_{\boldsymbol{k}}^\dagger b_{\boldsymbol{k}}] \ , \tag{177}$$

which is identical to Eq. (165) except for notations. As a model of a direct measurement, we assume that the atom is coupled with an apparatus A, which has a continuum of single-electron states, in such a way that as soon as the decayed electronic state $|b\rangle$ is occupied the electron tunnels into the continuum with a rate $\eta$ [83]. The observer knows the decay of the initial unstable state $|a\rangle$ through the population in the continuum. Denoting an energy eigenstate of A with energy $\mu$ by $|\mu\rangle$, we take the Hamiltonian of A and the interaction with S as

$$\hat{H}_{\mathrm{A}}^{\mathrm{direct}} + \hat{H}_{\mathrm{int}}^{\mathrm{direct}} = \int \mathrm{d}\mu\ \mu |\mu\rangle\langle\mu| + \int \mathrm{d}\mu \sqrt{\eta/2\pi} (|\mu\rangle\langle b| + |b\rangle\langle\mu|) \ . \tag{178}$$

[32] However, there are several other definitions of measurement error (Section 4.5.2).

Obviously, this model describes a direct measurement, for the measurement apparatus directly interacts with the atom in order to get information on the atom.

According to the above Hamiltonians, the state vector starting from the initial state $|a\rangle$ evolves in the subspace, spanned by $\{|a\rangle, b_{\boldsymbol{k}}^\dagger|b\rangle, b_{\boldsymbol{k}}^\dagger|\mu\rangle\}$, of the total Hilbert space. This situation is similar to the model of Section 5.1.1, for which the subspace is spanned by $\{\sigma_+|0\rangle, b_{\boldsymbol{k}}^\dagger|0\rangle, c_{\boldsymbol{k}\omega}^\dagger|0\rangle\}$ as Eq. (173). Actually, by regarding $|a\rangle \to \sigma_+|0\rangle$, $b_{\boldsymbol{k}}^\dagger|b\rangle \to b_{\boldsymbol{k}}^\dagger|0\rangle$, and $b_{\boldsymbol{k}}^\dagger|\omega - \epsilon_{\boldsymbol{k}}\rangle \to c_{\boldsymbol{k}\omega}^\dagger|0\rangle$, we can map the present model of a direct measurement exactly onto the model of Section 5.1.1 with the photon–detector coupling constant $\xi_{\boldsymbol{k}\omega} = \sqrt{\eta/2\pi}$. (Such a case, where $\xi_{\boldsymbol{k}\omega}$ has no$\boldsymbol{k}$-dependence, is called the case of "flat response" in this article and shall be discussed extensively in Section 5.3.) Thus, the model of a direct measurement, Eqs. (177) and 178is included as a special case of the model of an indirect measurement, Eqs. (165), (168) and (169).

### 5.2. Renormalization of form factor by measurement

As an inevitable counteraction of photon-counting measurements, the lifetimes of photons become finite. As a result, the energies of photons are broadened, and the form factor (see Section 2.3) suffers modification. Hereafter, we refer to the new form factor as the *renormalized* form factor. In this section, we discuss how the form factor is renormalized by the measurement, i.e., through the photon–detector interaction. It should be reminded that, when the system is not observed ($\hat{H}_{\rm int} = 0$), the *original* form factor is given by

$$|g_\mu|^2 = \int \mathrm{d}\boldsymbol{k}|g_{\boldsymbol{k}}|^2\delta(\epsilon_{\boldsymbol{k}} - \mu) \ . \tag{179}$$

In order to obtain the renormalized form factor, we first diagonalize the photon–detector part of the Hamiltonian, $\hat{H}_{\rm int} + \hat{H}_A$. For this purpose, we define the coupled-mode operator $B_{\boldsymbol{k}\mu}$ [41,82] by

$$B_{\boldsymbol{k}\mu} = \alpha_{\boldsymbol{k}}(\mu)b_{\boldsymbol{k}} + \int \mathrm{d}\omega\beta_{\boldsymbol{k}}(\mu,\omega)c_{\boldsymbol{k}\omega} \ , \tag{180}$$

$$\alpha_{\boldsymbol{k}}(\mu) = \frac{(\eta_{\boldsymbol{k}}/2\pi)^{1/2}}{\mu - \epsilon_{\boldsymbol{k}} + \mathrm{i}\eta_{\boldsymbol{k}}/2} \ , \tag{181}$$

$$\beta_{\boldsymbol{k}}(\mu,\omega) = \frac{\eta_{\boldsymbol{k}}/2\pi}{(\mu - \epsilon_{\boldsymbol{k}} + \mathrm{i}\eta_{\boldsymbol{k}}/2)(\mu - \omega + \mathrm{i}\delta)} + \delta(\mu - \omega) \ . \tag{182}$$

It can be confirmed that $B_{\boldsymbol{k}\mu}$ is orthonormalized as $[B_{\boldsymbol{k}\mu}, B_{\boldsymbol{k}'\mu'}^\dagger] = \delta(\boldsymbol{k} - \boldsymbol{k}')\delta(\mu - \mu')$. Inversely, the original operators, $b_{\boldsymbol{k}}$ and $c_{\boldsymbol{k}\omega}$, are given, in terms of $B_{\boldsymbol{k}\mu}$, by

$$b_{\boldsymbol{k}} = \int \mathrm{d}\mu\alpha_{\boldsymbol{k}}^*(\mu)B_{\boldsymbol{k}\mu} \ , \tag{183}$$

$$c_{\boldsymbol{k}\omega} = \int \mathrm{d}\mu\beta_{\boldsymbol{k}}^*(\omega,\mu)B_{\boldsymbol{k}\mu} \ . \tag{184}$$

Using the coupled-mode operators, the enlarged Hamiltonian $\hat{H}$ is transformed into the following form:

$$\hat{H} = \Omega\sigma_+\sigma_- + \int\int \mathrm{d}\boldsymbol{k}\,\mathrm{d}\mu\ \mu B^\dagger_{\boldsymbol{k}\mu}B_{\boldsymbol{k}\mu} + \int\int \mathrm{d}\boldsymbol{k}\,\mathrm{d}\mu\left[\frac{(\eta_{\boldsymbol{k}}/2\pi)^{1/2}g_{\boldsymbol{k}}}{\mu-\epsilon_{\boldsymbol{k}}-\mathrm{i}\eta_{\boldsymbol{k}}/2}\sigma_+B_{\boldsymbol{k}\mu}+H.c.\right]. \tag{185}$$

Now we extract the interaction mode $\bar{B}_\mu$ at energy $\mu$, employing the same method as used in Section 2.3. $\bar{B}_\mu$ is given by

$$\bar{B}_\mu = \bar{g}_\mu^{-1}\int \mathrm{d}\boldsymbol{k}\frac{(\eta_{\boldsymbol{k}}/2\pi)^{1/2}g_{\boldsymbol{k}}}{\mu-\epsilon_{\boldsymbol{k}}-\mathrm{i}\eta_{\boldsymbol{k}}/2}B_{\boldsymbol{k}\mu}\ , \tag{186}$$

$$|\bar{g}_\mu|^2 = \int \mathrm{d}\boldsymbol{k}|g_{\boldsymbol{k}}|^2\frac{\eta_{\boldsymbol{k}}/2\pi}{|\mu-\epsilon_{\boldsymbol{k}}-\mathrm{i}\eta_{\boldsymbol{k}}/2|^2}\ , \tag{187}$$

where $|\bar{g}_\mu|^2$ was determined so that $\bar{B}_\mu$ is orthonormalized as $[\bar{B}_\mu, \bar{B}^\dagger_{\mu'}] = \delta(\mu-\mu')$. Using the interaction modes, $\hat{H}$ is further rewritten as

$$\hat{H} = \Omega_0\sigma_+\sigma_- + \int \mathrm{d}\mu[(\bar{g}_\mu\sigma_+\bar{B}_\mu + \mathrm{H.c.}) + \mu\bar{B}^\dagger_\mu\bar{B}_\mu] + \hat{H}_{\mathrm{rest}}\ , \tag{188}$$

where $\hat{H}_{\mathrm{rest}}$ consists of coupled modes which do not interact with the atom.

In the final form of the Hamiltonian, Eq. (188), the atom is coupled to a one-dimensional continuum of $\bar{B}_\mu$ with the coupling function $\bar{g}_\mu$. Thus, $|\bar{g}_\mu|^2$ gives the form factor renormalized by measurement. It is easy to confirm that, in the limit of $\eta_{\boldsymbol{k}} \to 0$ for every $\boldsymbol{k}$, Eq. (187) reduces to the original form factor, Eq. (179).

Eqs. (179) and (187) clarify how the form factor is renormalized as a backaction of measurement. When the system is not observed, the form factor is an accumulation of delta functions, $|g_{\boldsymbol{k}}|^2\delta(\mu-\epsilon_{\boldsymbol{k}})$. When one tries to measure the decay of the system by detecting an emitted photon, the lifetime of the emitted photon becomes finite as inevitable counteraction of measurement. Thus, the contribution of photon $\boldsymbol{k}$ is energetically broadened as

$$|g_{\boldsymbol{k}}|^2\delta(\mu-\epsilon_{\boldsymbol{k}}) \quad\to\quad |g_{\boldsymbol{k}}|^2\frac{\eta_{\boldsymbol{k}}/2\pi}{|\mu-\epsilon_{\boldsymbol{k}}-\mathrm{i}\eta_{\boldsymbol{k}}/2|^2}\ , \tag{189}$$

satisfying a sum rule:

$$\int \mathrm{d}\mu|g_{\boldsymbol{k}}|^2\delta(\mu-\epsilon_{\boldsymbol{k}}) = \int \mathrm{d}\mu|g_{\boldsymbol{k}}|^2\frac{\eta_{\boldsymbol{k}}/2\pi}{|\mu-\epsilon_{\boldsymbol{k}}-\mathrm{i}\eta_{\boldsymbol{k}}/2|^2} = |g_{\boldsymbol{k}}|^2\ . \tag{190}$$

The renormalization of form factor is illustrated in Fig. 15.

As is observed in Section 2.6, the decay rate is approximately given by the FGR with high accuracy. We may thus estimate the decay rate under measurements by the FGR. In this case, note that when applying the FGR the final states must be defined as eigenstates of the system in the absence of the atom–photon interaction. Under measurements, the photon states ($b^\dagger_{\boldsymbol{k}}|0\rangle$) do not satisfy this condition because of the photon–detector interaction, whereas the coupled modes ($\bar{B}^\dagger_\mu|0\rangle$ or $B^\dagger_{\boldsymbol{k}\mu}|0\rangle$) do. Therefore, in order to

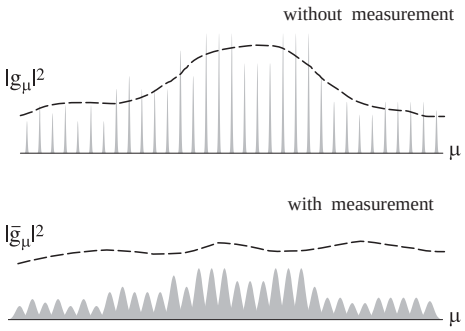


Fig. 15. Illustration of the renormalization of the form factor. The contribution of each photon mode is given by a delta function when photons are not counted, whereas it acquires finite width $\eta_{\boldsymbol{k}}$ as a counteraction of measurement. The form factor is an accumulation of contributions of all photon modes (broken line).

predict the decay rate correctly, the FGR should be applied not to the original form factor, Eq. (179), but to the renormalized form factor, Eq. (187). Then, we obtain the decay rate under measurement as

$$\Gamma(\{\tau_{\boldsymbol{k}}\}) = 2\pi|\bar{g}_\Omega|^2 = \int \mathrm{d}\boldsymbol{k}|g_{\boldsymbol{k}}|^2 \frac{\eta_{\boldsymbol{k}}}{|\Omega - \epsilon_{\boldsymbol{k}} - \mathrm{i}\eta_{\boldsymbol{k}}/2|^2} \ , \tag{191}$$

This quantity is the principal result on the QZE and AZE by the quantum measurement theory: the decay rate is modified through renormalization of form factor by measurement. If $\Gamma$ is smaller (larger) than the original decay rate without measurement, which is given by $\Gamma = 2\pi|g_\Omega|^2$, we regard that the QZE (AZE) is taking place. In Section 5.3, Eq. (191) is compared with Eq. (76), which gives the decay rate under repeated instantaneous measurements based on the projection postulate.

### *5.3. Continuous measurement with flat response*

The conventional theories of the Zeno effect (Section 3) assumed that each of the repeated measurements is instantaneous and ideal. On the other hand, we are treating here a continuous measurement. As pointed out in Section 4.6.3, these measurements are quite different from each other in general. For example, the response time $\tau_\mathrm{r} = 0$ and the measurement intervals $\tau_\mathrm{i} > 0$ in the former, whereas $\tau_\mathrm{r} > 0$ and $\tau_\mathrm{i} = 0$ in the latter. Regarding the Zeno effect, however, similarity between these different measurements has often been discussed [79]. In this subsection, we present a case where they indeed give similar results, whereas in Sections 5.4–5.6 we will present drastic cases where they give much different results.

To see the similarity, it is customary to consider that $\tau_\mathrm{r}$ (response time of the apparatus) would correspond to $\tau_\mathrm{i}$ (interval of repeated instantaneous measurements) with a possible multiplicative factor of order unity. Furthermore, it should be noted that, if one applies the projection postulate directly to the atomic states, the quantum coherences between the survived state ($\sigma_+|0\rangle$) and decayed states ($b^\dagger_{\boldsymbol{k}}|0\rangle$) are destroyed simultaneously, regardless of photon wavenumber $\boldsymbol{k}$. Therefore, the projection postulate implicitly assumes an idealized situation, in which the detector is sensitive to every photon mode with an identical response time $\tau_\mathrm{r}$. In the present model, such *flat response* is realized by putting

$$\eta_{\boldsymbol{k}} = \tau_\mathrm{r}^{-1} \quad \text{for every } \boldsymbol{k} \ . \tag{192}$$

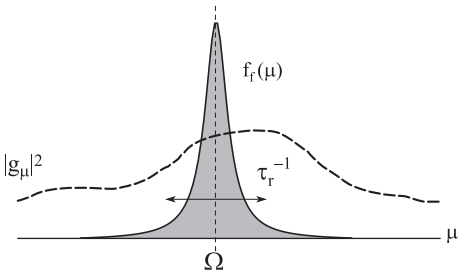


Fig. 16. Illustration of the calculation by Eq. (193) of the decay rate $\Gamma(\tau_r)$ under continuous measurement with flat response. $\Gamma(\tau_r)$ is given by integrating the form factor $|g_\mu|^2$ with a weight function $f_f(\mu)$.

In this section, using the formalism of Sections 5.1 and 5.2, we study the Zeno effect under a continuous measurement with such a detector, and compare the results with those obtained by the conventional theories.

*5.3.1. Decay rate under flat response*

When the condition of flat response [Eq. (192)] is satisfied, the general expression of the measurement-modified decay rate [Eq. (191)] is recast into the following form, using the definition of the form factor, Eq. (14):

$$\Gamma(\tau_r) = \int d\mu |g_\mu|^2 \times f_f(\mu) \ , \tag{193}$$

$$f_f(\mu) = \frac{\tau_r^{-1}}{|\mu - \Omega - i/2\tau_r|^2} \ , \tag{194}$$

Namely, the decay rate under a continuous measurement with flat response is given by integrating the original form factor $|g_\mu|^2$ with a weight function $f_f(\mu)$, as illustrated in Fig. 16. The weight function $f_f(\mu)$ has the following properties: (i) $f_f(\mu)$ is a Lorentzian centered at the atomic transition energy $\Omega$ with a spectral width $\sim \tau_r^{-1}$, and (ii) $f_f(\mu)$ is normalized as $\int d\mu f_f(\mu) = 2\pi$.

Now a close connection between repeated instantaneous measurements (Section 3.2) and continuous measurements with flat response has become apparent [84]: the difference between them lies merely in the functional forms of the weight functions $f_c(\mu)$ of Eq. (78) and $f_f(\mu)$. Thus, apart from slight quantitative discrepancy due to the difference between $f_c(\mu)$ and $f_f(\mu)$, the conventional theories presented in Section 3 based on the projection postulate can be essentially reproduced from the formalism of Sections 5.1 and 5.2 in the special case of flat response.

Furthermore, it is of note that the effects of these two measurements would coincide even at a quantitative level, when the measurement interval $\tau_i$ is a stochastic variable following a distribution function $P(\tau_i) = (2\tau_r)^{-1} \exp(-\tau_i/2\tau_r)$. In this case, the weight function for the repeated measurements is modified as follows:

$$\tilde{f}_c(\mu) = \int d\tau_i P(\tau_i) \times \tau_i \ \mathrm{sinc}^2 \left[ \frac{\tau_i(\mu - \Omega)}{2} \right] = \frac{\tau_r^{-1}}{|\mu - \Omega - i/2\tau_r|^2} \ , \tag{195}$$

which is identical to $f_f(\mu)$ [84].

Of course, the condition of flat response is not satisfied in general measurement processes, so interesting phenomena beyond the conventional theories are expected, which are the topics of Sections 5.4, 5.5 and 5.6. In the rest of Section 5.3, we confirm the qualitative agreement between these two formalisms with concrete numerical examples, based on the Lorentzian form factor [Eq. (51)], for which the Zeno effect by the conventional theories has already been revealed quantitatively in Section 3.

*5.3.2. Numerical results*

To calculate the three probabilities of physical interest, $s(t)$, $\varepsilon(t)$ and $r(t)$, we use the Green function method presented in Section 2.5. Here, an important modification is required due to the photon–detector interaction: The bare photon Green function $P(\omega, \boldsymbol{k})$, which appears in Eqs. (49) and (50), should be replaced by the dressed photon Green function $\bar{P}(\omega, \boldsymbol{k})$. Following Section 2.5, the dressed Green function is given by

$$\bar{P}(\omega, \boldsymbol{k}) = \frac{P(\omega, \boldsymbol{k})}{1 - \Sigma(\omega, \boldsymbol{k}) P(\omega, \boldsymbol{k})} , \tag{196}$$

where $P(\omega, \boldsymbol{k})$ and $\Sigma(\omega, \boldsymbol{k})$ are the bare Green function and the self-energy of the photon $\boldsymbol{k}$, respectively, which are given by

$$P(\omega, \boldsymbol{k}) = \frac{1}{\omega - \epsilon_{\boldsymbol{k}} + \mathrm{i}\delta} , \tag{197}$$

$$\Sigma(\omega, \boldsymbol{k}) = \int \mathrm{d}\mu \frac{|\xi_{\boldsymbol{k}\mu}|^2}{\omega - \mu + \mathrm{i}\delta} = -\frac{\mathrm{i}\eta_{\boldsymbol{k}}}{2} . \tag{198}$$

Substituting Eqs. (197) and (198) into Eq. (196), we obtain the dressed Green function of the photon $\boldsymbol{k}$ as

$$\bar{P}(\omega, \boldsymbol{k}) = \frac{1}{\omega - \varepsilon_{\boldsymbol{k}} + \mathrm{i}\eta_{\boldsymbol{k}}/2} . \tag{199}$$

The change from $P(\omega, \boldsymbol{k})$ to $\bar{P}(\omega, \boldsymbol{k})$ represents the renormalization effect, which is discussed in Section 5.2, in the language of the Green function method. We can calculate $s(t)$, $\varepsilon(t)$ and $r(t)$ numerically using $\bar{P}(\omega, \boldsymbol{k})$.

In Fig. 17, the temporal evolutions of the three probabilities are plotted. In Fig. 17(a), the response of the detector is assumed to be very slow ($\tau_{\mathrm{r}} \sim \gamma^{-1}$), in order to visualize the delay of the detector response. As a result, the decay dynamics $s(t)$ is almost unchanged from the unobserved case. We can confirm that $r(t)$ follows $1 - s(t)$ with a delay time $\sim \tau_{\mathrm{r}}$; thus, $\tau_{\mathrm{r}}$ may safely be regarded as the response time of the detector. Recall that as noticed in Section 4.5.1 $\tau_{\mathrm{r}}$ is actually the *lower limit* of the response time because additional delays in the response, such as delays in signal magnification processes, may occur in practical experiments. In discussing fundamental physics, the limiting value is more significant than practical values, which depend strongly on detailed experimental conditions. A typical value of $\tau_{\mathrm{r}}$ for GaAs is $10^{-15}$s, which is much shorter than the practical response times of commercial photodetectors, which range from $10^{-6}$ to $10^{-13}$s. In the case of measurement of the decay of an excited atom by semiconductor photodetectors, we can usually assume that $\tau_{\mathrm{r}} \ll \gamma^{-1}$ because $\gamma^{-1} \sim 10^{-9}$s typically. The results for such quick response are plotted in Fig. 17(b). Furthermore, $r(t)$ follows $1 - s(t)$ almost without decay, and that the measurement error $\varepsilon(t)$ almost vanishes for all time. It is observed that the decay is slowed down as compared with (a), i.e., the QZE occurs under a continuous measurement with quick and flat response.

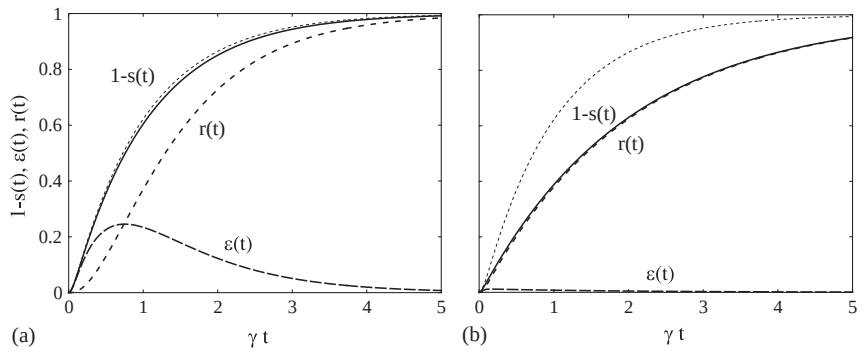


Fig. 17. Temporal evolutions of $1-s(t)$, $\varepsilon(t)$, and $r(t)$. The parameters are chosen as $\Delta = 20\gamma$ (i.e., $t_{\rm j} = 0.05\gamma^{-1}$), $|\Omega - \mu_0| = 0$. The response time of the detector is chosen as $\tau_{\rm r} = 0.5\gamma^{-1}$ in (a), and $\tau_{\rm r} = 0.025\gamma^{-1}$ in (b). $r(t)$ follows $1-s(t)$ with a delay time that is approximately given by $\tau_{\rm r}$. Thin dotted lines show the unobserved decay probability.

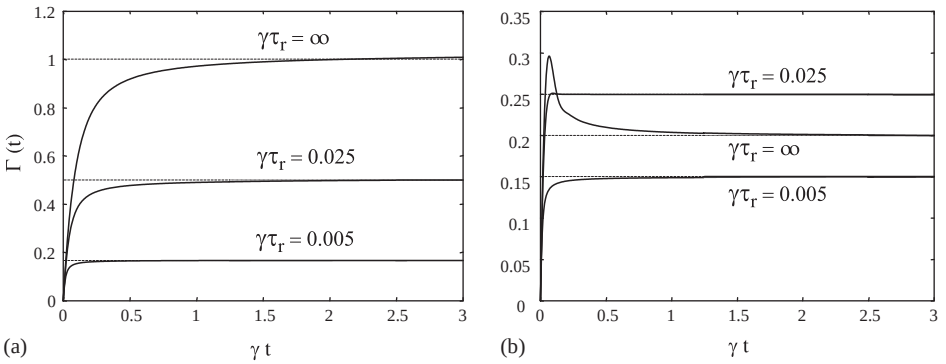


Fig. 18. Temporal evolution of $\Gamma(t)$, where $\Delta = 20\gamma$ (i.e., $t_{\rm j} = 0.05\gamma^{-1}$). $\Omega - \mu_0 = 0$ in (a), and $\Omega - \mu_0 = 2\Delta$ in (b). The values of the response time $\tau_{\rm r}$ are indicated in the figures. The decay rate agrees well with the FGR decay rate (thin dotted lines), which is given by Eq. (202).

In both Figs. 17(a) and (b), emitted photons are all counted by the detector. Therefore, $r(t) \to 1$ and $\varepsilon(t) \to 0$ as $t \to \infty$.

In order to see more details, $\Gamma(t) = -\ln s(t)/t$ is plotted in Fig. 18 for several values of the response time $\tau_{\rm r}$ of the detector. As for the initial behavior of $\Gamma(t)$, it is confirmed that $\Gamma(t)$ increases linearly in time as $\Gamma(t) = \gamma\Delta t$, regardless of the values of $\Omega - \mu_0$ and $\tau_{\rm r}$. This feature is completely the same as that of the free evolution of the atom–photon system (Fig. 7).[33] On the other hand, in the later stage of decay ($t \gtrsim t_{\rm j}$), it is confirmed that $\Gamma(t)$ approaches a constant value, indicating that the decay proceeds exponentially with a well-defined decay rate. It is also confirmed that the decay rate agrees well with the FGR decay rate applied to the renormalized form factor (thin dotted lines in Fig. 18), which will be

[33] The initial behavior of survival probability is given by $s(t) = 1 - (\langle \hat{H}^2 \rangle - \langle \hat{H} \rangle^2)t^2$, where $\langle \cdots \rangle = \langle {\rm i}| \cdots |{\rm i} \rangle$ and $\hat{H}$ is the enlarged Hamiltonian for S+A, given by Eq. (172). However, $\langle \hat{H}^2 \rangle - \langle \hat{H} \rangle^2 = \langle \hat{H}_S^2 \rangle - \langle \hat{H}_S \rangle^2$, i.e., the measurement terms $(\hat{H}_{\rm int} + \hat{H}_A)$ play no role in determining the initial behavior of $s(t)$.

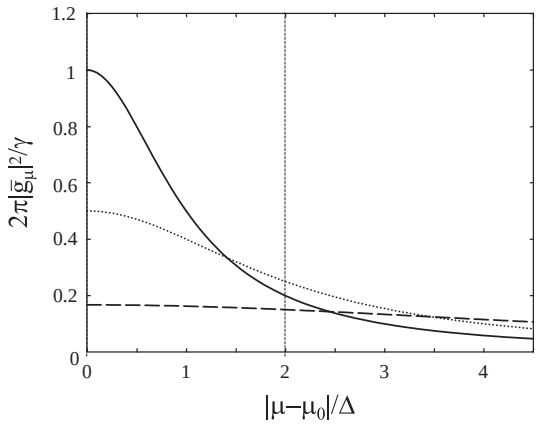


Fig. 19. Renormalization of the form factor. The original form factor is plotted by the solid line, and the renormalized form factors for $\tau_r = 0.025\gamma^{-1}$ (slow response) and $0.005\gamma^{-1}$ (fast response) are plotted by dotted and dashed lines, respectively. At $\mu = \mu_0$, $|\bar{g}_{\mu_0}|^2$ decreases monotonically as $\tau_r$ becomes shorter, which corresponds to Fig. 18(a). In contrast, at $\mu = \mu_0 + 2\Delta$, $|\bar{g}_{\mu_0+2\Delta}|^2$ is increased (decreased) for slow (fast) response, in comparison to the unobserved case. This feature corresponds to Fig. 18(b).

discussed in Section 5.3.3 in detail. Note also that in Fig. 18(a), where $\Omega - \mu_0 = 0$, the decay rate decreases monotonically as $\tau_r$ is shortened. In contrast, in Fig. 18(b), where $\Omega - \mu_0 = 2\Delta$, an increase of the decay rate (the AZE) is observed for large $\tau_r$, whereas suppression of decay (the QZE) is observed for small $\tau_r$.

*5.3.3. Renormalized FGR decay rate*

We can explain the above numerical results in terms of the renormalization of the form factor, which was discussed in Section 5.2. Using Eqs. (14), (51), (187) and (192), we obtain the renormalized form factor as

$$|\bar{g}_\mu|^2 = \frac{\gamma}{2\pi}\frac{\Delta(\Delta + (2\tau_r)^{-1})}{(\mu-\mu_0)^2 + (\Delta + (2\tau_r)^{-1})^2}\ , \tag{200}$$

which is, again, a Lorentzian centered at $\mu = \mu_0$. As a result of the continuous measurement, the width of the form factor is broadened as $\Delta \to \Delta + (2\tau_r)^{-1}$, satisfying the following sum rule;

$$\int \mathrm{d}\mu |\bar{g}_\mu|^2 = \frac{\gamma\Delta}{2}\ . \tag{201}$$

The renormalized form factor is plotted in Fig. 19. Applying the Fermi golden rule to Eq. (188), the atomic decay rate is calculated as [34]

$$\Gamma(\tau_r) = 2\pi|\bar{g}_\Omega|^2 = \gamma\frac{\Delta(\Delta + (2\tau_r)^{-1})}{(\Omega-\mu_0)^2 + (\Delta + (2\tau_r)^{-1})^2}\ . \tag{202}$$

It is confirmed from Fig. 18 that the FGR decay rate agrees well with the rigorous numerical results.

[34] One can also derive Eq. (202), combining Eqs. (51), (193) and (194).

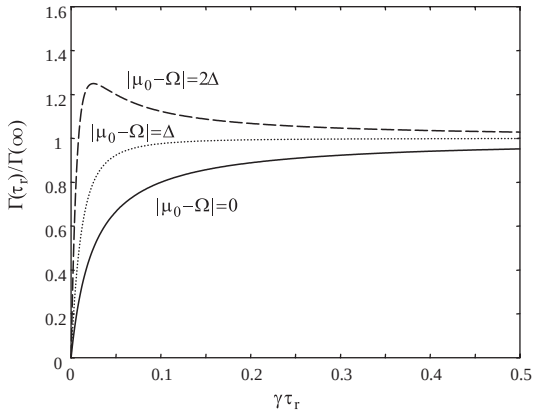


Fig. 20. Dependence of the normalized decay rate $\Gamma(\tau_r)/\Gamma(\infty)$ on the response time $\tau_r$ of detector, which is given by Eq. (203). The parameters are the same as Fig. 9; $\Delta = 20\gamma$ ($t_j = 0.05\gamma^{-1}$) and the values of $|\Omega - \mu_0|$ are indicated in this figure. For $|\Omega - \mu_0| = 2\Delta$, the decay rate is maximized when $\tau_r = 0.025\gamma^{-1}$.

In order to clarify the effect of measurement, the decay rate under the continuous measurement is normalized by the unobserved decay rate $\Gamma(\infty)$ in Fig. 20. It is given by

$$\frac{\Gamma(\tau_r)}{\Gamma(\infty)} = \frac{\Delta + (2\tau_r)^{-1}}{\Delta} \frac{(\Omega - \mu_0)^2 + \Delta^2}{(\Omega - \mu_0)^2 + (\Delta + (2\tau_r)^{-1})^2} \ . \tag{203}$$

This quantity for the case of repeated instantaneous ideal measurements has been calculated in Fig. 9. By comparing Figs. 9 and 20, we find that the results for the two cases agree semi-quantitatively with each other if we identify the measurement intervals $\tau_i$ of Fig. 9 with the response time $\tau_r$ of Fig. 20 as $\tau_i \simeq 2.64\tau_r$. (However, complete quantitative agreement is not attained: For example, the peak values of the decay rate for $|\mu_0 - \Omega| = 2\Delta$ (broken line) are different between Figs. 9 and 20.) Furthermore, Eq. (203) indicates that the Zeno effect becomes significant when $(2\tau_r)^{-1} \gtrsim \Delta$, i.e.,

$$\tau_r \lesssim \Delta^{-1} = t_j \ , \tag{204}$$

which is certainly confirmed in Fig. 18. A similar condition, Eq. (80), has been obtained also for repeated instantaneous ideal measurements by the conventional theory.

The above observations demonstrate that, in an idealized case where every photon is detected with the same response time (*flat* response), repeated instantaneous ideal measurements and a continuous measurement give similar results for the Zeno effect.

### *5.3.4. QZE–AZE phase diagram*

By analyzing Eq. (203) as a function of $|\Omega - \mu_0|$ and $\tau_r$, a 'phase diagram' discriminating the QZE and AZE is generated, which is shown in Fig. 21. The 'phase boundary' (solid curve) is given by

$$\tau_r^{(b)} = \frac{\Delta}{2[(\Omega - \mu_0)^2 - \Delta^2]} \ , \tag{205}$$

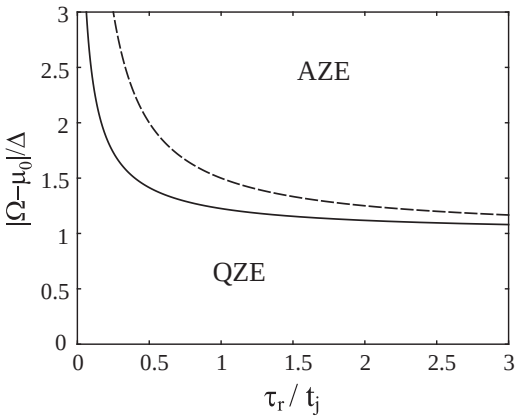


Fig. 21. The phase diagram for the QZE and the AZE, for a case of Lorentzian form factor and a continuous measurement with flat response. The solid curve divides the QZE region and the AZE region. The dotted line shows the value of $\tau_{\mathrm{r}}$ at which the decay rate is maximized for each value of $|\Omega-\mu_0|$.

on which the decay rate is not altered from the free rate, i.e., $\Gamma(\tau_{\mathrm{r}}^{(\mathrm{b})})=\Gamma(\infty)$. The decay rate takes the maximum value,

$$\frac{\Gamma(\tau_{\mathrm{r}}^{(\mathrm{m})})}{\Gamma(\infty)}=\frac{|\Omega-\mu_0|^2+\Delta^2}{2\Delta|\Omega-\mu_0|}-1\ , \tag{206}$$

on the dotted line, which is given by

$$\tau_{\mathrm{r}}^{(\mathrm{m})}=\frac{1}{2(|\Omega-\mu_0|-\Delta)}\ . \tag{207}$$

When the atomic transition energy is close to the center of the form factor ($|\Omega-\mu_0|\lesssim\Delta$), only the QZE is observed. However, in the opposite case ($|\Omega-\mu_0|\gtrsim\Delta$), the AZE is observed dominantly except for an extremely small response time. In this respect, one may say that the AZE is more widely expected than the QZE [51]. It should be remarked that Fig. 21 agrees semi-quantitatively with Fig. 10, which is the phase diagram for repeated instantaneous ideal measurements.

### *5.4. Geometrically imperfect measurement*

In the previous section, we have discussed the Zeno effect under an continuous measurement with flat response, in which all photons are detected with the same response time. In the following subsections, we discuss more realistic measurement processes, in which the response time may be different among different photon modes.

As an example of such realistic measurements, we consider in this subsection a *geometrically* imperfect measurement [85], in which the detector is inactive to photons in some modes because of a geometric condition. For example, suppose that the photoabsorptive medium composing the detector is sensitive only to the $x$-component of the electric field. Then, the photon–detector interaction becomes proportional to $\boldsymbol{e}_{\boldsymbol{k}\lambda}\cdot\boldsymbol{e}_x$, where $\boldsymbol{e}_{\boldsymbol{k}\lambda}$ is the polarization vector, which is perpendicular to $\boldsymbol{k}$, and $\boldsymbol{e}_x=(1,0,0)$. Therefore, such a detector is inactive to photons whose wavevector $\boldsymbol{k}$ is oriented in the $x$ direction, for example.

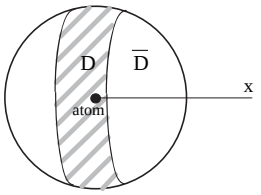


Fig. 22. Illustration of geometrically imperfect measurement. The detector covers only a part of the whole solid angle around the atom, and some of emitted photons are lost without being detected.

To discuss essential points of the geometrically imperfect measurements, we here consider a simplified example, in which the detector has an active solid angle $\mathscr{D}$ and an inactive solid angle $\bar{\mathscr{D}}$ around the atom, as illustrated in Fig. 22. We assume that the detector can catch an emitted photon with a unique response time $\tau_{\mathrm{r}}$ when the wavevector of the photon is oriented inside of $\mathscr{D}$; otherwise, the detector misses the photon. Thus, we put

$$\eta_{\boldsymbol{k}} = \begin{cases} \tau_{\mathrm{r}}^{-1} & (\boldsymbol{k} \in \mathscr{D}) \ , \\ 0 & (\boldsymbol{k} \in \bar{\mathscr{D}}) \ . \end{cases} \tag{208}$$

As for the atom–photon coupling, we assume the Lorentzian form factor again and take the following form:

$$\int_{\boldsymbol{k}\in\mathscr{D}} \mathrm{d}\boldsymbol{k} |g_{\boldsymbol{k}}|^2 \delta(\epsilon_{\boldsymbol{k}} - \mu) = \frac{(1-\varepsilon_\infty)\gamma}{2\pi} \frac{\Delta^2}{\Delta^2 + (\mu-\mu_0)^2} \ , \tag{209}$$

$$\int_{\boldsymbol{k}\in\bar{\mathscr{D}}} \mathrm{d}\boldsymbol{k} |g_{\boldsymbol{k}}|^2 \delta(\epsilon_{\boldsymbol{k}} - \mu) = \frac{\varepsilon_\infty\gamma}{2\pi} \frac{\Delta^2}{\Delta^2 + (\mu-\mu_0)^2} \ . \tag{210}$$

The newly introduced parameter $\varepsilon_\infty$ represents the probability that the emitted photon is lost without being detected. For example, if spontaneous emission occurs spherically symmetrically (i.e., $g_{\boldsymbol{k}}$ is independent of the direction of $\boldsymbol{k}$), and if the detector is sensitive only to the $x$-component of the electric field, then $\varepsilon_\infty = 1/3$. In general cases such as the case of the dipole radiation, $\varepsilon_\infty$ also depends on the direction of the transition dipole of the atom.

The temporal behaviors of $s(t)$, $\varepsilon(t)$ and $r(t)$ are plotted in Fig. 23. Contrarily to the case of flat response, which is plotted in Fig. 17, $\varepsilon(t) \to \varepsilon_\infty$ ($\neq 0$) and $r(t) \to 1-\varepsilon_\infty$ ($\neq 1$) even in the limit of $t \to \infty$. Using Eqs. (191), (187), (209), (210) and (208), we can calculate the decay rate as

$$\Gamma(\tau_{\mathrm{r}}, \varepsilon_\infty) = (1-\varepsilon_\infty)\gamma \frac{\Delta(\Delta + (2\tau_{\mathrm{r}})^{-1})}{(\Omega-\mu_0)^2 + (\Delta + (2\tau_{\mathrm{r}})^{-1})^2} + \varepsilon_\infty\gamma \frac{\Delta^2}{(\Omega-\mu_0)^2 + \Delta^2} \tag{211}$$

$$= \varepsilon_\infty \Gamma(\infty) + (1-\varepsilon_\infty)\Gamma(\tau_{\mathrm{r}}) \ . \tag{212}$$

Here, $\Gamma(\infty)$ is the free decay rate and $\Gamma(\tau_{\mathrm{r}})$ is the decay rate under continuous measurement with flat response, Eq. (202). Thus, the decay rate is simply given by these mixture under geometrically imperfect measurement. It is therefore clear that if $\varepsilon_\infty \sim 1$ then the decay rate in this case differs much from that under repeated instantaneous ideal measurements. Although this result may sound rather trivial, more surprising examples will be presented in the following subsections.

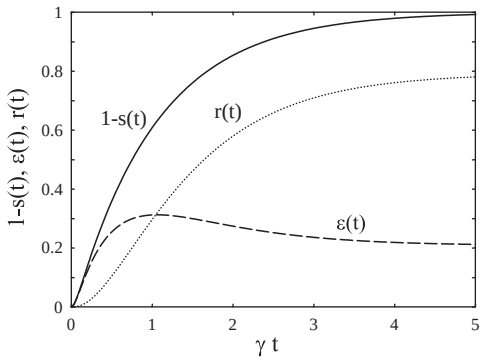


Fig. 23. Temporal evolutions of $1-s(t)$, $\varepsilon(t)$, and $r(t)$. The values of the parameters are the same as in Fig. 17 (i.e., $t_{\rm j}=0.05\gamma^{-1}$, $|\Omega-\mu_0|=0$, $\tau_{\rm r}=0.5\gamma^{-1}$) except that $\varepsilon_\infty=0.2$ in this figure.

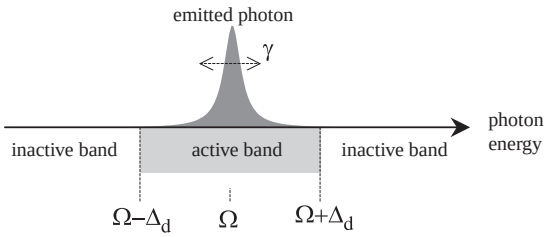


Fig. 24. Illustration of an energetically imperfect measurement. The gray spike represents the energy spectrum of an emitted photon, which is defined by $I(\omega)=\lim_{t\to\infty}\int {\rm d}\boldsymbol{k}\delta(\epsilon_{\boldsymbol{k}}-\omega)|\langle 0|b_{\boldsymbol{k}}{\rm e}^{-{\rm i}H_S t}\sigma_+|0\rangle|^2$. The detector is sensitive only to photons within the active detection band, which spans $(\Omega-\Delta_{\rm d},\Omega+\Delta_{\rm d})$. In the model of Sections 5.5 and 5.6, where Eq. (215) is assumed, $I(\omega)$ becomes proportional to the dressed atomic Green function $\bar{A}(\omega)$, which is given by Eq. (48).

### 5.5. *Quantum Zeno effect by energetically imperfect measurement*

Actual materials composing photodetectors are sensitive only to photons within a restricted energy range, which is the source of another kind of imperfectness of measurement. Thus, we are led to consider *energetically* imperfect measurement [24], where, as illustrated in Fig. 24, the range of the measurement of photons by the photodetector does not cover all the energy range of a photon. In other words, the photodetector has a finite detection band. To simplify the discussion, we consider the case where the detector responds with an identical response time $\tau_{\rm r}$ to a photon if its energy $\epsilon_{\boldsymbol{k}}$ falls in the detection band as $|\epsilon_{\boldsymbol{k}}-\Omega|<\Delta_{\rm d}$, whereas it does not respond to photons outside of this detection band. Thus, we take the following form for the photon–detector coupling:

$$\eta_{\boldsymbol{k}}=\eta_{\epsilon_{\boldsymbol{k}}}=\begin{cases}\tau_{\rm r}^{-1} & (|\epsilon_{\boldsymbol{k}}-\Omega|<\Delta_{\rm d})\ ,\\ 0 & (\text{otherwise})\ .\end{cases} \tag{213}$$

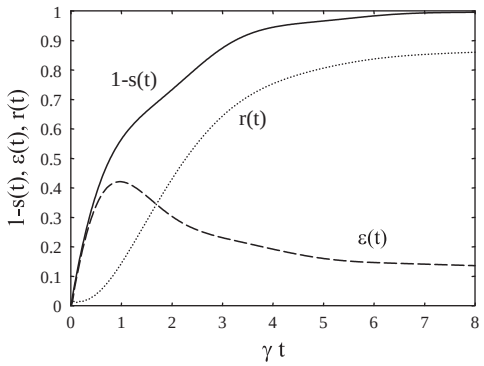


Fig. 25. Temporal evolutions of $1-s(t)$, $\varepsilon(t)$, and $r(t)$. The parameters are chosen as follows: $\Delta_{\rm d}=2\gamma$ and $\gamma\tau_{\rm r}=0.5$.

It is of note that when $\eta_{\boldsymbol{k}}$ depends only on the photonic energy, namely, $\eta_{\boldsymbol{k}}=\eta_{\epsilon_{\boldsymbol{k}}}$, the formula Eq. (187) for the renormalized form factor is recast into the following simplified form:

$$|\bar{g}_\mu|^2=\int {\rm d}\omega|g_\omega|^2\frac{\eta_\omega/2\pi}{|\mu-\omega-{\rm i}\eta_\omega/2|^2}\ . \tag{214}$$

*5.5.1. A model for an exact exponential decay*

As for the atom–photon coupling, we treat a special case where the unobserved form factor is given by a constant function:

$$|g_\mu|^2=\int {\rm d}\boldsymbol{k}|g_{\boldsymbol{k}}|^2\delta(\mu-\epsilon_{\boldsymbol{k}})=\frac{\gamma}{2\pi}\ , \tag{215}$$

which is the $\Delta\to\infty$ limit of a Lorentzian form factor. One reason why we have employed this form factor is that we expect that the qualitative results will not be much different for other cases if the unobserved form factor has a finite $\Delta$. Another reason, which is more important, is that the above model extracts most clearly a drastic feature of the Zeno effect under energetically imperfect measurement. To see this, we note the following points peculiar to the above form factor: (i) The survival probability exactly follows the exponential decay law as $s(t)=\exp(-\gamma t)$, i.e., the jump time $t_{\rm j}$ $(=\Delta^{-1})$ is zero (see Section 2.6). (ii) The conventional theory therefore predicts that the system undergoes neither the QZE nor the AZE (see Section 3.3). (iii) Neither effect can be induced in this system by a continuous measurement with flat response, which is proven to yield equivalent results to the conventional theory (see Section 5.3.1). However, we will show in the following part of this subsection that the QZE *can* be induced when the measurement is energetically imperfect.

*5.5.2. Numerical results*

First we present the numerical results based on the Green function method. Using the fact that the lineshape of emitted photons is an exact Lorentzian with width $\gamma/2$, the probability of obtaining the detector response is naively expected to be $r(\infty)=(2/\pi)\arctan(2\Delta_{\rm d}/\gamma)$. Therefore, significant measurement error will result when the detection bandwidth $\Delta_{\rm d}$ is small as $\Delta_{\rm d}\lesssim\gamma$. In Fig. 25, temporal behaviors of $1-s(t)$, $\varepsilon(t)$ and $r(t)$ are plotted, for a case of narrow detection band ($\Delta_{\rm d}=2\gamma$). The probability of photodetection

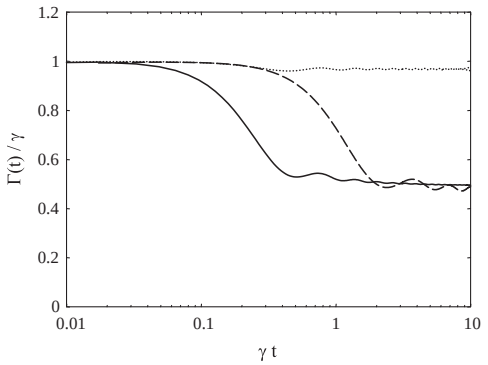


Fig. 26. Temporal evolution of $\Gamma(t)$. $\{\Delta_d, \tau_r\}$ are chosen at $\{10\gamma, 0.05\gamma^{-1}\}$ (solid line), $\{2\gamma, 0.25\gamma^{-1}\}$ (broken line) and $\{10\gamma, \gamma^{-1}\}$ (dotted line).

is in good agreement with naive estimation, $r(\infty) = (2/\pi)\arctan(2\Delta_d/\gamma) = 0.84$. By looking at the decay probability $1 - s(t)$, it is observed that the decay is slightly suppressed for $t \gtrsim \gamma^{-1}$.

The change of the decay rate is more emphasized in Fig. 26, where temporal evolution of $\Gamma(t) = -\ln s(t)/t$ is plotted for three different values of $\Delta_d$ and $\tau_r$. It should be recalled that $\Gamma(t)$ reduces to a constant function ($=\gamma$) when the atom is not measured. This feature is contrary to the models with a finite jump time, where $\Gamma$ always approaches zero as $t \to 0$ as a result of quadratic decrease of $s(t)$ (see, e.g., Fig. 7). We find the following two-stage behavior of $\Gamma(t)$ in Fig. 26: Initially, the decay rate is identical to the unobserved rate $\gamma$, whereas the decay proceeds with a suppressed rate in the later stage. For example, when $\Delta_d = 10\gamma$ and $\tau_r = 0.05\gamma^{-1}$ (solid line in Fig. 26), the decay rate changes from $\gamma$ to $0.5\gamma$ at $t \sim 0.1\gamma^{-1}$. Since the atom is kept almost undecayed at the crossover time [$s(t \sim 0.1\gamma^{-1}) \simeq 0.9$], significant decay occurs in the second stage with a suppressed rate. Thus, the QZE is surely taking place for the exponentially decaying system.

### 5.5.3. Conditions for QZE

Here, we explore the underlying mechanisms of the two-stage behavior of decay rate, and clarify the condition for inducing the QZE. Using Eqs. (213)–(215), the renormalized form factor is calculated as

$$|\bar{g}_\mu|^2 = \frac{\gamma}{4\pi^2}\int \mathrm{d}\omega \frac{\eta_\omega}{|\mu - \omega - \mathrm{i}\eta_\omega/2|^2} \tag{216}$$

$$= \frac{\gamma}{2\pi^2}\left[\pi\theta(|\mu - \Omega| - \Delta_d) + \arctan(2\tau_r(\mu - \Omega + \Delta_d)) - \arctan(2\tau_r(\mu - \Omega - \Delta_d))\right] , \tag{217}$$

where $\theta(x)$ is a step function. The renormalized form factor is plotted in Fig. 27 for three different values of $\tau_r\Delta_d$. The form factor is modified locally around the band edge in case of large $\tau_r\Delta_d$, whereas global modification occurs for small $\tau_r\Delta_d$. $|\bar{g}_\mu|^2$ approaches the unobserved value $\gamma/2\pi$ in the limit of $|\mu - \Omega| \to \infty$, regardless of $\tau_r\Delta_d$. Considering that the value of the form factor at $\mu = \Omega$ is given by $|\bar{g}_\Omega|^2 = (\gamma/\pi^2)\arctan(2\tau_r\Delta_d)$, we obtain the condition for significant decrease of the form factor at $\mu = \Omega$ as

$$\tau_r\Delta_d \lesssim 1 . \tag{218}$$

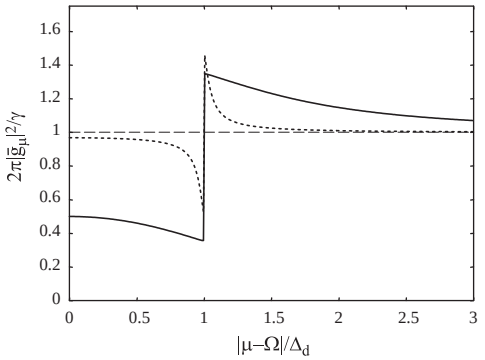


Fig. 27. Renormalization of form factor. The original form factor without measurement, which corresponds to $\tau_r \to \infty$ limit, is a constant function (thin broken line). The renormalized form factors are plotted for $\tau_r \Delta_d = 0.5$ (solid line) and $\tau_r \Delta_d = 10$ (broken line).

The two-stage behavior can be understood with a help of the perturbation theory in $g$. Applying the lowest-order perturbation to the renormalized Hamiltonian Eq. (188), we obtain the decay probability as

$$1 - s(t) = \int \mathrm{d}\mu \; |\bar{g}_\mu|^2 \frac{\sin^2[(\mu - \Omega)t/2]}{[(\mu - \Omega)/2]^2} \; . \tag{219}$$

Taking into account that the main contribution in the integral comes from the region of $\mu$ satisfying $|\mu - \Omega| \lesssim 2\pi t^{-1}$, we evaluate the right-hand side in two limiting cases: In the case of $t \ll \Delta_d^{-1}$, $|\bar{g}_\mu|^2$ can be approximated by $|\bar{g}_\infty|^2 = \gamma/2\pi$, which coincides with the free decay rate $1 - s(t) = \gamma t$; whereas in the opposite case of $t \gg \Delta_d^{-1}$, $|\bar{g}_\mu|^2$ can be approximated by $|\bar{g}_\Omega|^2$, which gives the suppressed decay rate $1 - s(t) = 2\pi |\bar{g}_\Omega|^2 t$. Thus, the decay rate changes from the free rate to the suppressed rate at $t \sim \Delta_d^{-1}$. We can confirm that this statement agrees with the results in Fig. 26.

Now the conditions for inducing the QZE in exponentially decaying systems are clarified: (i) The decay rate in the second stage should be significantly suppressed from the free decay rate. This condition is expressed by inequality (218). (ii) The transition from the first to the second stage should occur before the atom decays. Since the survival probability at the crossover time ($t \sim \Delta_d^{-1}$) is roughly given by $s(\Delta_d^{-1}) \simeq \exp(-\gamma/\Delta_d)$, this condition is expressed as $\exp(-\gamma/\Delta_d) \simeq 1$, i.e.,

$$\gamma \ll \Delta_d \; , \tag{220}$$

which means that the detection band should completely cover the radiative linewidth of the atom. Note that if the detection bandwidth is not so large ($\Delta_d \sim \gamma$) the *partial quantum Zeno effect* takes place, where suppression of decay starts during the decay (at $t \sim \gamma^{-1}$). The behavior of $s(t)$ in Fig. 25 serves as an example of the partial QZE.

To summarize this subsection, when the detector has a finite detection bandwidth the QZE can be induced even in a system which exactly follows the exponential decay law. The conditions for inducing the QZE on the response time and the bandwidth are given by inequalities (218) and (220), respectively. One might immediately notice that these results seemingly contradict with the well-known wisdom on the QZE, which states that neither the QZE nor the AZE takes place in exactly exponentially decaying systems, as has been shown in Section 3.3. This point will be discussed in Section 5.7.1.

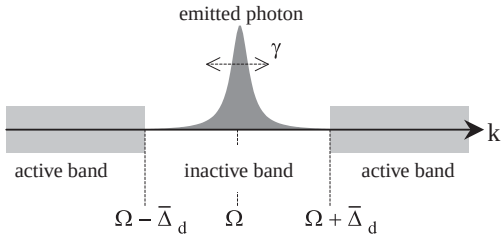


Fig. 28. Illustration of the false measurement. The detector is insensitive to photons within the inactive detection band, which spans $(\Omega - \bar{\Delta}_{\rm d}, \Omega + \bar{\Delta}_{\rm d})$.

### 5.6. Quantum anti-Zeno effect by false measurement

In Section 5.5, we have observed that the QZE can be induced even in systems which exactly follows the exponential decay law, when the measurement is energetically imperfect. There, the detector was assumed to be active only for photons close to the atomic transition energy, as shown in Fig. 24. In this section, we consider the opposite situation, where the active band of the detector does not match the energy of a photon emitted from the atom, as illustrated in Fig. 28 [25]. To study this case, we assume the following form for $\eta_{\boldsymbol{k}}$:

$$\eta_{\boldsymbol{k}} = \eta_{\epsilon_{\boldsymbol{k}}} = \begin{cases} \tau_{\rm r}^{-1} & (|\epsilon_{\boldsymbol{k}} - \Omega| > \bar{\Delta}_{\rm d}) \ , \\ 0 & (\text{otherwise}) \ . \end{cases} \tag{221}$$

A photon which has the atomic transition energy $\Omega$ cannot be detected by such an detector. We here refer to such measurements as *false measurements*. In most of previous discussions on the Zeno effects, it was assumed that measuring apparatus can detect the decay with a high efficiency, because the Zeno effect is supposed to appear only weakly if measurements on the target system are ineffective, as has been confirmed in Section 5.4 for the case of continuous measurement with flat response. However, we will show that the Zeno effect can take place even under false measurements.

#### 5.6.1. Natural linewidth

As for the atom–photon coupling, we again employ Eq. (215), by which the atomic decay follows an exact exponential decay law. The spectrum of the emitted photon therefore becomes a Lorentzian centered around the atomic transition energy $\Omega$ with width $\gamma$, as illustrated in Fig. 28.

If $\gamma$ were larger than $\bar{\Delta}_{\rm d}$, then the probability that an emitting photon is detected would become large. However, we consider the opposite case where $\gamma \ll \bar{\Delta}_{\rm d}$, for which the detection efficiency would be expected to be very small. When $\bar{\Delta}_{\rm d} = 10\gamma$, for example, we can estimate, noting that the lineshape is an exact Lorentzian, the fraction of photons emitted in the active band as $1 - (2/\pi)\arctan(2\bar{\Delta}_{\rm d}/\gamma) \simeq 3.2\%$. Therefore, it is naively expected that almost no photons would be counted by the detector and that such a false measurement would not affect the decay dynamics of the atom significantly. We will show that this naive expectation is wrong, by numerically solving the Schödinger equation in the next subsection. The conditions for inducing the Zeno effect will be described in Section 5.6.3.

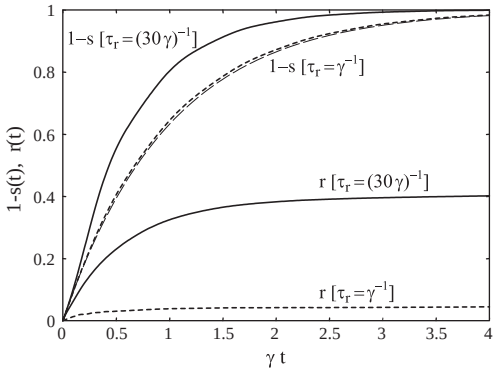


Fig. 29. Temporal evolutions of $1-s(t)$ and $r(t)$. The dotted and solid lines show the results for $\tau_r=\gamma^{-1}$ (slow detector response) and $\tau_r=(30\gamma)^{-1}$ (fast detector response). The inactive bandwidth $\bar{\Delta}_d$ is $10\gamma$. The thin broken line shows the decay probability for unobserved case, where $1-s(t)=1-e^{-\gamma t}$.

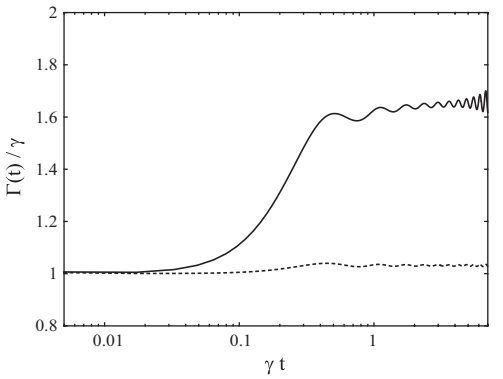


Fig. 30. Temporal evolution of $\Gamma(t)$, where $\bar{\Delta}_d=10\gamma$, and $\tau_r=\gamma^{-1}$ (dotted line) and $(30\gamma)^{-1}$ (solid line). The system decays with the unobserved decay rate $\gamma$ for $t\lesssim\bar{\Delta}_d^{-1}$, and with the enhanced decay rate $2\pi|\bar{g}_\omega|^2$ for $t\gtrsim\bar{\Delta}_d^{-1}$.

### *5.6.2. Numerical results*

The temporal behaviors of $1-s(t)$ and $r(t)$ are drawn in Fig. 29, where the inactive bandwidth $\bar{\Delta}_d$ $(=10\gamma)$ is much larger than $\gamma$, and the *false* measurement is realized. When the detector response is slow ($\tau_r=\gamma^{-1}$, dotted lines in Fig. 29), the decay probability is almost unchanged from that of the unobserved case, i.e., $1-s(t)\simeq 1-e^{-\gamma t}$. In this case, although a photon is emitted upon decay, detection of the emitted photon is almost unsuccessful, i.e., $r(t)\simeq 0$. Such behaviors of $1-s(t)$ and $r(t)$ agree with the above naive expectation on false measurements.

However, when the detector response is fast ($\tau_r=(30\gamma)^{-1}$, solid lines in Fig. 29), we find that the detection probability of the emitted photon becomes surprisingly large ($\sim 40\%$). Furthermore, the decay is significantly promoted, which is nothing but the AZE. In Fig. 30, $\Gamma(t)=-\ln s(t)/t$ is plotted to visualize the decay rate. The figure clarifies that the decay rate changes from the unobserved rate $\gamma$ to the enhanced rate $\bar{\gamma}$ ($\simeq 1.6\gamma$) at $t\sim 0.1\gamma^{-1}$. Because the atom is kept almost excited at that moment, it decays with the enhanced rate. This result would be quite unexpected, considering that the energy of the

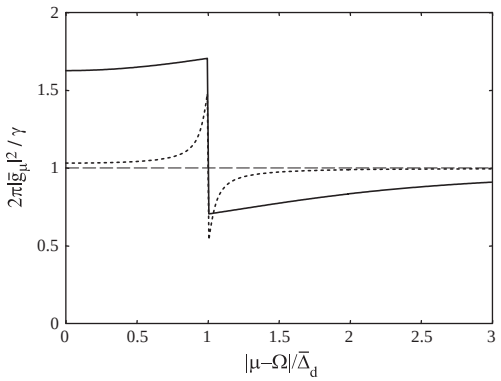


Fig. 31. Plot of the renormalized form factor $|\bar{g}_\mu|^2$ under the measurement, for $\tau_r\bar{\Delta}_d = \infty$ (thin broken line), 10 (dotted line), and 1/3 (solid line).

emitted photon lies almost completely in the inactive band of the detector and therefore that the detector seemingly cannot touch the target system.

### 5.6.3. *Conditions for AZE*

The unexpected results shown in Section 5.6.2 can be understood in terms of the renormalized form factor. It is given by

$$|\bar{g}_\mu|^2 = \frac{\gamma}{2\pi^2}[\pi + \pi\theta(\bar{\Delta}_d - |\mu-\Omega|) + \arctan(2\tau_r(\mu-\Omega-\bar{\Delta}_d)) - \arctan(2\tau_r(\mu-\Omega+\bar{\Delta}_d))] \ , \tag{222}$$

which is plotted in Fig. 31. Contrary to Fig. 27, the form factor is increased at the atomic transition energy, $\mu = \Omega$. In case of false measurements, the form factor is always increased inside the inactive band, which implies that false measurements always result in the enhancement of decay (the AZE).[35]

Following Section 5.5.3, the conditions for inducing the AZE is summarized as follows: (i) The decay rate in the second stage $\bar{\gamma}$ should be significantly enhanced from the free decay rate. This condition is expressed by the following inequality:

$$\tau_r\bar{\Delta}_d \lesssim 1 \ , \tag{224}$$

because $\bar{\gamma}$ is given by

$$\bar{\gamma} = 2\pi|\bar{g}_\Omega|^2 = \gamma[2 - 2\pi^{-1}\arctan(2\tau_r\bar{\Delta}_d)] \ . \tag{225}$$

[35] When $\eta_{\boldsymbol{k}}$ depends only on the photonic energy as $\eta_{\boldsymbol{k}} = \eta_{\epsilon_{\boldsymbol{k}}}$ and the detector has an inactive band $I$, the decay rate Eq. (191) is recast into the following form:

$$\Gamma = 2\pi|\bar{g}_\Omega|^2 = \int_{\omega\notin I} d\omega|g_\omega|^2 \frac{\eta_\omega}{|\Omega-\omega-i\eta_\omega/2|^2} + 2\pi\int_{\omega\in I} d\omega|g_\omega|^2\delta(\Omega-\omega) \ , \tag{223}$$

where $|g_\omega|^2$ is the original form factor [not restricted to the flat ones, Eq. (215)]. In case of false measurements where $\Omega \in I$, the second term gives the unobserved decay rate, $2\pi|g_\Omega|^2$. Because the first term is positive, $\Gamma \geqslant 2\pi|g_\Omega|^2$ in general.

(ii) The transition from the first to the second stage should occur before the atom decays. This condition is expressed as

$$\gamma \ll \bar{\Delta}_{\mathrm{d}} \ , \tag{226}$$

which means that the probability of detecting a photon is naively expected to be very *small*.

The former condition can be understood intuitively as follows: The lifetime of a virtually emitted photon in the active band is estimated by $\delta t \sim (\delta E)^{-1} \sim \bar{\Delta}_{\mathrm{d}}^{-1}$, using the uncertainty principle. The anti-Zeno effect takes place if the detector response $\tau_{\mathrm{r}}$ is quick enough to fix a virtual photon, which is accomplished by $\tau_{\mathrm{r}} \lesssim \bar{\Delta}_{\mathrm{d}}^{-1}$.

### *5.7. Discussions*

#### *5.7.1. Relation to conventional theories*

We have observed that the QZE or AZE can be induced even in exactly exponentially decaying systems, for which $t_{\mathrm{j}} \to 0$, if the measurement is energetically imperfect. This fact seemingly contradicts with the conventional theories, which state that neither the QZE nor the AZE can be induced in such systems. However, it should be stressed that this conventional wisdom was proved only for repeated instantaneous ideal measurements. Therefore, the relation of the present theory to the conventional theories can be seen by taking the limits of flat response,[36] as we have done in Section 5.3, as follows.

Regarding the case of Section 5.5, the limit of flat response is obtained by taking $\Delta_{\mathrm{d}} \to \infty$. Then, inequality (218) can never be satisfied by a finite $\tau_{\mathrm{r}}$ for exponentially decaying systems, and the QZE does not take place. Similarly, regarding the case of Section 5.6, the flat response is obtained by putting $\bar{\Delta}_{\mathrm{d}} \to 0$. Then, inequality (226) can never be satisfied for exponentially decaying systems, and the AZE does not take place. We have thus obtained the conventional wisdom from the present formalism by taking the limit of flat response. It is therefore seen that the present theory serves as an extension of the conventional theories to realistic situations, where the detection range of the detector is always finite.

#### *5.7.2. Physical interpretation*

In Sections 5.5 and 5.6, the following two opposite effects of measurement has been revealed: (a) Measurement on photons whose energies are close to the atomic transition energy $\Omega$ tends to suppress the decay of the atom. (b) Measurement on photons whose energies are far from $\Omega$ tends to accelerate the decay of the atom. When the detector is active for all photons, these two opposite effects appear simultaneously and weaken each other. This is the reason why a 'worse' detector which possesses a finite inactive band is more advantageous in inducing the QZE or AZE than a 'better' detector which is sensitive to all photons. Particularly, when the unobserved form factor is a constant function (in other words, the system decays with an exact exponential decay law), the two opposite effects cancels out completely; the form factor suffers no modification at all, no matter how short $\tau_{\mathrm{r}}$ would be. This cancellation mechanism can be understood with a help of Fig. 15; although every photonic mode is energetically broadened as a counteraction of measurement, such individual broadenings

[36] The flat response is one of necessary conditions for reducing to repeated instantaneous ideal measurements. Therefore, it is sufficient for the present purpose to show that the Zeno effect disappears for the flat response.

are perfectly smeared out by the $\boldsymbol{k}$-integration in Eq. (187), and are not reflected in the renormalized form factor.

In general systems with a nonzero jump time, however, effects (a) and (b) are not completely canceled out even in the case of the flat response. For example, in case of a Lorentzian form factor with finite $\Delta$, the system suffers the QZE or AZE by a continuous measurement with flat response, as discussed in Section 5.3. There, it was observed that the QZE (AZE) dominantly takes place when the atomic transition energy $\Omega$ is close to (far from) the central energy $\mu_0$ of the form factor. This fact can also be understood in terms of the competition between effects (a) and (b): When $\Omega$ and $\mu_0$ is close, effect (a) dominates effect (b), resulting in the QZE; when $\Omega$ and $\mu_0$ is far apart, effect (b) dominates effect (a), resulting in the AZE.

*5.7.3. Discussions and remarks on the model*

In this section, we have analyzed the Zeno effect using a specific model, Eqs. (165)–(167). We expect that the results based on this model would cover most of essential elements of the Zeno effect. For example, although the model assumes an indirect measurement we have shown in Section 5.1.3 that direct measurements are included as a special case of this model. However, the following points are worth mentioning about the model.

Firstly, the model is linear, i.e., Eqs. (165)–(167) are bilinear in the creation and annihilation operators. Although this seems to be a good approximation to an effective Hamiltonian for photon-counting measurements by standard photodetectors, the model cannot describe other experimental setups, of course. For other experimental setups, the quantitative results of this section would become much different, although we think that the qualitative results would be similar.

Secondly, we have computed the response time and the measurement error as relevant parameters characterizing measurements. As discussed in Section 4.5.1, they are actually the lower limits of the response time and measurement error, respectively, within the model of Eqs. (165)–(167), because,because additional delay and/or measurement error can take place in subsequent processes such as the signal magnification process in a photodetector. Although the performance of actual measuring devices would be worse, the limiting values are most important in discussing fundamental physics, as emphasized in Section 4.5.1.

Thirdly, we have assumed that the detector signal is obtained from the average population, which is given by Eq. (176), of the elementary excitations. This may be detected by subsequent magnifying processes through, say, avalanche processes. Note however that Eqs. (165)–(167) do not exclude the possibility of other methods of getting the detector signal. For example, the signal may be obtained from the off-diagonal elements $f^*_{\boldsymbol{k}\omega}(t)f_{\boldsymbol{k}'\omega'}(t)$, where $f_{\boldsymbol{k}\omega}(t)$ is defined in Eq. (173). What method is used is not uniquely determined by Eqs. (165)–(167), which describe the dynamics of the systems inside the Heisenberg cut (Section 4.3.2). To determine the full experimental setup, we must also specify the systems outside the Heisenberg cut. Among many methods of getting the signal using Eqs. (165)–(167), we,we have assumed that the detection of the average population would be the most efficient method, thus giving the fastest response. Since we are interested in the lower limit of the response time as discussed in Section 4.5.1, the calculation of the average population suffices for our purpose.

Finally, our model assumes a homogeneous photoabsorptive media for the photodetector. The case where the photodetector is separated spatially from the atom will be discussed in Section 6.4.

## 6. Relation to cavity quantum electrodynamics

### 6.1. Relation between the Zeno effect and other phenomena

If one is interested in the Zeno effect in the broad sense (Section 4.5.4), only the decay rate will be relevant, whereas quantities characterizing measurements, such as the measurement error and the amount of information obtained by measurement, would be irrelevant. In such a case, any change of the decay rate of the target system, which is induced by interaction with external systems, could be called a Zeno effect even when no information can be obtained by the interaction process. Therefore, the Zeno effect in the broad sense is not necessarily connected with measurements (as discussed in Section 4.5.4), and, consequently, is closely related to various phenomena in many different fields of physics [28–30].

Such phenomena include, for example, (i) the motional narrowing [67,86,87], in which the width of an excitation in a solid is reduced by perturbations from external noises or environments, (ii) Raman scattering processes [88,89], in which the transition rate between atomic levels is modulated by external fields of photons or phonons, and (iii) the cavity quantum electrodynamics (abbreviated as the *cavity QED*) [45,90,91], in which electrodynamics is modified by the presence of optical cavities. These phenomena can be considered as examples of the Zeno effect in the broad sense, and vice versa.

Regarding the models of continuous measurements which are employed in Section 5, in particular, the physical configurations are quite similar to those of the cavity QED. In fact, in Section 5 we have studied effects of photon-counting measurements on the decay dynamics of an excited atom, assuming that the photon-counting measurement is accomplished by the interaction between photons and photoabsorptive media. Therefore, if we focus only on the decay dynamics of the atom it can be simply said that we have studied effects of the photoabsorptive media surrounding the atom on the decay rate. This is a subject of the cavity QED. Because of this similarity, we discuss in this section the relation between the cavity QED and the results of Section 5.

### 6.2. Modification of form factor in cavity QED

In discussions of the cavity QED, the optical media surrounding an atom are usually treated as passive media. That is, the dynamics of (elementary excitations in) the optical media is usually disregarded. This should be contrasted with the discussions in Section 5, where microscopic dynamics of the photoabsorptive media plays an important role as the readout of the measuring apparatus. If we focus only on the dynamics of the atom, however, both the cavity QED and the Zeno effect can be understood from a unified viewpoint, using the form factor of the atom–photon interaction. To see this, note that the form factor is sensitive to the optical environment. For example, the form factor has a continuous spectrum when the atom is in the free space (see Section 2.3.2). However, when the atom is surrounded by mirrors, the eigenmodes are discretized and the form factor becomes a line spectrum (see Section 2.3.3). The decay dynamics is affected by the optical environment through the modification of the form factor. This explains the cavity QED, as well as the Zeno effect in the broad sense.

In the discussions of the cavity QED, the optical environment is treated as a passive media, which is characterized by the dielectric constant $\varepsilon(\boldsymbol{r})$. It may depend on the space coordinate $\boldsymbol{r}$ because the optical environment is spatially inhomogeneous in general. Since $\varepsilon(\boldsymbol{r})$ takes complex values, its effects on the form factor may be classified into two: One is the effect of the real part, which results in reconstruction of

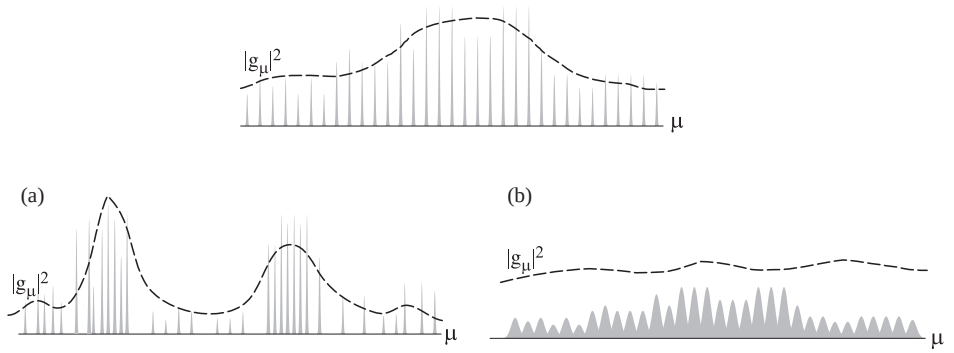


Fig. 32. Two mechanisms for modification of a form factor in the cavity-QED: (a) reconstruction of eigenmodes; and (b) broadenings of eigenmodes.

optical eigenmodes, and the other is the effect of the imaginary part, which induces energetic broadening of optical eigenmodes. We will explain them in the following subsections.

*6.2.1. Reconstruction of eigenmodes*

Suppose a situation where non-absorptive optical media is distributed in space [92]. Non-absorptive optical media are characterized by real dielectric constants. The Maxwell equation for the electric field is given by

$$\nabla \times \nabla \times \boldsymbol{E}(\boldsymbol{r}, t) = -\varepsilon(\boldsymbol{r}) \frac{\partial^2}{\partial t^2} \boldsymbol{E}(\boldsymbol{r}, t) \ , \tag{227}$$

where $\varepsilon(\boldsymbol{r})$ is a real function, representing the spatial distribution of dielectric constant. Then, a set of eigenmode functions $\boldsymbol{f}_j(\boldsymbol{r})$ and eigenfrequencies $\epsilon_j$, where $j$ is an index of eigenmodes, are obtained as the stationary solutions of the Maxwell equations. When the atom is placed at $\boldsymbol{r}$, the atom–photon coupling constant is given by Eq. (19). Thus, the eigenenergies $\epsilon_j$ of the photon modes are dependent on the spatial distribution $\varepsilon(\boldsymbol{r})$ of the dielectric constant; the atom–photon coupling constant $g_j$ is dependent also on the atomic position $\boldsymbol{r}$, in addition to $\varepsilon(\boldsymbol{r})$. It should be remarked that, when the optical media is spatially homogeneous, the eigenmode functions are given by plane waves. Then, $\boldsymbol{r}$-dependence of $g_j$ appears only in the phase of $g_j$ and the magnitude $|g_j|^2$ is independent of $\boldsymbol{r}$, so the atomic decay takes place independently of its position. However, in general, $|g_j|^2$ depends on the atomic position when optical media are distributed inhomogeneously in space; as a result, the dynamics of the atom becomes strongly sensitive to the atomic position $\boldsymbol{r}$.

The form factor, which is given by

$$|g_\mu|^2 = \sum_j |g_j|^2 \delta(\epsilon_j - \mu) \ , \tag{228}$$

is modified through $\epsilon_j$ and $g_j$. Modification of the form factor by reconstruction of eigenmodes is illustrated in Fig. 32(a). The contribution of each photonic mode remains a delta function in this case, but the strength ($|g_j|^2$) and position ($\epsilon_j$) of a delta function is modified.

Two representative examples of this type of modification of the form factor are as follows: (i) Only the atomic position $\boldsymbol{r}$ is changed, keeping the spatial distribution $\varepsilon(\boldsymbol{r})$ unchanged. Then, the positions of the delta functions ($\epsilon_j$) are unchanged, but the strength ($|g_j|^2$) is changed, depending on the eigenmode function $\boldsymbol{f}_j(\boldsymbol{r})$. (ii) When the size of a perfect cavity is increased, the eigenenergies are red-shifted. $|g_j|^2$ shows a complicated behavior, depending on the relative position of the atom to the cavity as explained in (i). Generally, $|g_j|^2$ is decreased proportionally to the inverse of the cavity volume.

### *6.2.2. Broadening of eigenenergies*

We now consider the case where absorption of photons by optical media is significant. In photoabsorptive media, photons are converted within finite lifetimes to elementary excitations in the media, such as electron-hole pairs, excitons, etc. Therefore, in the presence of photoabsorptive media, eigenmodes of photons do not exist in a strict sense; they should be regarded as quasi-eigenmodes with finite lifetimes. The situation is phenomenologically described by a complex eigenenergy of the mode, the imaginary part of which is inversely proportional to the lifetime of the mode.

We have already observed an example of broadening of eigenenergies in Section 5 in the context of the Zeno effect. The schematic view is given again in Fig. 32(b). When there is no absorption of photons, the form factor is composed of delta functions, each of which represents the contribution of each eigenmode. In the presence of a detector, which absorbs photons with finite lifetimes, a delta function is broadened to be a Lorentzian as in Eq. (189), satisfying a sum rule, Eq. (190).

It should be remarked that the broadening of a cavity mode was observed in Section 2.3.4, through the coupling between the cavity mode and external photon modes. The difference between the systems considered in Sections 2.3.4 and 5 lies in the point that both the cavity mode ($a$) and external modes ($b_\omega$) are of photonic origin in Section 2.3.4, whereas a photon mode ($b_{\boldsymbol{k}}$) is coupled to non-photon modes (elementary excitations in the detector, $c_{\boldsymbol{k}\omega}$) in Section 5. In the system of Section 2.3.4, a diagonalized mode ($B_\omega$) still represents a photonic eigenmode, which extends over the whole space, both inside and outside of the cavity. Actually, by solving the Maxwell equation treating the mirrors as an optical medium with real dielectric constants, one can obtain eigenmode functions for $B_\omega$. Thus, the broadening of a cavity mode observed in Section 2.3.4 should be classified as an example of reconstruction of eigenmodes, discussed in Section 6.2.1.

## *6.3. Atom in a homogeneous absorptive medium*

In the previous subsection, two mechanisms for modification of the form factor in general cavity-QED systems are described. In most photoabsorptive materials, these two mechanisms usually appear simultaneously. In order to see this point, we revisit the Hamiltonian for an atom embedded in a homogeneous photoabsorptive media, which was used in Section 5 for discussion of the Zeno effect. Here, we consider a case without the flat-band assumption, Eq. (170). Following the same mathematics as Section 5.2, one can confirm that the contribution of the photon $\boldsymbol{k}$ to the form factor is modified as follows:

$$|g_{\boldsymbol{k}}|^2\delta(\mu-\epsilon_{\boldsymbol{k}}) \to \frac{|g_{\boldsymbol{k}}|^2}{2\pi}\left(\frac{\mathrm{i}}{\mu-\epsilon_{\boldsymbol{k}}+\int \mathrm{d}\omega \dfrac{|\xi_{\boldsymbol{k}\omega}|^2}{\omega-\mu-\mathrm{i}\delta}}+\mathrm{c.c.}\right). \tag{229}$$

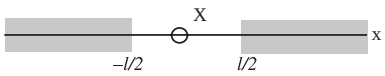


Fig. 33. Arrangement of the target atom and absorptive media composing detectors. The atom is located at $x = X$, whereas the absorptive media are placed in the regions $x \leqslant -l/2$ and $\geqslant l/2$.

The integral in the denominator of the RHS of Eq. (229) becomes significant when $|\mu - \epsilon_{\boldsymbol{k}}|$ is small. We may therefore approximate this quantity roughly by

$$\int \mathrm{d}\omega \frac{|\xi_{\boldsymbol{k}\omega}|^2}{\omega - \mu - \mathrm{i}\delta} \simeq \int \mathrm{d}\omega \frac{|\xi_{\boldsymbol{k}\omega}|^2}{\omega - \epsilon_{\boldsymbol{k}} - \mathrm{i}\delta} \tag{230}$$

$$= P \int \mathrm{d}\omega \frac{|\xi_{\boldsymbol{k}\omega}|^2}{\omega - \epsilon_{\boldsymbol{k}}} + \mathrm{i}\pi |\xi_{\boldsymbol{k},\epsilon_{\boldsymbol{k}}}|^2 \tag{231}$$

$$\equiv -\Delta\epsilon_{\boldsymbol{k}} + \mathrm{i}\eta_{\boldsymbol{k}}/2 \,. \tag{232}$$

Using the above quantity, Eq. (229) is transformed into a more transparent form:

$$|g_{\boldsymbol{k}}|^2 \delta(\mu - \epsilon_{\boldsymbol{k}}) \to |g_{\boldsymbol{k}}|^2 \frac{\eta_{\boldsymbol{k}}/2\pi}{|\mu - (\epsilon_{\boldsymbol{k}} + \Delta\epsilon_{\boldsymbol{k}}) + \mathrm{i}\eta_{\boldsymbol{k}}/2|^2} \,. \tag{233}$$

Eqs. (231) and (232) reveal that asymmetry in the photon–medium coupling $|\xi_{\boldsymbol{k}\omega}|^2$ about the photon energy $\epsilon_{\boldsymbol{k}}$ results in a shift of the eigenfrequency, $\Delta\epsilon_{\boldsymbol{k}}$. Generally, the photon–medium coupling simultaneously induces both broadening and energy shift.

In the discussion of the Zeno effect in Section 5, shifts of the eigenenergy are neglected by the flat-band assumption, Eq. (170), and only the broadening effect is picked up. Under this approximation, fairly good agreement with the conventional theories of the Zeno effect has been achieved, as has been shown in Section 5.3. It would be important to point out that only the broadening effect is assumed in the conventional theory of the Zeno effect: by using the projection postulate to the atomic state, coherences between the undecayed ($|x\rangle$) and decayed ($|g, \boldsymbol{k}\rangle$) states are lost without shifting the energy of photons. In actual photon counting processes, eigenenergies of photons would be slightly shifted through the interaction with a detector, which also affect the atomic decay rate.

### *6.4. Atom in an inhomogeneous absorptive medium*

In discussion of the Zeno effect in Section 5, we have considered a situation in which an atom is embedded in a homogeneous absorptive material. However, in actual situations of photon counting, photodetectors composed of photoabsorptive material are spatially separated from the target atom, as illustrated in Fig. 33. In the following two subsections, we discuss what would be expected for the decay rate when the detectors are spatially separated from the atom. We shall describe results of the cavity QED in Section 6.4.1, and apply them to the Zeno effect in Section 6.4.2.

#### *6.4.1. Cavity QED*

For simplicity, we consider the following situation here: The space is assumed to be one-dimensional, extended in the $x$-direction, and the photon field is treated as a scalar field. The optical materials are

modeled by bulk absorptive dielectric materials occupying $|x| > l/2$, which has a complex dielectric constant $\epsilon(\omega) = [\eta(\omega) + i\kappa(\omega)]^2$.

First, we preliminarily consider a case where the medium is not absorptive and its dielectric constant is given by $\epsilon(\omega) = \eta^2$ in the relevant frequency region under consideration. In this case, as has been discussed in Section 6.2.1, photonic eigenmodes are reconstructed according to the following equation:

$$-\frac{\partial^2}{\partial x^2}E = -\varepsilon(x)\frac{\partial^2}{\partial t^2}E \tag{234}$$

which is a scalar field version of Eq. (227). Reviving the light velocity $c$ here, the eigenmodes at frequency $\omega$ are given by

$$f_{\omega,+}(x) = \begin{cases} \dfrac{C_1}{\sqrt{C_1^2 + C_2^2}}\cos\eta kx + \dfrac{C_2}{\sqrt{C_1^2 + C_2^2}}\sin\eta k|x| & (|x| \geqslant l/2)\ , \\ \dfrac{1}{\sqrt{C_1^2 + C_2^2}}\cos kx & (|x| \leqslant l/2)\ , \end{cases} \tag{235}$$

$$f_{\omega,-}(x) = \begin{cases} \dfrac{x}{|x|}\dfrac{D_1}{\sqrt{D_1^2 + D_2^2}}\cos\eta kx + \dfrac{D_2}{\sqrt{D_1^2 + D_2^2}}\sin\eta kx & (|x| \geqslant l/2)\ , \\ -\dfrac{1}{\sqrt{D_1^2 + D_2^2}}\sin kx & (|x| \leqslant l/2)\ , \end{cases} \tag{236}$$

where $k = \omega/c$, and the index $\pm$ represents the parity of the eigenmode. The coefficients, $C_1$, $C_2$, $D_1$ and $D_2$, are given by

$$\begin{pmatrix} C_1 \\ C_2 \end{pmatrix} = \begin{pmatrix} \cos(\eta kl/2) & -\sin(\eta kl/2) \\ \sin(\eta kl/2) & \cos(\eta kl/2) \end{pmatrix} \begin{pmatrix} \cos(kl/2) \\ -\eta^{-1}\sin(kl/2) \end{pmatrix}\ , \tag{237}$$

$$\begin{pmatrix} D_1 \\ D_2 \end{pmatrix} = \begin{pmatrix} \cos(\eta kl/2) & -\sin(\eta kl/2) \\ \sin(\eta kl/2) & \cos(\eta kl/2) \end{pmatrix} \begin{pmatrix} \sin(kl/2) \\ \eta^{-1}\cos(kl/2) \end{pmatrix}\ , \tag{238}$$

As has been clarified in Sections 2 and 5, the atomic decay rate can be well evaluated by the Fermi golden rule. The decay rate (normalized by the decay rate $\Gamma_0$ in a free space) is given by

$$\Gamma(X)/\Gamma_0 = \eta^{-1}\sum_{\sigma=+,-}|f_{\Omega,\sigma}(X)|^2\ , \tag{239}$$

which is plotted in Fig. 34 by a thin dotted line as a function of the atomic position $X$. It is observed that the atomic decay rate becomes strongly sensitive to the atomic position $X$, reflecting the spatial form of the eigenmodes at the atomic transition energy $\Omega$. In other words, the cavity effect appears strongly both in the vacuum region ($|X| \leqslant l/2$) and the medium region ($|X| \geqslant l/2$).

Next, we proceed to discuss a case where the medium is absorptive ($\kappa \neq 0$) and plays the role of a photodetector. In order to handle this case, the absorptive material is modeled by an assembly of harmonic oscillators, and the canonical quantization is performed for both the photon field and the material [93]. As the absorptivity $\kappa$ is increased, the effect of broadening of eigenmodes (Section 6.2.2) becomes more significant. The position dependence of the decay rate is plotted in Fig. 34, for weakly

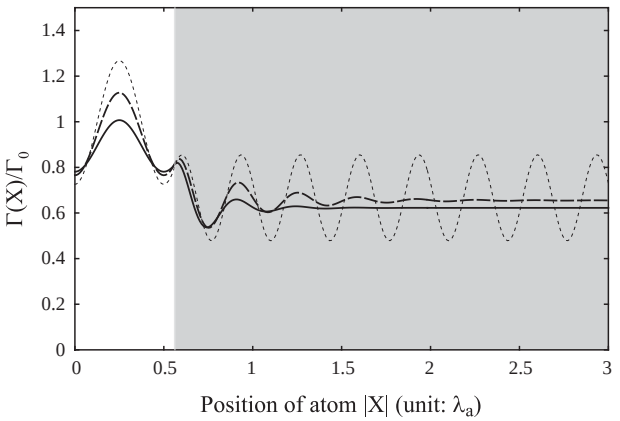


Fig. 34. Position dependence of the decay rate (normalized by the decay rate in free space). Only the $X > 0$ region is plotted because $\Gamma(X)$ is an even function. The length of the vacuum region is chosen at $l = (9/8)\lambda_a$, where $\lambda_a = 2\pi c/\Omega$ is the wavelength of the emitted photon. $\eta = 1.5$ and $\kappa = 0$ (thin dotted line), 0.2 (broken line), and 0.4 (solid line).

absorptive ($\kappa = 0.2$, broken line) and strongly absorptive ($\kappa = 0.4$, solid line) cases. It is observed that, when the atom is placed deeply inside of the material ($|x| - l/2 \gg \lambda_a/\kappa$, where $\lambda_a = 2\pi c/\Omega$ is the wavelength of emitted photon), the cavity effect is completely smeared out and the decay rate becomes identical to that of an atom embedded in an homogeneous medium. In this case, the decay is solely determined by the nature of the material, as in Section 6.3. Contrarily, when the atom is placed in the vacuum region, the position dependence remains even when the material is strongly absorptive. Fig. 34 indicated that the decay rate in this case is basically determined by the eigenmodes for the non-absorptive case ($\kappa = 0$).

To summarize the results derived from the cavity QED, the decay rate would surely be affected by the presence of the optical materials even when they are placed separately from the atom (Fig. 33). In this case, the physical origin of modification of the decay rate should mainly be attributed to reconstruction of eigenmodes, not to broadening of eigenmodes. In other words, the boundary effect would dominate. Although a one-dimensional case is considered here, the same qualitatively prediction would follow in the three-dimensional case also, if the optical materials well surround the atom to form an optical cavity.

### *6.4.2. Zeno effect by detectors spatially separated from the target atom*

It is sometimes argued that the term 'Zeno effect' should be restricted to experiments where pieces of measuring apparatus exert a non-local negative-result effect on a microscopic system [10]. We can discuss the Zeno effect in this restricted sense as follows, using the results of the cavity QED presented above and consideration about the causality.

First of all, we must distinguish the following three cases. Let the distance between the atom and the detectors be $l/2$, as shown in Fig. 33. Suppose that the detectors are placed at $t = t_d$,[37] and the atom is

[37] Or, one can change the absorption spectrum of the detector materials, which was previously placed at $t < t_d$, through, e.g., the electro-optical effect [88] by applying an electric field at $t = t_d$.

excited to an unstable state at $t = 0$. The three cases to be distinguished are:

(a) The detectors are placed long before the atom is excited, i.e., $t_d < 0$ and $c|t_d| \gg l$, where $c$ is the light velocity.
(b) The detectors are suddenly placed after the atom is excited, i.e., $t_d > 0$.
(c) The detectors are placed long before the atom is excited, but are suddenly removed at $t = t'_d$ after the atom is excited, i.e., $t_d < 0 < t'_d$ and $c|t_d| \gg l$.

In case (a), the calculations in Section 6.4.1 hold, except for a very short time scale ($< 1/\Omega$) for which the rotating-wave approximation employed in Eq. (165) may be wrong. Therefore, the results of Section 6.4.1 are valid at least when $t_j > 1/\Omega$. We thus conclude that the Zeno effect can take place in case (a). Physically, this may be understood as follows. The materials composing the detectors modify the vacuum state of photons [90,94]. Although the modification requires a finite time to complete, it is completed before the atom is excited. Therefore, the dynamics of the atom is affected by the modified photon vacuum [90,94]. i.e., by the presence of the detectors.

In case (b), on the other hand, the modification of the photon vacuum is not completed when the atom is excited. It is obvious from the causality that the dynamics of the atom is not affected during $t < l/2c$. Therefore, if the free decay rate $\gg c/l$, then the decay rate is not modified, i.e., the Zeno effect does not occur. If, on the other hand, the free decay rate $\lesssim c/l$, then the Zeno effect can take place. To analyze case (b) in detail, one must take account of the dynamics of the photon field, as in Refs. [95,96]. Note that, as shown there, photons will be emitted from the 'false vacuum' during the modification process of the photon vacuum.

Case (c) is in some sense a combination of cases (a) and (b). The dynamics of the atom is affected by the detector materials during $t < t'_d + l/2c$. Therefore, the Zeno effect can take place if the modified decay rate $\gtrsim 1/(t'_d + l/2c)$. If, on the other hand, the modified decay rate $\ll 1/(t'_d + l/2c)$, then the observed decay rate will become the free decay rate.

Although we believe these conclusions at the time of writing, more elaborate works may be necessary to draw more definite conclusions. A related discussion is given in Ref. [97].

## 7. Experimental studies on the Zeno effect

In the preceding sections, we have discussed the Zeno effect, assuming the photodetection measurement on a radiatively decaying excited atom as a typical of quantum unstable states and measurements on them. However, it is difficult to confirm experimentally the Zeno effect in such a system for the following reasons: (i) The response time $\tau_r$ of the detector cannot be controlled easily, because it is determined by the material parameters, i.e., the interaction between photons and constituting materials of the detector. (ii) The jump time $t_j$ is small and therefore the decay dynamics is not easily perturbed by measurement. If we simply estimate, taking the positiveness of photon energies into account, the bandwidth of the form factor by $\Delta \sim \Omega$ (transition frequency), $t_j$ is estimated at $t_j \sim \Omega^{-1} \sim 10^{-15}$ s.

It is generally believed that the jump time is very short in most of truly decaying states, whose form factors are energetically broad. Therefore, in most attempts at experimental confirmation of the Zeno effect, oscillating systems are selected as the target system [76,98–102]. In such systems, the initial quadratic behavior lasts for a much longer time as compared with truly decaying states, and the Zeno

effect is expected to be induced more easily. For this reason, experiments on the Zeno effect have been performed mainly for oscillating systems such as Rabi-oscillating atoms [26,27,103–105]. However, significance of the Zeno effect is obscured in oscillating systems, particularly when one considers long-time behaviors of the survival probability.

Recently, there are several attempts to observe the Zeno effect in truly decaying states. Here we introduce two of them, both of which have long duration of deviation from the exponential law (i.e., large jump time, $t_j$) and well devised measuring methods with high controllability of measurement intervals. One is the first observation of both effects in atomic tunneling phenomena [34,106]. The other one is theoretical indication in the parametric down conversion processes [107–110]. In addition to presenting them, we will also discuss in this section how to *avoid* the Zeno effect in general measurements, which are designed not to detect the Zeno effect but to measure the free decay rate accurately.

### 7.1. Atomic tunneling phenomenon

The experimental observation of the Zeno effect in truly unstable states is a difficult problem. Although the initial deviation from the exponential decay law is predicted in theory, the duration of this period is supposed to be extremely short and the deviation is undetectable in most unstable states. Recently, however, this deviation was successfully observed in tunneling phenomena of trapped atoms in an optical potential [34,106].

In their experiment, ultracold sodium atoms are trapped in standing wave of light, which serves as an optical potential. The optical potential is controllable in time and may be accelerated as follows:

$$V(x,t) = V_0 \cos(2k_L x - k_L a t^2) \ . \tag{240}$$

where $k_L$ is the wavenumber of light and $a$ is the acceleration. The trapped atoms are driven by this potential. In the moving frame fixed to the potential ($x' = x - at^2/2$), the atoms suffer inertial force and the effective potential for the atoms becomes

$$V(x') = V_0 \cos(2k_L x') + max' \ , \tag{241}$$

where $m$ is the atomic mass. Thus, a tilted washboard potential can be obtained, which contains a controllable parameter $a$.

The forms of the potential $V(x')$ is drawn in Fig. 35. When the acceleration is small ($a = a_{\text{trans}}$), high potential barriers are formed, as shown in Fig. 35(a). By adequate choice of $V_0$ and $a_{\text{trans}}$, Fischer et al. have realized a situation where only the lowest state is bounded in each potential minimum. This bound state is almost isolated from other modes by high potential barriers around the minimum. Contrarily, under a large acceleration ($a = a_{\text{tunnel}}$), the left (right) potential is lowered (heightened), as shown in Fig. 35(b). In this case, the bound state can couple through the left barrier to external modes, which extend semi-infinitely in the negative $x'$ region and therefore constitute a continuum in energy. The bound state is no more stable and decays to unbound states with a finite lifetime. Thus, one may freely switch these two sorts of situations (isolated bound state and unstable bound state) by controlling the parameter $a$.

The measurement of the survival probability is devised as follows. (i) As the initial state, the system is prepared in the potential of Fig. 35(a) by taking $a = a_{\text{trans}}$ for $t < 0$. (ii) For $0 < t < t_{\text{tunnel}}$, the atoms are accelerated strongly with $a = a_{\text{tunnel}}$ and the effective potential is changed to that of Fig. 35(b). In this period, tunneling to unbound states may take place. (iii) For $t_{\text{tunnel}} < t < t_{\text{tunnel}} + t_{\text{interr}}$, $a$ is set to $a_{\text{trans}}$ again and bounded atoms are isolated. In this period, the bounded atoms are accelerated by the

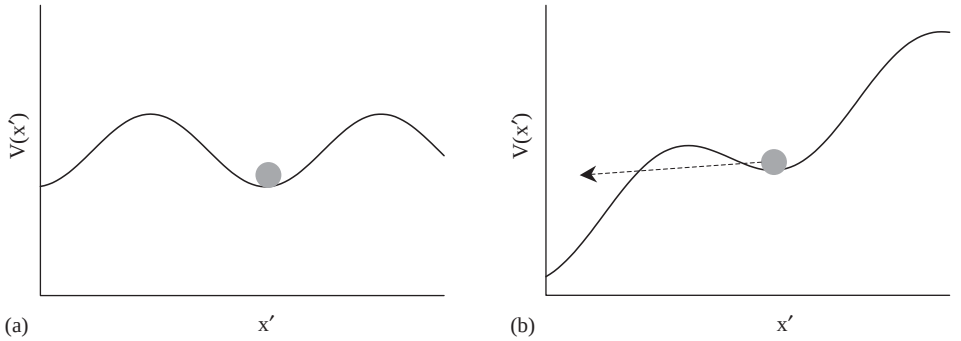


Fig. 35. The shape of the washboard potential Eq. (241), under (a) small acceleration and (b) large acceleration. The bound state is almost isolated in (a), whereas, in (b), it may decay to unbounded modes extending in the negative $x'$ region.

potential whereas the escaped atoms are not, resulting in separating the survived (bounded) atoms and decayed (unbounded) atoms in the velocity space. (iv) Finally, the optical potential is removed and the velocity distribution is measured, from which one can infer the survival probability $s(t_{\text{tunnel}})$. If $t_{\text{interr}}$ is long enough to guarantee complete separation in the velocity space, this process serves as an ideal measurement of survival of the atoms.

In this manner, the survival probability under free temporal evolution was successfully measured, and deviations from the exponential decay law was confirmed experimentally for the first time. The measured jump time is very long ($t_{\text{j}} \sim 10\,\mu\text{s}$) in this system. Furthermore, by inserting several periods of small acceleration (in which the survival and decayed atoms are separated) into the tunneling period, they measured the survival probability under repeated measurements, and succeeded in confirming both the QZE and the AZE.

However, it is worth mentioning that the measurement process through (iii) to (iv) is a sort of direct measurements, the Zeno effect by which is often criticized as not being the genuine Zeno effect, as discussed in Section 4.6.1. In fact, the potential for the atoms is altered when the measurement is performed. Furthermore, the horizontal axes of Figs. 3–5 of the excellent experiment of Ref. [106] are not the real time $t$ but $t-$(measuring times). More elaborate experiments, which are free from these points, are therefore desired to observe the Zeno effect more clearly.

### *7.2. Parametric down conversion process*

In this subsection, we introduce a theoretical indication of the possibility of observing the Zeno effect in parametric down conversion process [107–110]. Although actual experimental observation of the effects has not been reported in this system yet, this system is an interesting candidate for actual experiments, because the procedures for both continuous and discrete measurements are proposed in this system.

In this process, a pump photon (frequency $\omega_{\text{p}}$) spontaneously decays in a second-order nonlinear material into a pair of signal and idler photons (frequencies $\omega_{\text{s}}$ and $\omega_{\text{i}}$) satisfying the energy conservation law, $\omega_{\text{p}} = \omega_{\text{s}} + \omega_{\text{i}}$. Using the semiclassical approximation for the pump field and switching to the interaction representation, the effective Hamiltonian for the signal and idler photons are

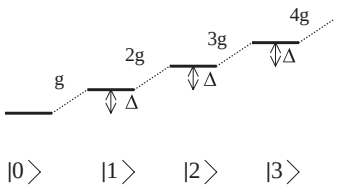


Fig. 36. The energy diagram of Hamiltonian (242). $|n\rangle = (n!)^{-1}(a_s^\dagger a_i^\dagger)^n|0\rangle$ denotes the $n$ photon pair state.

given by

$$\mathscr{H} = \frac{\Delta}{2}(a_s^\dagger a_s + a_i^\dagger a_i) + g(a_s^\dagger a_i^\dagger + a_s a_i) \ , \tag{242}$$

where $a_s$ and $a_i$ are the annihilation operators for the signal and idler photons. $\Delta$ is determined by the phase mismatch, and $g$ depends on the intensity of the pump beam and the second-order susceptibility of the material. Here, the space coordinate in the propagating direction is regarded as the time coordinate. Initially, there are no photons in the signal and idler modes, the quantum state of which is denoted by $|0\rangle$.

The instability of the vacuum state is understood by regarding Eq. (242) as a tight-binding Hamiltonian in the photon number space. Fig. 36 shows the energy diagram of the Hamiltonian. $|n\rangle = (n!)^{-1}(a_s^\dagger a_i^\dagger)^n|0\rangle$ denotes a state with $n$ photon pairs. The hopping energy between $|n\rangle$ and $|n+1\rangle$ is given by $(n+1)g$, whereas there is an energy mismatch of $\Delta$ between neighboring sites. The energy diagram becomes similar to Fig. 1 after diagonalizing $n \geqslant 1$ states. When $g \gg \Delta$, the eigenstates of the Hamiltonian are delocalized in the number space, and the initial state can decay to larger number states. Contrarily, when $g \ll \Delta$, the eigenstates are almost localized in each site. In such a case, the initial state cannot decay completely. Indeed, the survival probability is analytically given by

$$s(t) = \left[\cosh^2\left(\sqrt{g^2 - \Delta^2/4}\ t\right) + \frac{\Delta^2}{4g^2 - \Delta^2}\sinh^2\left(\sqrt{g^2 - \Delta^2/4}\ t\right)\right]^{-1} . \tag{243}$$

Therefore, the system becomes a truly decaying one when $|\Delta|$ is small enough to satisfy $|\Delta| < 2g$. The jump time in this system is given, for $\Delta = 0$, by

$$t_j \sim g^{-1} \ . \tag{244}$$

This means that the jump time may be controllable in terms of the pump intensity, which is a suitable nature for experimental observation of the Zeno effect.

The decay products in this experiment are the down-converted photons. As for the measurement of them, two schemes, discrete and continuous, are proposed. First, we introduce the discrete type. To this end, one divides the nonlinear crystal into several pieces, and insert mirrors after each piece in order to remove the idler photon. By detecting the removed photon by a photodetector, one can perform a discrete photon number measurement for each piece of nonlinear crystals. The measurement intervals are determined by the length of each piece, so the control of the measurement intervals is flexibly done in this scheme. Or, if one is only interested in the Zeno effect in the broad sense (Section 4.5.4), the photodetector for the removed photon is not necessary because the removed photon will soon become entangled with environmental mechanical degrees of freedom, which results in the decoherence between

the states with no photon pair (survived state) and one photon pair (decayed state). This suffices for the modulation of the decay rate, as discussed generally in Sections 4.5.4 and 6.1.

Next, we introduce a continuous type of measurement. In order to measure the photon number continuously, one let the idler mode interact with the meter mode $b$, which propagates in parallel with the idler mode, through the third-order non-linearity. The Hamiltonian reads

$$\mathscr{H} = \mathscr{H} + \kappa a_{\mathrm{i}}^{\dagger} a_{\mathrm{i}} b^{\dagger} b \ . \tag{245}$$

The inference of the decayed moment is carried out as follows: If the meter mode travels with an idler photon for time $t$, the amplitude of the meter mode acquires a phase shift by $\phi = \kappa t$. By measuring this phase shift, one may infer the decayed moment. As for the response time of this detecting device, the uncertainty in the inferred time of decay should be interpreted as the response time. Noticing that the uncertainty $\Delta\phi$ in the phase measurement is evaluated by $\langle b^{\dagger} b\rangle^{-1}$, the response time $\tau_{\mathrm{r}}$ is approximately given by

$$\tau_{\mathrm{r}} = \Delta t \sim \frac{1}{\kappa\langle b^{\dagger} b\rangle} \ . \tag{246}$$

Thus, the response time is revealed to be determined by the intensity of the meter mode, which is easily controllable.

### *7.3. Evasion of the Zeno effect in general experiments*

So far, we have discussed how to observe the Zeno effect. On the other hand, in general experiments, one usually wants to *avoid* the Zeno effect in order to get correct results [85,111]. Considering recent rapid progress of experimental techniques and diversification of experimental objects, we expect that the QZE or AZE would slip in results of advanced experiments not designed to detect it. To avoid the Zeno effect, one must design the experimental setup to break at least one of the conditions for observing these effects [85].

For example, when performing an experiment with a high time resolution such that $\tau_{\mathrm{r}} \lesssim t_{\mathrm{j}}$, then the results of Section 5.4 suggest that $\varepsilon_{\infty}$ should be *increased*. If $\varepsilon_{\infty}$ cannot be increased to keep the sensitivity of such a high-speed measurement, then one should adjust parameters in such a way that $\tau_{\mathrm{r}}$ lies on the boundary between the QZE and AZE, i.e., on the solid line in Fig. 21. Or, alternatively, one should calibrate the observed value using our results, such as Eq. (203), to obtain the free decay rate. Such consideration would become important to future experiments.

## 8. Summary

The quantum Zeno effect (QZE) and the quantum anti-Zeno effect (AZE), which are simply called the Zeno effect, have been clearly understood for the case of repeated instantaneous ideal measurements, for which one can take account of influence of the measurements simply by application of the projection postulate to the target system. However, real physical measurements are not instantaneous and ideal. Theories of the Zeno effect induced by such general measurements have been developed only recently. In this article, after reviewing the results of conventional theories, we have presented the results of such general theories of the Zeno effect. We have also reviewed briefly the quantum measurement theory, on

which these general theories are based, as well as experimental studies on the Zeno effect on monotonically decaying states.

In Section 2, we have reviewed the quantum dynamics of an unstable state of an isolated system. The dynamics is completely determined by the form factor $g_\mu$, defined by Eq. (14). It is shown that the survival probability $s(t)$ of the unstable state decreases quadratically with time at the beginning of decay, and later follows the exponential decay law, the rate of which is given by Eq. (16). Such an initial deviation from the exponential decay law plays a vital role in the Zeno effect.

In Section 3, combining the projection postulate with the result for $s(t)$ obtained in Section 2, we have reproduced the results of the conventional theories for the Zeno effect by repeated instantaneous ideal measurements. The decay rate under the measurement is plotted as a function of the measurement intervals $\tau_{\rm i}$ in Fig. 9. This figure demonstrates that repeated measurements does not necessarily result in suppression of decay: Depending on $\tau_{\rm i}$ and the form factor $g_\mu$, the opposite effect, i.e., acceleration of decay, may take place, which is called the AZE.

These conclusions have been drawn under the assumptions that measurements are instantaneous and ideal. However, as discussed in Section 4.5.6, real measurements are not strictly instantaneous and ideal. To explore the Zeno effect by realistic measurement processes, we should apply the quantum measurement theory, which is briefly summarized in Section 4. Its key observation is that not only the system S to be observed but also the measuring apparatus A should obey the laws of quantum theory. Therefore, one must analyze the time evolution of the joint quantum system S+A using the laws of quantum theory, as schematically shown in Figs. 11 and 12. The information about the observable $Q$ to be measured is transferred to the readout observable $R$ of A, through an interaction $\hat{H}_{\rm int}$ between S and A. The measurement of $Q$ is thus reduced to a measurement of $R$ by another apparatus (or observer) A′. Actually, A′ may be measured by a third apparatus A″, and A″ by A‴, and so on. Such a sequence, as shown in Fig. 13, is called the von Neumann chain, the basic notions of which are summarized in Section 4.3. We have summarized the prescription for analyzing general measurements in Section 4.4. As explained in Section 4.5, properties of general measurements are characterized by the response time, measurement error, range of measurement, the amount $I$ of information obtained by measurement, backaction of measurement, and so on. An interaction process between S and A can be called a measurement process only when $I$ is large enough, at least $I \gtrsim 1$. Although this point is crucial when discussing many problems about measurement, it is disregarded in discussions of the Zeno effect in the broad sense (Section 4.5.4). To discuss the Zeno effect, we have summarized in Section 4.6 more characterizations of measurements, including direct, indirect, positive-result, and negative-result. It is sometimes argued that the terms QZE and AZE should be restricted to effects induced by indirect and negative-result measurements. We have also explained repeated measurements, including repeated instantaneous measurements and continuous measurement. A simple explanation of the Zeno effect using the quantum measurement theory is given in Section 4.7. It is also shown that within the unitary approximation, which is explained in Section 4.6.4, one does not have to use the projection postulate in the analysis of the Zeno effect. A few more points, which will help the reader, concerning the quantum measurement theory are described in Section 4.8.

In Section 5, we have analyzed the Zeno effect using the quantum measurement theory. We employ a model which describes a continuous indirect negative-result measurement of an unstable state (Section 5.1). A typical example described by this model is the continuous measurement of the decay of an excited atom using a photodetector, which detects a photon emitted by the atom upon decay. The measuring apparatus (photodetector) is modeled by bosonic continua coupled to photons, and the quantum dynamics is investigated for the enlarged system composed of the atom, photon and photodetector. In Section 5.2,

it is shown that the form factor is renormalized as a counteraction of the measurement, as illustrated in Fig. 15. The renormalized form factor $\bar{g}_\mu$ determines whether the decay is suppressed (the QZE) or enhanced (the AZE). In Section 5.3, we have applied this formalism to the case where the response of the detector is flat, i.e., the photodetector responds to every mode of photons with an identical response time. The decay rate is plotted as a function of the response time $\tau_\mathrm{r}$ in Fig. 20. The results almost coincide with those of the conventional theories of Section 3, which assume repeated instantaneous ideal measurements, if we identify (apart from a multiplicative factor of order unity) the measurement intervals $\tau_\mathrm{i}$ of Fig. 9 with the response time $\tau_\mathrm{r}$ of Fig. 20. In contrast, we show in Sections 5.4–5.6 that drastic differences emerge if the response is not flat. The non-flat response may be interpreted as imperfectness in the measurement, such as geometrical imperfectness and energetic imperfectness. In Section 5.4, a geometrically imperfect measurement is discussed, where the photodetector does not cover the full solid angle around the atom. In this case, the Zeno effect takes place partially, the amount of which is proportional to $1-\varepsilon_\infty$, the asymptotic photodetection probability. In Section 5.5, an energetically imperfect measurement is discussed, where the photodetector responds to photons within a limited energy range $\Delta_\mathrm{d}$, called the active band. Surprisingly, when the detector is energetically imperfect, the Zeno effect can take place even for systems which follow the exact exponential decay law, which was believed never to undergo the Zeno effect according to the conventional theories. This fact serves as an counterexample to an intuition that imperfect measurements are disadvantageous for inducing the Zeno effect. In Section 5.6, a false measurement is discussed, where the detector cannot detect a photon whose energy is close to the atomic transition energy $\Omega$, because the active band of the detector does not cover this energy. Interestingly, the AZE takes place even by such a false measurement if the detector response $\tau_\mathrm{r}$ is quick enough. Relation between these results and the conventional theories are discussed in Section 5.7.1, and the physical interpretation in Section 5.7.2. Discussions and remarks on our model are described in Section 5.7.3.

In Section 6, relation between the Zeno effects and other phenomena, such as the motional narrowing, is discussed. In particular, we discuss the close relationship between the cavity quantum electrodynamics (QED) and the Zeno effect by a continuous indirect measurement. Using the results of the cavity QED, we also discuss in Section 6.4 the Zeno effect in the case where the detectors are spatially separated from the target atom.

Finally, in Section 7, we discuss experimental studies on the Zeno effect. In most attempts at experimental confirmation of the QZE, oscillating states were selected as the unstable states. However, significance of the Zeno effect is obscured in oscillating systems. We have introduced two attempts to observe the Zeno effect in truly decaying systems (Sections 7.1 and 7.2), both of which have long duration (i.e., long $t_\mathrm{j}$) of deviation from the exponential decay law and well devised measuring methods with high controllability of measurement intervals. We have also discussed in Section 7.3 how to *avoid* the Zeno effect in general measurements, which are designed not to detect the Zeno effect but to measure the free decay rate accurately.

In conclusion, the quantum measurement theory has revealed many interesting and surprising facts about the Zeno effect by general measurements. We hope that future works, both experimental and theoretical, will confirm and/or extend these results, and thereby explore more deeply into the Zeno effect.

## References

[1] J. von Neumann, Die Mathematishe Grundlangen der Quantenmechanik, Springer, Berlin, 1932.
[2] J.J. Sakurai, Modern Quantum Mechanics, Addison-Wesley, Reading, MA, 1985.

[3] A. Beskow, J. Nilsson, Ark. Fys. 34 (1967) 561.
[4] L.A. Khalfin, JETP Lett. 8 (1968) 65.
[5] B. Misra, E.C.G. Sudarshan, J. Math. Phys. 18 (1977) 756.
[6] L.S. Schulman, J. Phys. A 30 (1997) L293.
[7] C. Presilla, R. Onofrio, U. Tambini, Ann. Phys. 248 (1996) 95.
[8] H. Nakazato, M. Namiki, S. Pascazio, Int. J. Mod. Phys. B 10 (1996) 247.
[9] A.D. Panov, Ann. Phys. 249 (1996) 1.
[10] D. Home, M.A.B. Whitaker, Ann. Phys. 258 (1997) 237.
[11] A.M. Lane, Phys. Lett. A 99 (1983) 359.
[12] A.G. Kofman, G. Kurizki, Phys. Rev. A 54 (1996) R3750.
[13] B. Kaulakys, V. Gontis, Phys. Rev. A 56 (1997) 1131.
[14] P. Facchi, S. Pascazio, in: E. Wolf (Ed.), Progress in Optics, vol. 42, Elsevier, Amsterdam, 2001, p. 147.
[15] L.D. Landau, R. Peierls, Z. Phys. 69 (1931) 56.
[16] R.J. Glauber, Phys. Rev. 130 (1963) 2529.
[17] W.G. Unruh, Phys. Rev. D 18 (1978) 1764.
[18] M. Ozawa, Phys. Rev. Lett. 60 (1988) 385.
[19] A. Shimizu, K. Fujita, in: H. Ezawa, Y. Murayama (Eds.), Quantum Control and Measurement, North-Holland, Amsterdam, 1993, p. 191 (e-Print: quant-ph/9804026).
[20] A. Shimizu, in: M. Tokuyama, H.E. Stanley (Eds.), Statistical Physics, American Institute of Physics, 2000, p. 611 (e-Print: quant-ph/9911102).
[21] C.W. Gardiner, P. Zoller, Quantum Noise, second ed., Springer, Berlin, 2000.
[22] E. Arthurs, M.S. Goodman, Phys. Rev. Lett. 85 (2000) 688.
[23] M. Ozawa, Phys. Rev. A 67 (2003) 042105.
[24] K. Koshino, A. Shimizu, Phys. Rev. Lett. 92 (2004) 030401.
[25] K. Koshino, Phys. Rev. Lett. 93 (2004) 030401.
[26] R.J. Cook, Phys. Scripta T 21 (1988) 49.
[27] W.M. Itano, D.J. Heinzen, J.J. Bollinger, D.J. Wineland, Phys. Rev. A 41 (1990) 2295.
[28] R.F. Sawyer, Phys. Rev. Lett. 69 (1992) 2457.
[29] B. Nagels, L.J.F. Hermans, P.L. Chapovsky, Phys. Rev. Lett. 79 (1997) 3097.
[30] A. Beige, D. Braun, B. Tregenna, P.L. Knight, Phys. Rev. Lett. 85 (2000) 1762.
[31] P. Meystre, M. Sargent III, Elements of Quantum Optics, second ed., Springer, Berlin, 1990.
[32] L. Mandel, E. Wolf, Optical Coherence and Quantum Optics, Cambridge University Press, Cambridge, 1995.
[33] C. Bernardini, L. Maiani, M. Testa, Phys. Rev. Lett. 71 (1993) 2687.
[34] S.R. Wilkinson, C.F. Bharucha, M.C. Fischer, K.W. Madison, P.R. Morrow, Q. Niu, B. Sundaram, M.G. Raizen, Nature 387 (1997) 575.
[35] K. Unnikrishnan, Phys. Rev. A 60 (1999) 41.
[36] Y. Toyozawa, M. Inoue, J. Phys. Soc. Japan 21 (1966) 1663.
[37] Y. Kayanuma, H. Nakayama, J. Phys. Soc. Japan 67 (1998) 3718.
[38] K. Friedrichs, Commun. Pure Appl. Math. 1 (1948) 361.
[39] E. Fermi, Rev. Mod. Phys. 4 (1932) 87.
[40] M.J. Collett, C.W. Gardiner, Phys. Rev. A 30 (1984) 1386.
[41] U. Fano, Phys. Rev. 124 (1961) 1866.
[42] A.L. Fetter, J.D. Walecka, Quantum Theory of Many-Particle Systems, McGraw-Hill, New York, 1971.
[43] G.D. Mahan, Many-Particle Physics, second ed., Plenum Press, New York, 1990.
[44] G. Rempe, H. Walther, N. Klein, Phys. Rev. Lett. 58 (1987) 353.
[45] S. Haroche, D. Kleppner, Phys. Today January (1989) 24.
[46] H. Walther, Phys. Rep. 219 (1992) 263.
[47] A.M. Wolsky, Found. Phys. 6 (1976) 367.
[48] K. Kraus, Found. Phys. 11 (1981) 547.
[49] E. Joos, Phys. Rev. D 29 (1984) 1626.
[50] A. Marchewka, Z. Schuss, Phys. Rev. A 61 (2000) 052107.
[51] A.G. Kofman, G. Kurizki, Nature 405 (2000) 546.

[52] I. Antoniou, E. Karpov, G. Pronko, E. Yarevsky, Phys. Rev. A 63 (2001) 062110.
[53] P. Facchi, H. Nakazato, S. Pascazio, Phys. Rev. Lett. 86 (2001) 2699.
[54] A.D. Panov, Phys. Lett. A 298 (2002) 295.
[55] L.D. Landau, E.M. Lifshitz, Quantum Mechanics, Pergamon Press, Oxford, 1977.
[56] N. Imoto, H.A. Haus, Y. Yamamoto, Phys. Rev. A 32 (1985) 2287.
[57] A. Shimizu, Phys. Rev. A 43 (1991) 3819.
[58] V.B. Braginsky, Y.I. Vorontsov, K.S. Thorne, Science 209 (1980) 547.
[59] C.M. Caves, K.S. Thorne, R.W.P. Drever, V.D. Sandberg, M. Zimmermann, Rev. Mod. Phys. 52 (1980) 341.
[60] M. Ueda, N. Imoto, H. Nagaoka, Phys. Rev. A 53 (1996) 3808.
[61] H. Araki, M. Yanase, Phys. Rev. 120 (1963) 2529.
[62] A. Shimizu, in: H. Sakaki, H. Noge (Eds.), Nanostructures and Quantum Effects, Springer Series in Material Science, vol. 31, Springer, Heidelberg, 1994, p. 35 (e-Print: quant-ph/9804027).
[63] A. Shimizu, T. Miyadera, Phys. Rev. Lett. 89 (2002) 270403.
[64] T. Morimae, A. Sugita, A. Shimizu, Phys. Rev. A 71 (2005) 032317.
[65] T.M. Cover, J.A. Thomas, Elements of Information Theory, Wiley, New York, 1991.
[66] J. Ruseckas, Phys. Rev. A 66 (2002) 012105.
[67] R. Kubo, M. Toda, N. Hashitsume, Statistical Physics II, second ed., Springer, New York, 1995 (Chapter 4).
[68] C.W. Helstrom, Quantum Detection and Estimation Theory, Academic Press, New York, 1976.
[69] M.A. Nielsen, I.L. Chuang, Quantum Computation and Quantum Information, Cambridge University Press, Cambridge, 2000.
[70] E.P. Wigner, Z. Phyzik 131 (1952) 101.
[71] W.E. Lamb, Phys. Today 22 (1969) 23.
[72] See, e.g., Papers in: Y.A. Ono, K. Fujikawa (Eds.), Quantum Coherence and Decoherence, North-Holland, Amsterdam, 1999.
[73] T. Petrosky, S. Tasaki, I. Prigogine, Phys. Lett. A 151 (1990) 109.
[74] V. Frerichs, A. Schenzle, Phys. Rev. A 44 (1991) 1962.
[75] E. Block, P.R. Berman, Phys. Rev. A 44 (1991) 1466.
[76] S. Pascazio, M. Namiki, Phys. Rev. A 50 (1994) 4582.
[77] A. Beige, G.C. Hegerfeldt, Phys. Rev. A 53 (1996) 53.
[78] E. Mihokova, S. Pascazio, L.S. Schulman, Phys. Rev. A 56 (1997) 25.
[79] L.S. Schulman, Phys. Rev. A 57 (1998) 1509.
[80] A. Klein, E.R. Marshalek, Rev. Mod. Phys. 63 (1991) 375.
[81] A.L. Ivanov, H. Haug, L.V. Keldysh, Phys. Rep. 296 (1998) 237.
[82] B. Huttner, S.M. Barnett, Phys. Rev. A 46 (1992) 4306.
[83] P. Facchi, S. Pascasio, Fortschr. Phys. 49 (2001) 941.
[84] K. Koshino, Phys. Rev. A 71 (2005) 034104.
[85] K. Koshino, A. Shimizu, Phys. Rev. A 67 (2003) 042101.
[86] P.W. Anderson, P.R. Weiss, Rev. Mod. Phys. 25 (1953) 269.
[87] G.J. Milburn, J. Opt. Soc. Am. B 5 (1988) 1317.
[88] Y.R. Shen, The Principles of Nonlinear Optics, Wiley, New York, 1991.
[89] K. Thun, J. Perina, J. Krepelka, Proc. SPIE Int. Soc. Opt. Eng. 5259 (2003) 1.
[90] P.R. Berman (Ed.), Cavity Quantum Electrodynamics, Academic Press, San Diego, 1994.
[91] H. Mabuchi, A.C. Doherty, Science 298 (2002) 1372.
[92] J.D. Joannopoulos, R.D. Meade, J.N. Winn, Photonic Crystals, Princeton University Press, New Jersey, 1995.
[93] K. Koshino, A. Shimizu, Phys. Rev. A 53 (1996) 4468.
[94] A.A. Abrikosov, L.P. Gorkov, I.E. Dzyaloshinski, Methods of Quantum Field Theory in Statistical Physics, Dover, New York, 1963 (Chapter 6).
[95] T. Okushima, A. Shimizu, Jpn. J. Appl. Phys. 34 (1995) 4508.
[96] A. Shimizu, T. Okushima, K. Koshino, Mater. Sci. Eng. B 48 (1997) 66.
[97] M. Hotta, M. Morikawa, Phys. Rev. A 69 (2004) 052114.
[98] P. Kwiat, H. Weinfurter, T. Herzog, A. Zeilinger, M.A. Kasevich, Phys. Rev. Lett. 74 (1995) 4763.
[99] M. Kitano, K. Yamane, T. Ikushima, Phys. Rev. A 59 (1999) 3710.

[100] T. Nakanishi, K. Yamane, M. Kitano, Phys. Rev. A 65 (2002) 013404.
[101] P. Facchi, Y. Nakaguro, H. Nakazato, S. Pascazio, M. Unoki, K. Yuasa, Phys. Rev. A 68 (2003) 012107.
[102] A. Luis, Phys. Rev. A 67 (2003) 062113.
[103] L.E. Ballentine, Phys. Rev. A 43 (1991) 5165.
[104] W.M. Itano, D.J. Heinzen, J.J. Bollinger, D.J. Wineland, Phys. Rev. A 43 (1991) 5168.
[105] Chr. Balzer, R. Huesmann, W. Neuhauser, P.E. Toschek, Opt. Commun. 180 (2000) 115.
[106] M.C. Fischer, B. Gutierrez-Medina, M.G. Raizen, Phys. Rev. Lett. 87 (2001) 040402.
[107] A. Luis, J. Perina, Phys. Rev. Lett. 76 (1996) 4340.
[108] J. Rehacek, J. Perina, P. Facchi, S. Pascazio, L. Mita Jr., Phys. Rev. A 62 (2000) 013804.
[109] J. Rehacek, J. Perina, P. Facchi, S. Pascazio, L. Mita, Opt. Spectrosc. 91 (2001) 501.
[110] A. Luis, Phys. Rev. A 66 (2002) 012101.
[111] V. Kidambi, A. Widom, C. Lerner, Y.N. Srivastava, Am. J. Phys. 68 (2000) 475.